INSTITUTO SUPERIOR DE ENGENHARIA DO PORTO
MESTRADO EM ENGENHARIA ELECTROTÉCNICA E DE COMPUTADORES

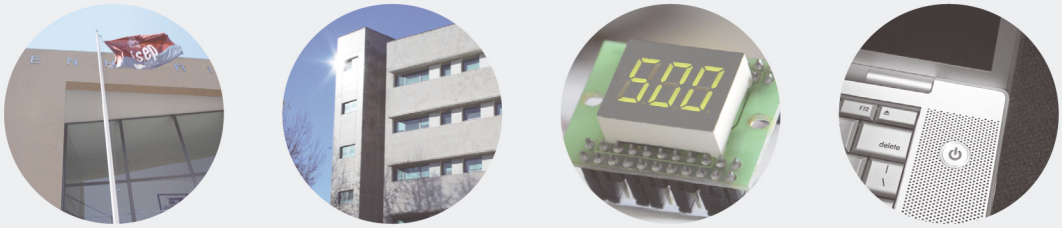

Energy Monitoring of Intralogistics Systems

RICARDO JORGE EVARISTO OLIVEIRA
dezembro de 2021

POLITÉCNICO
DO PORTO

INSTITUTO SUPERIOR DE ENGENHARIA DO PORTO
MESTRADO EM ENGENHARIA ELECTROTÉCNICA E DE COMPUTADORES

Energy Monitoring of Intralogistics Systems

RICARDO JORGE EVARISTO OLIVEIRA
Outubro de 2021

POLITÉCNICO
DO PORTO

Instituto Superior de Engenharia do Porto

ENERGY MONITORING OF INTRALOGISTICS SYSTEMS

Ricardo Jorge Evaristo Oliveira
Outubro de 2021

Departamento de Engenharia Eletrotécnica

Mestrado em Engenharia Eletrotécnica e de Computadores

Área de Especialização em Automação

This report satisfies partially the requirements to the subject of Thesis / Dissertation of - Electrical and Computer Engineers MSc.

Candidate: Ricardo Jorge Evaristo Oliveira, Nº 1160652, 1160652@isep.ipp.pt

Scientific Orientation: Dr. António Quadros Flores, aqf@isep.ipp.pt

Company: Körber Supply Chain Portugal

Supervisor: Eng. André Morais, andre.morais@koerber.com

Departamento de Engenharia Eletrotécnica

Mestrado em Engenharia Eletrotécnica e de Computadores

Área de Especialização em Automação e Controlo

2021

Acknowledgements

Firstly, to all those who accompany me throughout my life, I thank you for your motivation and unconditional support throughout my academic career.

I would like to thank Körber Supply Chain Portugal mainly to the Engineering and Customer Service departments for having guaranteed me all the condition to carry out the present project, as well as for having provided me with an internship full of learning moments.

To the scientific adviser, Dr. António Quadros Flores, I would like to thank the promptness and quality with which always received and helped me.

In particular, to the supervisor, Eng. André Morais, I would like to thank all accompaniment and all knowledge transmitted, essential for my professional and personal development.

Abstract

Intralogistics systems, in line with current technological development, seek to improve their performance in order to achieve high levels of efficiency, becoming an essential sustainable means of transporting goods and merchandise. Within this purpose, the present project aims to develop energy monitoring solutions capable of monitoring, in real time, the energy dynamics of intralogistics systems, allowing a perception of how energy flows along its movements. Therefore, the project relies on the use of monitoring equipment, Metrel MI 2892 Power Meter, easily adaptable to the physical and operational requirements of each system. This project is dedicated to monitoring the three main intralogistics systems, namely the stacker crane, the conveyors and the rail-guided vehicle (RGV) system.

Based on the analysis of the monitoring carried out for the relevant movements of each intralogistic system, the project presents a market study that highlights a set of monitoring equipment valid for the intralogistic systems under study. The equipment mentioned not only fits the energy monitoring requirements but also other requirements, such as protocols communications, important in the integration of these solutions.

The monitoring carried out throughout the project allow inferring the added value of its use in the design, operation analysis and support for predictive and corrective maintenance of intralogistics systems. Additionally, it turns out that the low acquisition and integration cost is quickly amortized by the benefits they present. Thereby, the monitoring solutions introduce energy, operational and financial benefits for the customer.

Keywords

Energy Monitoring, Efficiency, Intralogistics Systems, Stacker Crane, Conveyors, RGV system, Monitoring Solutions, Measuring Device

Resumo

Os sistemas intralogísticos, a par do atual desenvolvimento tecnológico, procuram aprimorar o seu funcionamento de modo a atingir elevados níveis de eficiência tornando-se um meio sustentável imprescindível no transporte de bens e mercadorias. Enquadrado neste propósito, o presente projeto visa o desenvolvimento de soluções de monitorização energética capazes de em tempo real monitorizar a dinâmica energética de sistemas intralogísticos permitindo uma perceção de como a energia flui ao longo dos seus movimentos. Para tal, o projeto conta com a utilização de um equipamento de monitorização, Metrel MI 2892 Power Meter, facilmente adaptável às exigências físicas e operacionais de cada sistema. Este projeto dedica-se à monitorização dos três principais sistemas intralogísticos sendo eles o transelevador, os transportadores e o sistema de veículos guiados por carril (RGV).

Com base na análise das monitorizações realizadas para os movimentos relevantes de cada sistema intralogístico, o projeto apresenta um estudo de mercado em que destaca um conjunto de equipamentos de monitorização validos para os sistemas intralogísticos em estudo. Os equipamentos referidos enquadram-se não apenas nas exigências de monitorização energéticas como também outras exigências tais como protocolos de comunicação importantes na integração destas soluções.

As monitorizações realizadas ao longo do projeto permitem inferir a mais valia da sua utilização no dimensionamento, análise de funcionamento e apoio à manutenção preditiva e corretiva de sistemas intralogísticos. Adicionalmente, verifica-se que o baixo custo de aquisição e de integração é rapidamente amortizado pelas mais valias que apresentam. Assim, as soluções de monitoramento trazem benefícios energéticos, operacionais e financeiros para o cliente.

Palavras-Chave

Monitorização Energética, Eficiência, Transelevador, Transportadores, Sistema RGV, Soluções de Monitorização, Equipamento de medição

Table of Contents

List of Figures

List of Tables

Acronyms

aMFS	–	Automated Material Flow Systems
CT	–	Current Transformer
ERP	–	Enterprise Resource Planning
PCC	–	Point of Common Coupling
PF	–	Power Factor
PWM	–	Pulse Width Modulation
RGV	–	Rail Guided Vehicle
RMS	–	Root Mean Square
TDD	–	Total Demand Distortion
THD	–	Total Harmonic Distortion
UPS	–	Uninterruptible Power Supply
VIM	–	International Vocabulary Metrology
VSD	–	Variable Speed Drive

1. INTRODUCTION

Since the mid-18th century with the first Industrial Revolution, the industry has gone through subsequent revolutions with radical changes in the production processes, from water and steam-powered machines to smart factories with autonomous systems and machine learning.

The progressively complexity, automation and sustainability of the manufacturing processes allow a worker to operate and analyse an industrial system easily, efficiently, and constantly. For this reason, the industry and its continuous evolution perform a crucial position in our world [1].

According to the European Council (2014) energy efficiency in the European Union is to be increased by 27% by the year 2030 to reduce primary requirements [2]. This prospect of improvement is largely supported by the great potential of the industrial sector. However, to exploit this potential it is necessary to monitor and understand in detail the energy needs of the production process and its dynamic variations. Only then a comprehensive

optimization of energy efficiency for a production system can be realized. Consequently, it is often that these data are not available to consider in a real-time control of production systems, which is why energy efficiency presently stills a minor optimization objective in production planning [3]. Endowing the industry with adaptive production systems enables a detailed monitoring of all pertinent production variables such as electrical power consumption, through diversified sensor technology. Thus, it is possible to include the consumption and influence of electrical energy from all operational resources in the decision-making process [4].

Intralogistics is increasingly a matter of research and development enabling the flow of resources and information along diverse logistics nodes in an organization as well as the entire supply chain [5]. It is possible through optimization, automation, and management supported by a multi-disciplinary ability, encompassing a wide range of essential skills that comprise strategic planning and logistics design, process engineering and analysis, facilities design and automation, systems design, integration, implementation and material handling technology [6].

The major components of most in-plant logistic systems are Automated Material Flow Systems (aMFS). The energy consumption of internal logistics increases in proportion to the size of the MFS implemented. For this reason, energy efficiency becomes an eminently important issue in terms of operational, environmental, and economic sustainability [7]. Efforts need to be made in order to overcome this inconvenience, resulting in a reduction of energy consumption throughout the physical part of the supply chain. The physical part of the supply chain besides transport systems includes intralogistics facilities where high-bay warehouses take an important performance [8].

The present industrial revolution, Industry 4.0, is concerned about efficient use of resources and cost optimization as well as improving the entire supply chain. Industry 4.0 enhances the productivity of the manufacturing industry giving crucial competitive benefits for companies. Additionally, interconnected autonomous control systems allies to digitalization will also help to improve agility and diversification. Industry 4.0 does not propose improvements only inside of the value chain of the company, but also through the entire supply chain in an industry [9].

While industry 4.0 has focused on digitalisation and artificial intelligence for rising the efficiency and flexibility of production, the oncoming industrial revolution, 5.0, includes responsible innovation based on three principles: human-centric, resilient, and sustainable. The introduction of the "human-centric" concept in industry means that production processes consider human needs and interests. Industry processes also must be sustainable by reducing waste and environmental impact in order to respect the planet and its limitations.

The present project aims to combine the fundamental principles of industry 5.0 with industry 4.0 and so explore the potential of smart factories in increasing the sustainability of its processes responding to the human and planet needs. Thus, a solution is proposed for energy monitoring of intralogistics systems allowing a real-time analysis of the flow of energy throughout the system and a perception of the way it works. The project also aims to be an easily addable solution in the implemented intralogistics systems as well as a fundamental tool for predictive maintenance and electrical system dimensioning. It is pretended that the potential benefits of the solution will be reflected on efficient use of customer energy increasing the operation quality of the intralogistics systems and reducing costs for the customer.

1.1. CONTEXT

The present project is accomplished at Körber Supply Chain Portugal (KSC PT) with the purpose of developing an energy monitoring solution for intralogistics systems designed and commercialized by the company. Since there is no energy monitoring of the referred systems, this project fits in that sense, enhancing the advantage of a systems continuous analysis. The matching with a personal interest in this area has motivated me to present this project as the theme of the master's thesis in Electronic Computer Engineering in the Automation and Systems branch at *Instituto Superior de Engenharia do Porto* (ISEP).

1.2. DESCRIPTION OF HOST COMPANY

The Körber Group is an international technology group with around 10,000 employees all over the world. It unites technologically leading companies with more than 100 production, service and sales locations and offers its customers solutions, products and services in the business areas of Körber Digital, Logistics Systems, Pharma Systems, Tissue and Tobacco. The Logistics Systems business area is the leading supplier of fully integrated solutions for optimizing complex internal and external logistics processes. Körber Supply Chain offers solutions in the fields of warehouse and conveying technology, palletization plants, software and logistics network controls as well as system integration.

1.3. OBJECTIVE

This project aims to design a solution for energy monitoring of intralogistics systems since it allows an analysis of the flow of energy throughout the system and a perception of the way it works. It is pretended that the solution to develop assists in the design and maintenance of KSC PT solutions with energy, operational and financial benefits for the customer. To achieve the proposed objective, the work is subdivided into the partial goals described below:

- Identify the main equipment and respective electrical infrastructure in the intralogistics systems developed by KSC PT;
- Study of the automation system integrated in the intralogistics solutions;
- Identify the main electrical parameters from the point of view of energy analysis;
- Definition of main monitoring points;
- Introduction of monitoring equipment into the system;
- Extraction and data processing from electrical parameters;
- Energy analysis based on acquired data;
- Research of market solutions for energy monitoring and analysis;
- Analysis of the solution's impact in terms of easy integration and flexibility.

1.4. SCHEDULING

In order to achieve the objective established in the previous section, the project is divided into some tasks that encompass the different stages of the project and whose execution is important for the correct project execution. Table 1 depicts how these tasks are divided and the presumptive relative time for their execution.

Table 1 Planned workflow

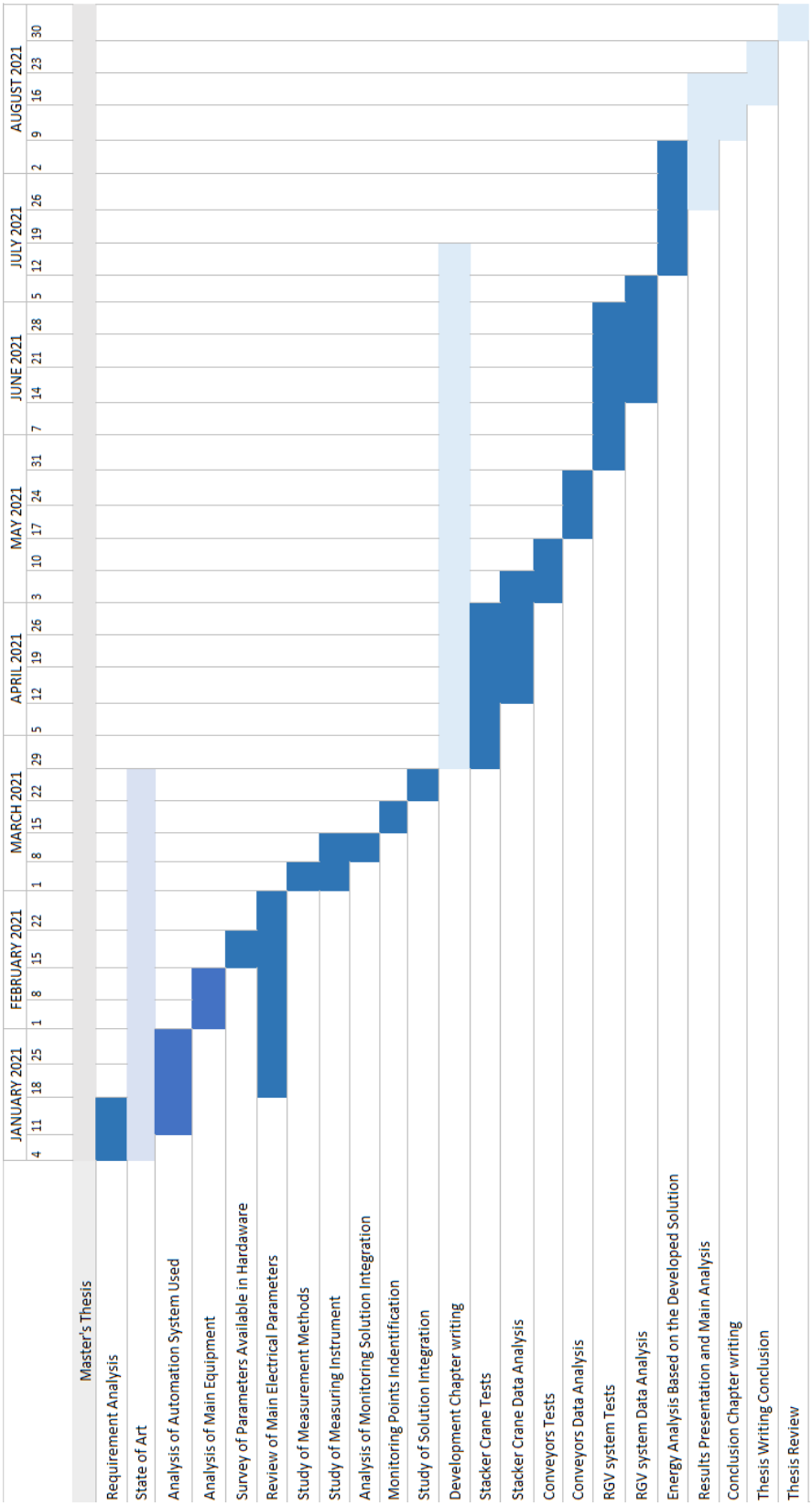

1.5. REPORT ORGANIZATION

Regarding the purpose of the project, it is viable divide the work into some steps and present them in seven chapters.

In the first chapter, a brief introduction to the theme is given, followed by a contextualization of the project. The aim of the project and its task organization is also presented.

The second chapter contains an important theoretical base to get the necessary expertise to develop the project. Understanding the electrical infrastructure and the variables available in the hardware of the automation systems currently used, as well as the main electrical parameters of energy monitoring is essential for the energy behaviour analysis of intralogistics systems.

Then, the third chapter is dedicated to the presentation of measurement methods, followed by monitoring equipment and its integration into the intralogistics systems under study with an emphasis on monitoring the electrical parameters.

In turn, chapter four describes the measuring process which includes the recording tests carried out, the description of the monitoring points for the various systems under analysis, and the introduction of the monitoring equipment at these points.

The energy monitoring tests are described throughout chapter five. This chapter also introduces considerations for the sizing, operation and maintenance of each system based on the monitoring analysis carried out.

In chapter six, monitoring equipment is presented and compared, followed by the evaluation of its integration in the intralogistics systems under study.

Finally, the seventh chapter is dedicated to the main conclusions and contributions of this project, as well as the presentation of suggestions for future work.

2. STUDY OF INTRALOGISTICS AUTOMATION SYSTEMS

The study of intralogistics automation systems begins with a description of the main systems on which this project is dedicated. Given the operating principle identical to each system, it is equally important to consider its main equipment. This first approach allows to infer which parameters are relevant in the monitoring of the intralogistics systems.

As these systems have some control units with direct communication to the logic units, certain parameters relevant to energy monitoring can be directly monitored. Although useful, the available parameters are insufficient for energy monitoring, so this chapter presents a theoretical analysis of electrical parameters with greater emphasis on energy monitoring of the intralogistic systems under study.

2.1. MAIN AUTOMATION SYSTEMS

Given the specificity of the systems under analysis, each of the systems to be monitored is presented below, namely the stacker cranes, the conveyors, and the rail-guided vehicle (RGV) system. For each system, its characteristics, functions and main elements are described with greater emphasis. The presentation of each system also includes a three-dimensional graphical representation.

2.1.1. STACKER CRANES

Stacker cranes are designed to travel automatically along aisles, efficiently handling the storage and retrieval of palletized goods in high-bay warehouses. Controlled by a warehouse management system, stacker cranes offer much greater load and height

capabilities than manually operated forklifts with significantly more accuracy, speed, softness, and safety. The stacker cranes can be configured in terms of size, load capacity, building height and cycle times.

Stacker cranes move along three axes, as shown in Figure 1 a), these being the hoisting axis, Y, the travelling axis, X, and the storage axis, Z.

The type of STK used for the project under analysis, similar to Figure 1 b), has a double mast system with a total weight of approximately 28 tons. Given the machine's energetic dynamics, it is relevant to highlight the hoisting and travelling axis.

About the translation axis, this is responsible for moving the STK along 110 meters using two 30 kW three-phase AC induction motors with a nominal current of 99 A, power factor of 0,84 and efficiency class IE1. Motors are controlled in parallel by a variable speed drive.

In turn, the hoisting axis allows moving two pallets simultaneously, with a total maximum weight of 2100 kg, up to 30 meters high. For this purpose, the STK has a 37 kW three-phase induction motor with a nominal current of 121 A, power factor of 0,82 and efficiency class IE1. The hoisting motor is controlled by a variable speed drive which is associated with a regenerative module whose function is to return the energy generated during the lowering and braking movements to the network.

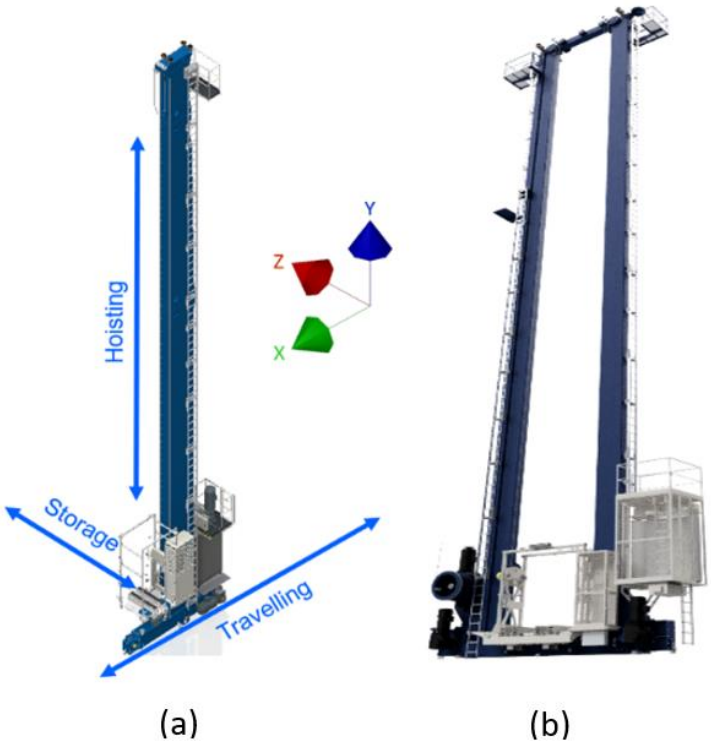

Figure 1 (a) Stacker Crane axes (b) Double Mast Stacker Crane.

2.1.2. CONVEYORS

Conveyors are an essential system to ensuring the fast, efficient, and accurate transportation of goods between all operational areas.

Conveyor systems cover the movement of products throughout the entire logistics chain, from product entry to the export area. For that, conveyor systems include a wide range of solutions that include powered or gravity roller conveyors, chain conveyors, belt conveyors and slat conveyors. These systems can be coupled to other devices such as lifts, stackers, and quality check stations.

The analysed conveyor, similar to Figure 2, is a powered roller conveyor located in the entrance area of an empty pallet container used in the filling process. This conveyor has a 0,55 kW three-phase AC induction motor associated with a VSD responsible for the roller's rotation.

Figure 2 Roller Conveyor.

2.1.3. RAIL GUIDED VEHICLE (RGV)

Rail Guided Vehicle (RGV) System is based on automated monorail carries travelling along circuit loops and is applicable to a wide range of pallet transport applications. It is an efficient, cost-effective, and high-speed option for the connection of very distant points with a light infrastructure. RGVs can be adapted to suit a vast range of load handling applications such as conveyors and telescopic forks.

The RGV system has a floor-fixed track rail that can include running rails load transfer stations, rail switching devices, lifts, and maintenance areas. Figure 3 (a) illustrates an overview of a possible RGV loop system.

The studied RGV system is composed of 37 monorails fed by a conductor rail divided into three sections. The connection between the conductor rail and each RGV is accomplished by a brushes system with two brushes by phase linked to the same entry point. Every rail-guided vehicle works along the storage and travelling axes as demonstrated in Figure 3 (b). For loading and unloading, the RGV has a conveyor roller with identical characteristics to the conveyor described above. To move around, the RGV has a 3 kW three-phase induction motor equally controlled by a VSD. The movement dynamic of all RGV inside the loop is carried out through a master controller.

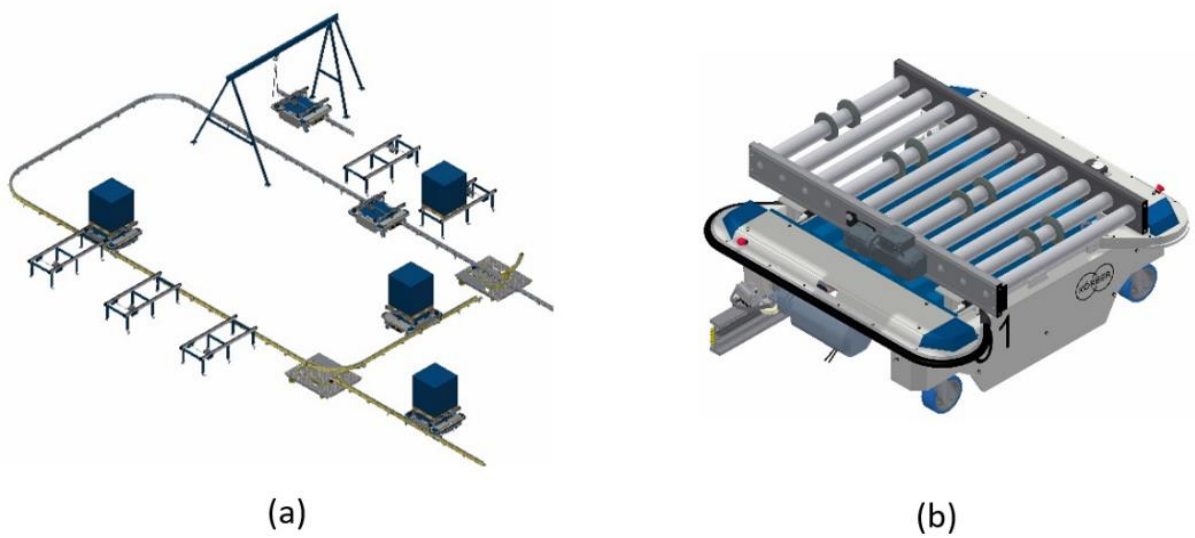

Figure 3 (a) RGV loop system (b) RGV with roller conveyor.

2.2. MAIN EQUIPMENT

Although with different dimensions and requirements, the three intralogistics systems under analysis are made up of two equipment that are essential for their operation: the three-phase AC Induction Motor and the Variable Speed Drive. For this reason, the present section briefly describes this equipment always singular.

2.2.1. THREE-PHASE AC INDUCTION MOTOR

The three-phase induction motor is the alternating current machine most used in industrial applications to drive mechanical loads due to its facility of use, robustness, efficiency, and reliability [10].

The constitution of an asynchronous machine is based on the following main elements:

- **Stator** (fixed part) - consists of magnetic leaf disks with low loss density that carry the windings responsible for magnetizing the air gap, forming the stator magnetic circuit. The three-phase, symmetrical, wound inductor circuit with a certain number of poles is formed by a winding with three spaced coils $\frac{2\pi}{3}$ rad, which are fed by each of the phases of a three-phase voltage system [10].

The three-phase winding can be illustrated by:

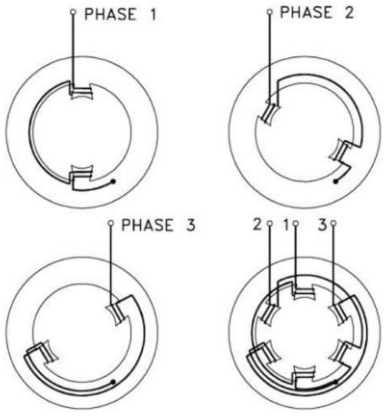

Figure 4 Three-phase winding [11].

- **Rotor** - refers to the rotating part coupled to the shaft that drives a mechanical load. Like the stator core, the rotor magnetic core is also clad and constructed with the same type of magnetic plate. In the rotor, the magnetic plates have a circular crown shape with closed grooves near the outer periphery. In order to avoid the appearance of noise during normal engine operation, the number of rotor slots is equal to the number of stator slots [10].

  Although there are different types of rotors, it is only intended to highlight the squirrel cage rotor used in the type of motors implemented in the intralogistics solutions under analysis.

  The squirrel cage rotor is formed by a laminated ferromagnetic core with slots where conductor bars fit, being short-circuited at the ends by copper or aluminium rings [12][13].

2.2.1.1. Basic Principles of Motor Operation

The stator electrical circuit is fed by a three-phase voltage system that causes the circulation of current in the coil conductors referring to the phases that form the winding. The resulting magnetic field, the stator's rotating field, moves in the air gap at the synchronous speed, n_s, described by the ratio between the network frequency, **f**, and the number of poles pairs of the stator winding, **p** [13]:

$$n_s = \frac{2 \times 60 \times f}{p} \quad (1)$$

The stator's magnetic field, B_s, as it moves, will cut the rotor winding, inducing currents on it. The currents induced in the rotor will cause a rotating magnetic field in response, B_r. The movement of the rotor tends to counteract the cause that gave rise to it and, due to the action of the electromagnetic torque, it tends to approach the speed of the rotating field.

The difference between the synchronous speed, n_s, and the rotor physical rotation speed, n_r, is called slip, s [10]:

$$s = \left(\frac{n_s - n_r}{n_s}\right) \quad (2)$$

While the synchronous speed has a fixed value, the rotor speed is entirely dependent on the coupled load.

B_s when moving, cuts the rotor bus, inducing an electromotive force, emf, given by [12]:

$$emf = (\vec{v} \times \vec{B}) * l \quad (3)$$

On what:

v -> Speed of bar/rotor conductor relative to magnetic field

B-> Magnetic flux density vector

l-> length of conductor that cuts the magnetic field

Since the stator rotating field moves counter clockwise and given the inductive nature of the rotor, the induced current will be lagging the induced electromotive force causing a rotating magnetic field in the rotor. The interaction between B_s and B_r generates a binary that moves equally counter clockwise. Figure 5 graphically outlines, for a given moment in time, the relationships exposed in the previous paragraph [12].

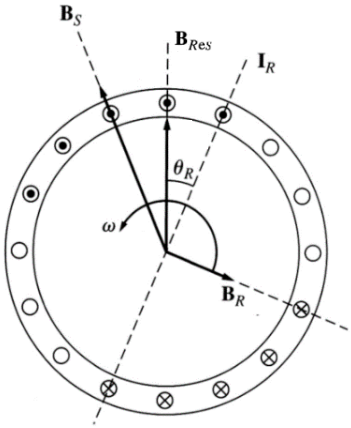

Figure 5 The development of induced torque in an induction motor [12].

Where:

B_S -> Rotating magnetic field acting on the stator

I_R -> Rotor current

B_R-> Rotating magnetic field acting on the rotor

θ_R-> Offset angle between the resulting magnetic field and the rotor current

B_{Res}-> Magnetic field resulting from the composition of B_S with B_R

ω -> Rotating field rotation speed

The resulting torque, τ, can be equated as follows [12]:

$$\tau = k\vec{B}_r \times \vec{B}_s \quad (4)$$

K refers to motor's constructive aspects.

2.2.1.2. OPERATING MODES

The three-phase induction motors can operate according to three modes: normal mode of operation, brake mode or generator mode. The curve presented in Figure 6 illustrates the relationship between torque and synchronism speed as well as the respective slip for each operating region.

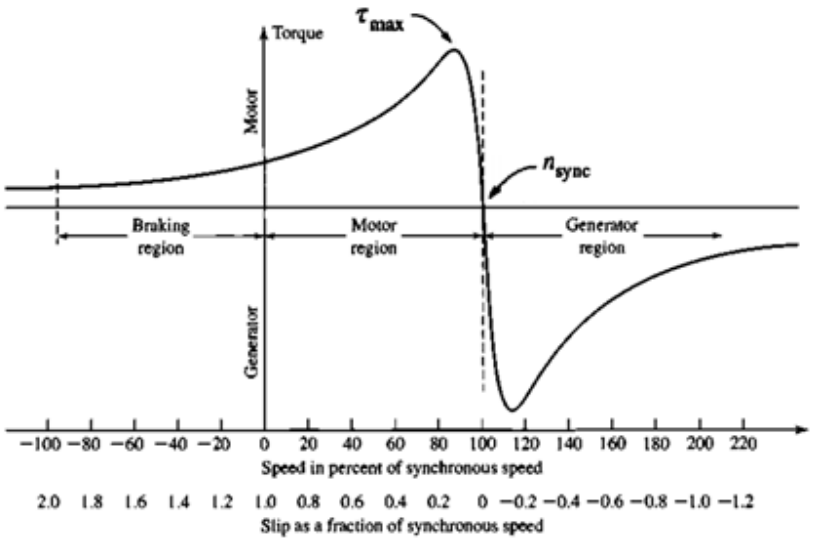

Figure 6 Induction-machine torque-slip curve showing braking, motor, and generator regions [14].

Motor Mode

In this operating mode, the motor operates at a speed between the stop speed and the synchronous speed, with a positive slip between 0 and 1. In no-load, the electromotive force on the rotor is very low, the impedance of the rotor circuit is practically inductive, and the current is enough to develop a torque capable of keeping the rotor in operation. When a mechanical load is coupled to the shaft, the rotor slows down and the slip increases which leads to an increase of electromotive force in magnitude and frequency, producing more current and torque [15].

Brake Mode

If the motor is driven in the opposite direction of displacement, it still produces a forward torque and therefore acts as a brake, absorbing the mechanical power in the rotor loss. At this stage, the rotor has a high slip and enters braking mode. The velocity decreases to zero and the machine can be stopped. This method of stopping a motor is denominated "plugging" [15].

Generator Mode

During a mechanical load action, the motor torque and the resistive torque can act in the same direction. When this phenomenon occurs, the motor speed exceeds the synchronism speed, making the motor work as a generator. To work as a generator, the magnetization of the motor depends on the reactive energy provided by the source. As electrical energy is produced, it can be dissipated by a resistance (rheostatic braking) or returned to the grid (regenerative braking) [10].

2.2.2. VARIABLE SPEED DRIVE

An AC motor operating with direct recourse to the AC voltage from the supply network can only regulate its speed to a fixed value according to the number of poles and the frequency supplied from the supply network. However, when an application requires a controllable speed, a suitable solution is to introduce in the system a variable speed drive (VSD) [16]. A VSD works by converting fixed frequency to adjustable frequency to control AC induction motor in variable speed based on the load's changes.

A VSD operating principle is based on converting the incoming electrical supply into a variable frequency and voltage that is provided to the motor with a direct influence on the motor speed and torque. The voltage and frequency should keep a regular ratio in order to produce a suitable torque. The standard design of a VSD consists of three sequential stages [17]. The first stage, AC to DC Converter, consists of a rectifier that converts the incoming AC supply voltage into DC. Then, the DC voltage ripples are smoothed using capacitors. This section is commonly introduced as DC link. In the last stage, DC to AC converter, the

rectified and conditioned DC supply back into an AC supply of variable frequency and voltage. This conversion is carried out by power electronic devices such as IGBT power transistors using the Pulse Width Modulation (PWM) technique. The output voltage is turned on and off at a high frequency, with the interval of on-time, or pulse width, managed to approach a sinusoidal waveform [18]. As exemplified in Figure 7, the resulting PWM waveform is regulated according to the requested frequency and voltage.

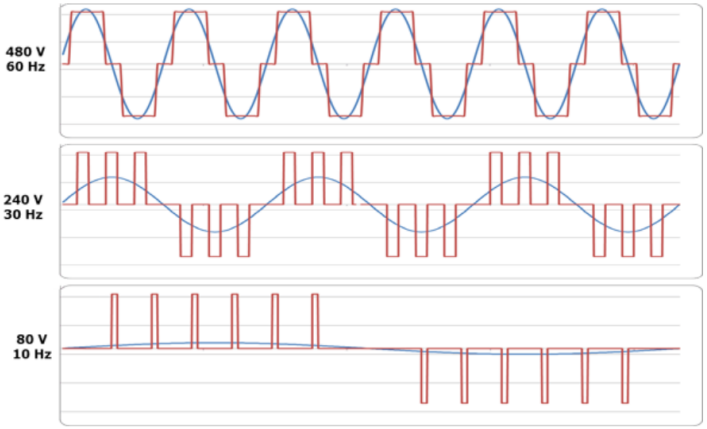

Figure 7 PWM waveforms for different frequencies and voltages requested [19].

In short, Figure 8 presents the standard design of a VSD and the waveform changes along the described stages.

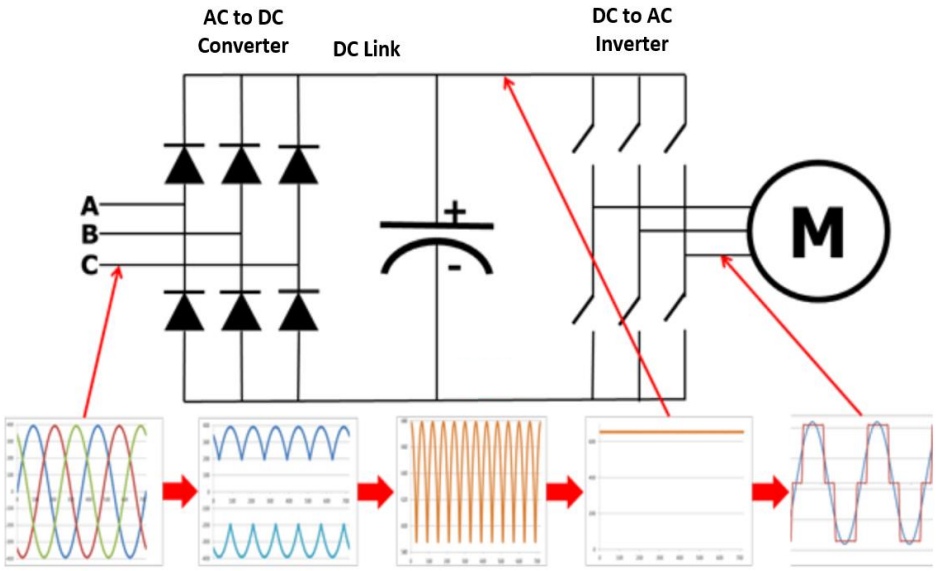

Figure 8 VSD stages and respective waveform treatment process [19].

2.3. Available Variables in Existing Hardware System Useful for Energy Monitoring

All intralogistics systems under analysis have a similar operating logic. The execution orders from the user or the Warehouse Management System (WMS) are provided to the system through an interface that directs the information to a Programmable Logic Controller (PLC). The PLC is a digital computer with an operating system dedicated to automating industrial electromechanical processes. It is highly specialized and optimized to handle incoming events in real-time. The PLC is also considered the essential element of the system once it is responsible for the articulation between all system elements [20].

The PLC has input lines, analogue or digital, through which it receives the orders to be executed as well as information on how the process is being performed from the control units. Then, based on the input data, the PLC executes the appropriate output function. These orders are transmitted to actuators responsible for acting or signalling reactions. To clarify the implemented systems functioning, Figure 9 presents a block diagram of its base logic.

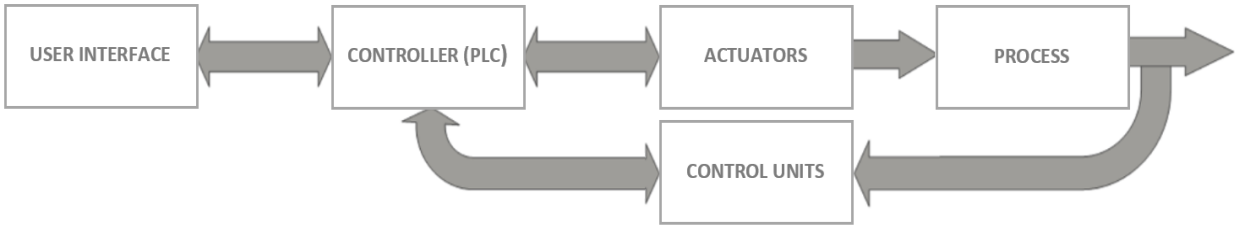

Figure 9 Block diagram of system base logic.

The connection between the PLC and some actuators or control units is bidirectional which allows the PLC to transmit important system variables to the user level. These variables can be useful to detect errors, understand how the system works, count the number and type of movements and the operation hours. It is also advantageous to seize some available variables to complement the energy monitoring of the systems under analysis. The available variables in the existing hardware system useful for energy monitoring are:

- Movement speed per axis;
- Distance between initial, actual and final position per axis;
- VSD actual current per axis;
- Motor temperatures;
- Carriage Temperature and relative humidity;
- Cabinet Temperature and relative humidity;
- Carriage vibration;
- Topmast vibration.

It is possible to carry out a logical analysis or a register of the above-mentioned variables during a certain period using the PLC-ANALYZER software.

The PLC-ANALYZER allows the acquisition, representation, and evaluation of signals from the PLC as input, output, flags, timer, counter and data of data blocks. This software is a useful tool for failure diagnosis, detection of sporadic errors, cycle time optimization, long-term recording of measured values, installation, development, and maintenance [21].

2.4. MAIN ELECTRICAL PARAMETERS FOR ENERGY MONITORING

Over the last decades, concerns with quality and energy efficiency of suppliers and large consumers have become more prominent. The increasing use of power electronics in the industry and the impact of energy on the overall quality of the system have become key issues for different types of research.

2.4.1. POWER QUALITY

The actual evolution of the industrial integrated process increases the real concern of the future impact on system capabilities and its power efficiency given that the failure of any equipment can condition directly the correct functioning of the entire system. This is one of the most important reasons why there is a need to guarantee a high-power quality.

According to IEEE, the term power quality refers to a wide variety of electromagnetic phenomena that characterize the voltage and current at a given time and at a given location on the power system [22].

In order to describe electromagnetic phenomena at a specific electric power circuit, power quality monitoring is an essential condition. Monitoring can be used to analyse the electrical environment as well as to develop a power quality baseline. Monitoring also has a profitable contribution to forecast power quality mitigating devices or future performance [23].

The losses associated with electrical system problems are high, considerably impairing the quality of the energy with anomalies on the products and on the process operations. Equipment damage can also be a consequence of electromagnetic phenomena requiring that the damaged equipment either be recycled or castoff.

Next are described the most important aspects related to the consequences of low power quality in the industry:

- **Loss of production:** Forced stoppage of production leads to a loss of margin for products that are not sold because they are not produced.
- **Manufacturing interruption:** The shutdown caused by a power quality disturbance has an impact on the correct functioning of the entire system.
- **Loss of revenue:** Delayed production and sales schedules can be caused by any interruption to a manufacturing process.
- **Decreased competitiveness:** Customer disappointment and poor-quality product as a result of power quality in the manufacturing environment.
- **Product damage:** Power quality problems during the production process can often result in damaged products. Failure to detect a malfunction can be expensive and lead to the disposal of equipment.
- **Decreased equipment lifetime:** Detected and undetected disturbances have resulted in decreased equipment life.

The effects designated above are firmly associated with problems caused in electrical energy. These problems are [24].

- **Harmonic Distortion:**

The non-linear loads introduce current with a harmonic component to the electrical network. This harmonic component affects power quality through voltage drops and distorted voltage waveforms. Figure 10 describes this phenomenon.

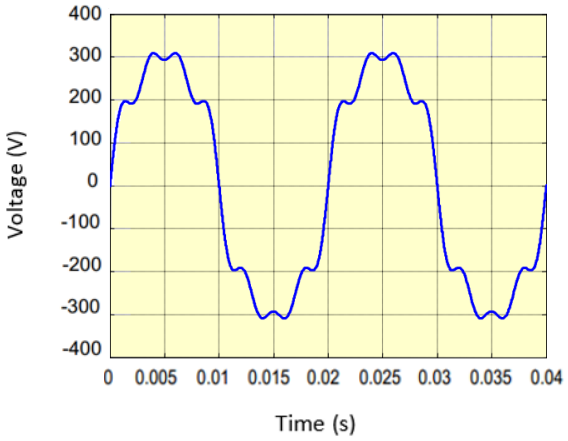

Figure 10 Harmonic Distortion [24].

- **Noise (electromagnetic interference):**

Corresponds to high-frequency electromagnetic noise, which can, for example, be produced by the fast switching of electronic power converters. Figure 11 represents a sinusoidal wave affected by noise.

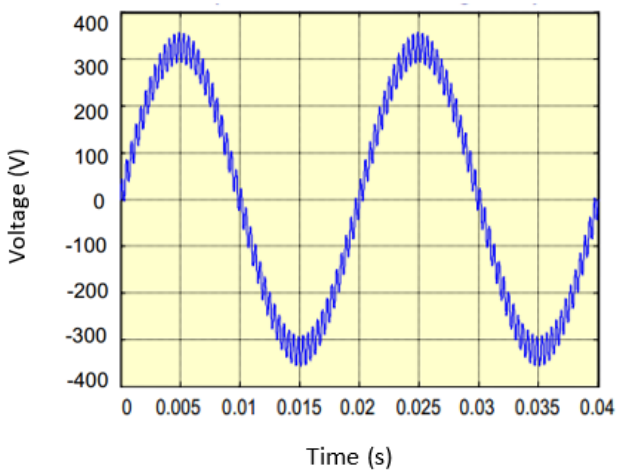

Figure 11 Noise [24].

- **Inter-harmonics:**

Inter-harmonics are inserted on current when its currents are not related to fundamental current. The inter-harmonics introduce current fluctuations as shown in Figure 12.

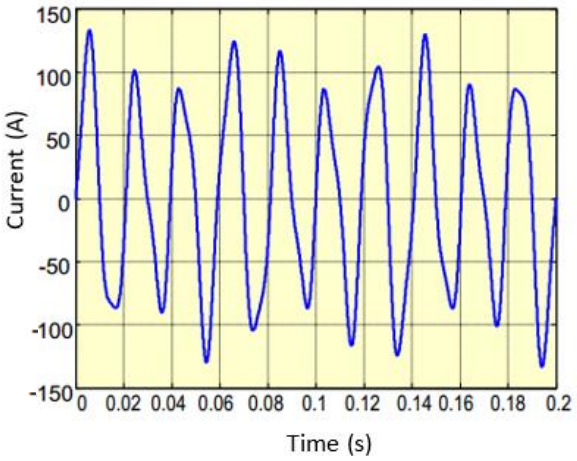

Figure 12 Inter-harmonics [24].

- **Momentary interruption:**

Momentary interruption happens as a result of a short circuit that makes a circuit breaker open. Circuit breakers with recloser have the capability of closing automatically after a few milliseconds, as shown in Figure 13.

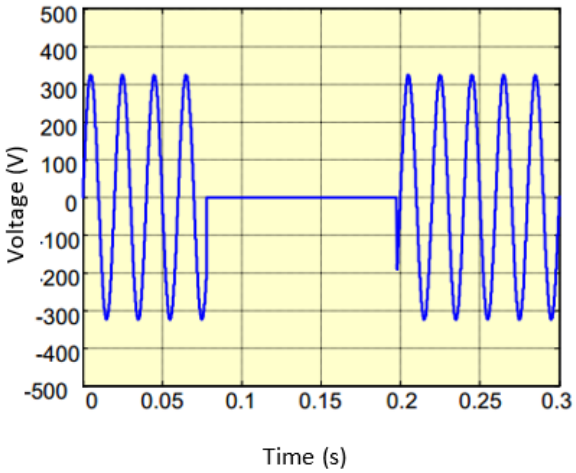

Figure 13 Momentary interruption [24].

- **Voltage sag:**

It is a short duration reduction in rms voltage which can be caused by a short circuit, overload, or starting of electric motors. Figure 14 represents an example of a voltage sag.

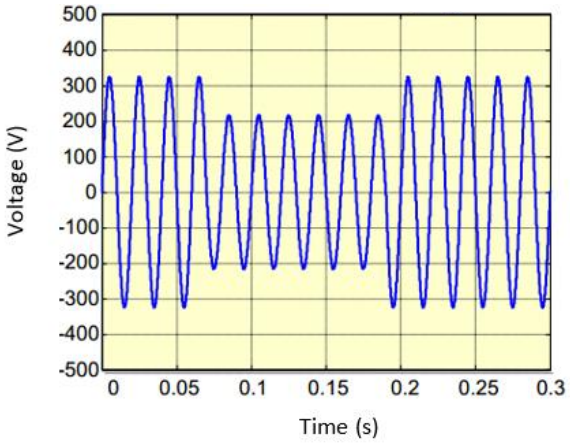

Figure 14 Voltage sag [24].

- **Voltage swell:**

Voltage swell defines surges in voltage of 10% or more above usual voltage. It can originate equipment issues and overall power quality. Swells arise when a large load (such as a large motor) is turned OFF and voltage on the power line increases for a short period of time [25]. The voltage Swell phenomenon is exhibited in Figure 15.

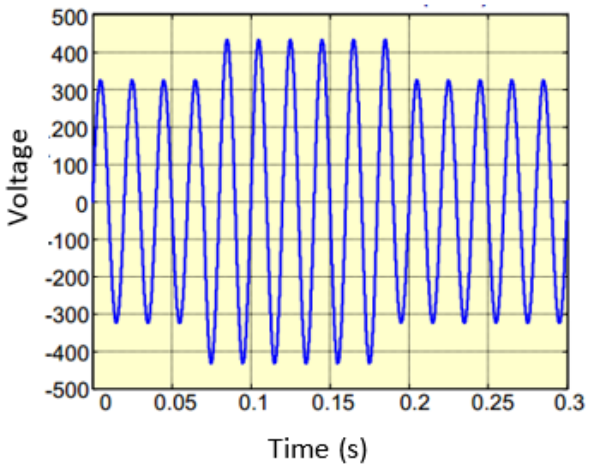

Figure 15 Voltage Swell [24].

- **Flicker:**

The irregular swing of certain loads provokes oscillations in the supply voltages, as shown in Figure 16.

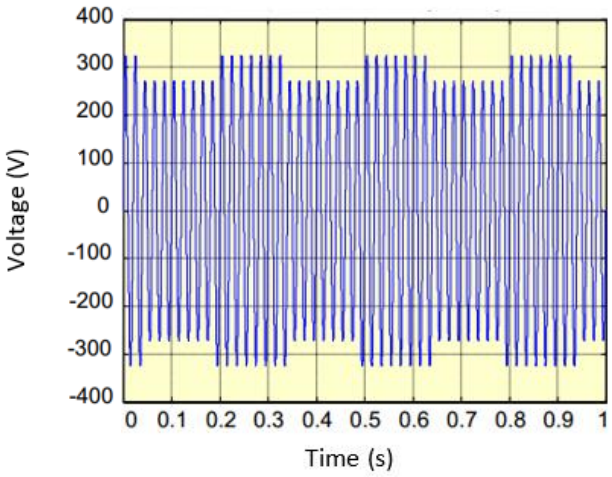

Figure 16 Flicker [24].

- **Transient**

It is a temporary unwanted voltage in an electrical circuit that ranges from a few volts to several thousand volts and lasts microseconds. This phenomenon is visible in Figure 17.

Transient voltages are caused by the sudden release of stored energy due to incidents such as lightning strikes, unfiltered electrical equipment, contact bounce, arcing, capacitor bank or generators being switched ON and OFF [25].

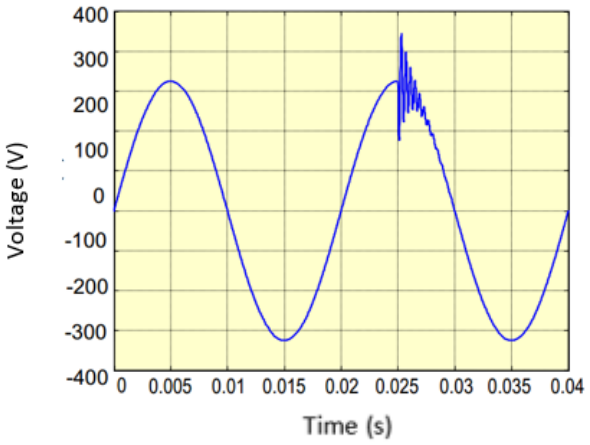

Figure 17 Transient [24].

- **Current and Voltage Crest factor**

The ratio of the peak current to the RMS current, expressed in equation 5, is designated as "current crest factor".

$$CFi = \frac{I_{peak}}{I_{RMS}} \quad (5)$$

In a similar way, the "voltage crest factor" describes the ratio of the peak voltage to the RMS voltage. This definition is represented by equation 6.

$$CFu = \frac{U_{peak}}{U_{RMS}} \quad (6)$$

Nonlinear loads like variable speed drives or battery chargers, induce high crest factors that usually has a low impact when metering the whole industrial load. However, a high crest factor in individual loads causes inaccurate readings. Therefore, it is important to be conservative in selecting the Current Transformers rated current [26].

2.4.2. HARMONIC ANALYSIS

Whereas initially the term power quality referred to the capability of the electric utilities to supply electric power without interruption, today power quality includes any deviation from a perfect sinusoidal waveform from short-term transients to continuous state distortions. Harmonics can be present in current, voltage, or both being that power system harmonics are a continuous state problem with dangerous results.

There are no benefits brought by the intense quantity of harmonics, but on the other hand, its mitigation can be translated into benefits for imperative industry processes such as IT systems and data centres. Preventing excessive harmonics can also reduce the installation cost, reduce the energy bill, and protect the installation against process breaks or equipment anomalies [27].

In the early 1800s, the French mathematician Jean Baptiste Fourier formulated that a periodic non-sinusoidal function of a fundamental frequency may be expressed as the sum

of sinusoidal functions of frequencies which are multiples of the fundamental frequency [28].

Considering a non-sinusoidal voltage, the mathematical expression of this definition is:

$$x(t) = \sum_{k=0}^{N} x_k \sin(k \cdot w_0 t + \emptyset_k) \quad (7)$$

Expanding equation 7 gives:

$$x(t) = x_k \sum_{k=0}^{N} \sin(k \cdot w_0 t) \cos(\emptyset_k) + \cos(k \cdot w_0 t) \sin(\emptyset_k) \quad (8)$$

Where:

$N \rightarrow$ Total number of harmonics

$k \rightarrow$ Order of harmonic

$w_0 \rightarrow$ Fundamental frequency

$\emptyset_k \rightarrow$ Phase angle of harmonic k

$x(t) \rightarrow$ Electrical signal

$x_k \rightarrow$ Electrical amplitude of harmonic k

Substituting $x_k \cos(\emptyset_k)$ for A and $x_k \sin(\emptyset_k)$ for B in equation 8, obtains:

$$x(t) = \sum_{k=0}^{N} \mathrm{A}\sin(k \cdot w_0 t) + \mathrm{B}\cos(k \cdot w_0 t) \quad (9)$$

At time t = 0, equation 9 reduces further to

$$A(0) = x(0) \quad (10)$$

Subsequently, the equation required to analyse the harmonic is:

$$x(t) = A(0) + \sum_{k=1}^{N} \mathrm{A}\sin(k \cdot w_0 t) + \mathrm{B}\cos(k \cdot w_0 t) \quad (11)$$

Equation 7 is a trigonometric form of finite series defined by Fourier [29].

In the decomposition into individual sinusoidal waveforms, the fundamental waveform will be the one for k = 1, and the multiples of this are designated harmonics of “k” order, for “k” ranging from 2 and above (it can be $N \rightarrow \infty$). A(0) represents the DC component. Assuming a signal with no DC component, it can be expressed by:

$$x(t) = x_1(t) + \sum_{k=2}^{N} x_k(t) \quad (12)$$

For a fundamental frequency, e.g. 50 Hz, the third harmonic would be 150 Hz and the fifth harmonic would be 250 Hz, as shown in Figure 18.

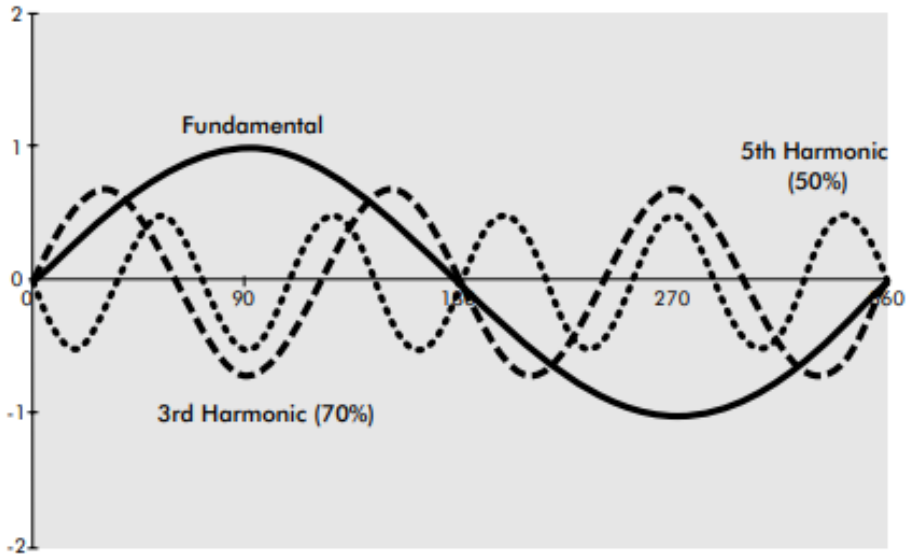

Figure 18 Fundamental with third and fifth harmonics [30].

Figure 19 exhibits a fundamental with 70 % third harmonic and 50 % fifth harmonic added. The waveform is the sum of the fundamental with harmonic frequencies. It is evidently not a sinewave [30].

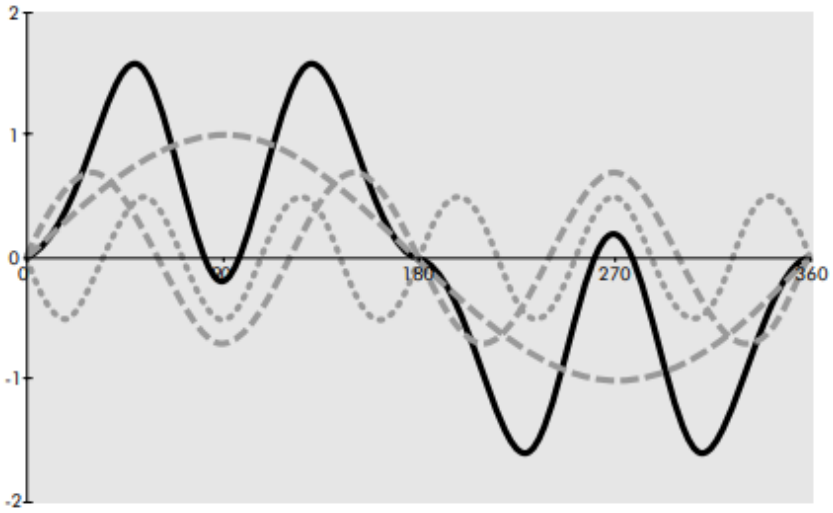

Figure 19 Distorted current waveform [30].

Effects

Harmonics flowing in supply networks cause instabilities in the regular flow of electricity. Thus, the quality of electrical power is deteriorated, the efficiency of the system is decreased, and electrical equipment or installations can be severely affected. Some of these effects are:

- Overload of distribution networks due to the rise of Root Mean Square (RMS) current;
- Supplementary efficiency losses;
- Unpredicted resonances;
- Logical faults in digital solutions;
- Instability in electronic equipment;
- Undesirable overload (or need to oversize) for wirings;
- Failures and premature ageing of motors, circuit breakers, and generators as well as increased transformer noise;
- Intermittent circuit breaker trip;
- Fuses blowing.

Point of Common Coupling (PCC)

Point of Common Coupling is understood as the point between the end user system and the utility system where evaluations of harmonic distortion are typically performed. If multiple systems are served from the primary of the transformer, the PCC is then positioned at the primary as shown in Figure 20 scheme (a). On the other hand, as demonstrated in Figure 20 scheme (b), if multiple systems are attended from the secondary of the transformer, the PCC is located at the secondary. Because of this, it is possible to conclude that the PCC can be placed on the primary or secondary side of the service transformer depending on the systems supplied by the transformer [31].

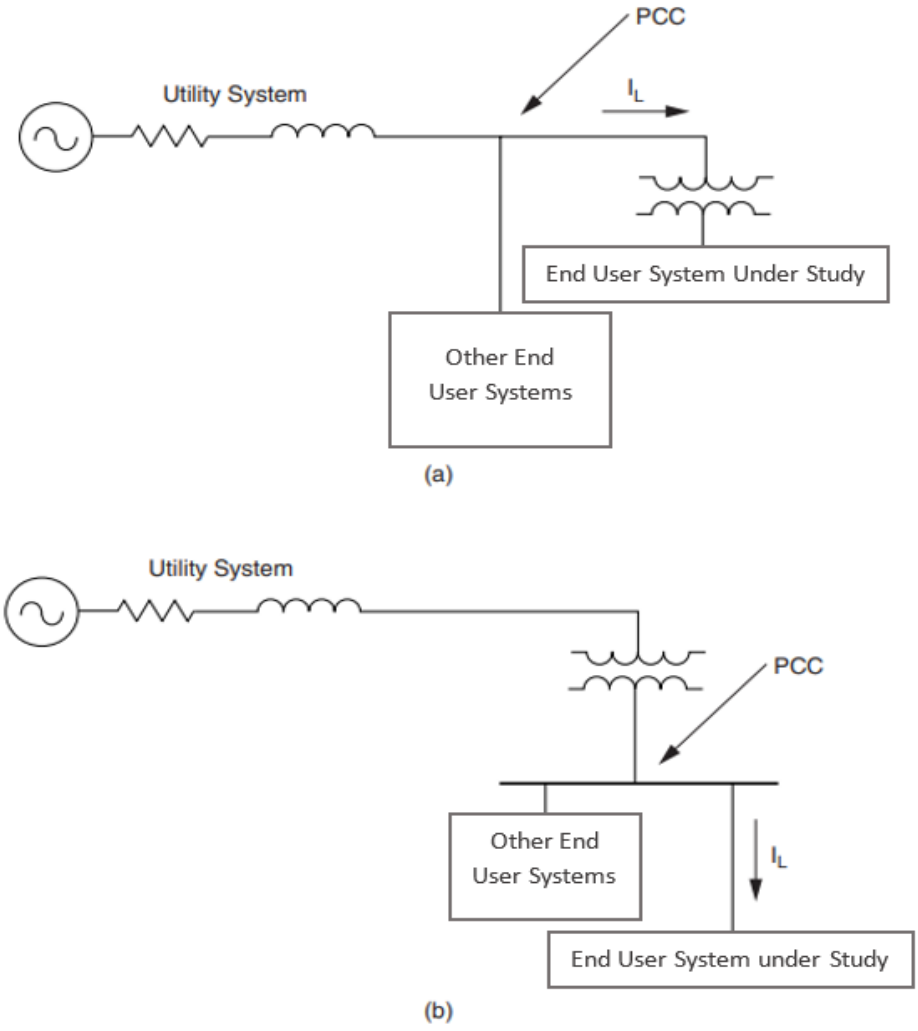

Figure 20 (a) PCC at the transformer primary where multiple customers are served (b) PCC at the transformer secondary where multiple customers are served [31].

Total Harmonic Distortion (THD)

The voltage waveform outside the ideal sine wave in the mains supply voltage is caused by a non-sinusoidal current consumption essentially rich in harmonics. Once electrical and electronic application designers cannot act on the voltage source waveform directly, it is important to minimize the harmonic component on the current wave shape and certify that the wave shape deviation caused by non-linear loads is as close as possible to the current fundamental sinusoid. Thus, the voltage distortion on the primary source supply will be minimized [32].

THD is defined as the ratio between the equivalent RMS voltage of all the harmonic frequencies, from the second harmonic on, and the RMS voltage of the fundamental frequency (first harmonic).

Equation 13 represents the voltage distortion factor (VTHD) [33].

$$VTHD = \frac{\sqrt{\sum_{k=2}^{\infty} V_{k_{RMS}}^2}}{V_{fund_{RMS}}} \cdot 100\% \qquad (13)$$

Where:

V_{k_RMS} → RMS voltage of the k^{th} harmonic

V_{fund_RMS} → RMS voltage of the fundamental frequency

Total Demand Distortion (TDD)

The ratio between the RMS current of all harmonic frequencies, from the second harmonic on, and the RMS current of the fundamental frequency is denominated Total Demand Distortion (TDD). TDD is algebraically expressed by equation 14 [33].

$$TDD = \frac{\sqrt{\sum_{k=2}^{\infty} I_{k\_RMS}^2}}{I_{fund\_RMS}} \cdot 100\% \qquad (14)$$

Where:

I_{k_RMS} → RMS current of the k^{th} harmonic

I_{fund_RMS} → RMS current of the fundamental frequency

The result is a percentage correlating the harmonic components with the fundamental component of a signal. So, the higher the percentage, the greater the distortion present in the signal.

Due to the impact of the harmonic component and its broad fluctuation within different parts at the same distribution system as well as the interaction with it through straight system connections, it is becoming ever more crucial to understand the fundamentals of harmonics and set the electrical systems to be capable to identify and monitor the occurrence of harmful harmonics [34]. For this reason, IEEE std 519-2014 recommends acceptable values for harmonic distortion and their limits are recommended for voltages and currents.

2.4.3. POWER FACTOR

Power Factor of an alternating current system is defined as the ratio of the real power absorbed by the load to the apparent power flowing in the circuit. For an ideal sinusoidal voltage and current waveforms, if there is a phase difference, φ, between them, the total apparent power, S, can be modelled as being composed of two components: one in phase with the input voltage, P, and the other 90° out of phase (in quadrature) with it, Q. The cosine of phase difference, $\cos\varphi$, is designated displacement power factor, DPF, and for a pure sinusoidal signal, it is equal to the power factor. This relationship can be expressed by the equation 15 and is visually noticeable in Figure 21.

$$PF = \frac{P}{S} = \cos\varphi = DPF \tag{15}$$

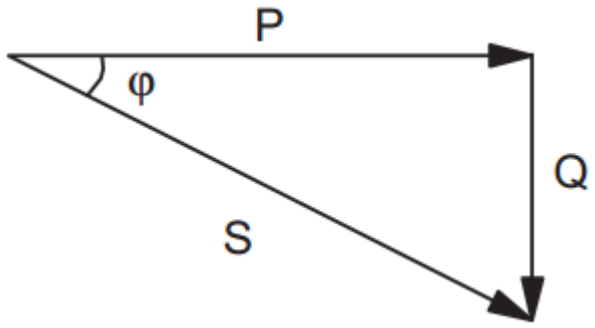

Figure 21 Power vectors of ideal sinusoidal signals [35].

Where:

$P = V_{RMS} \cdot I_{RMS} \cdot \cos\varphi$ → Real Power (kVA)

$Q = V_{RMS} \cdot I_{RMS} \cdot \sin\varphi$ → Reactive Power (kVAr)

$S = V_{RMS} \cdot I_{RMS}$ → Total Apparent Power (kW)

Considering the RMS value for the mains voltage as an ideal sinusoidal voltage waveform:

$$V_{RMS} = \frac{V_{peak}}{2} \tag{16}$$

If the current has been distorted into a periodic non-sinusoidal waveform, applying a Fourier transform gives:

$$I_{RMS(total)} = \sqrt{I_o + I_{1\,RMS}^2 + I_{2\,RMS}^2 + \cdots + I_{n\,RMS}^2} \qquad (17)$$

Where:

I_o → DC component current

$I_{1\,RMS}$ → Current of the fundamental harmonic

$I_{2\,RMS}$ → Current of the second harmonic

$I_{n\,RMS}$ → Current of the remaining harmonics

The fundamental of the RMS current can be modelled as a Real component $I_{1\,RMS\,P}$ and a Reactive component $I_{1\,RMS\,Q}$. Then, the RMS current can be introduced as:

$$I_{RMS(total)} = \sqrt{I_o + I_{1\,RMS\,P}^2 + I_{1\,RMS\,Q}^2 + \sum_{n=2}^{\infty} I_{n\,RMS}^2} \qquad (18)$$

Assuming the displacement angle between the input voltage and the reactive component of the fundament current represented by φ_1, $I_{1\,RMS\,P}$ is defined as:

$$I_{1\,RMS\,P} = I_{1\,RMS} \cdot \cos\varphi_1 \qquad (19)$$

Then, the Real Power is assumed as the RMS voltage multiplied by the reactive component current so:

$$P = V_{RMS} \cdot I_{RMS} \cdot \cos\varphi_1 \qquad (20)$$

Once the Apparent Power, S, is expressed by:

$$S = V_{RMS} \cdot I_{RMS\,total} \qquad (21)$$

Considering that the True Power Factor (TPF) takes into consideration the influence from all active power, both fundamental and harmonic frequencies, the TPF is specified as the ratio between the average power and the product of the rms values of the input current and voltage [36]:

$$TPF = \frac{P}{S} = \frac{V_{RMS} \cdot I_{1\,RMS} \cdot cos\varphi_1}{V_{RMS} \cdot I_{RMS\,(total)}} = \frac{I_{1\,RMS} \cdot cos\varphi_1}{I_{RMS\,(total)}} \quad (22)$$

If the phase angle between $I_{1\,RMS}$ and $I_{RMS\,(total)}$ is defined as θ, the cos θ is:

$$\cos\theta = \frac{I_{1\,RMS}}{I_{RMS\,(total)}} \quad (23)$$

The cos θ can also be denominated as Distortion Factor, DF, and defined as the ratio of TPF to DPF [36]:

$$cos\ \theta\ =\ DF = \frac{TPF}{DPF} = \sqrt{\frac{1}{1+(THD)^2}} = \frac{I_{1\,RMS}}{I_{RMS\,(total)}} \quad (24)$$

The oscillation of the harmonic content of the current will affect the θ and consequently the cos θ.

In the end, the Power Factor can be expressed accordingly with equation 25 as well as the power angles and vectors shown in Figure 22.

$$P = cos\ \theta \cdot \cos\varphi_1 \cdot S \quad (25)$$

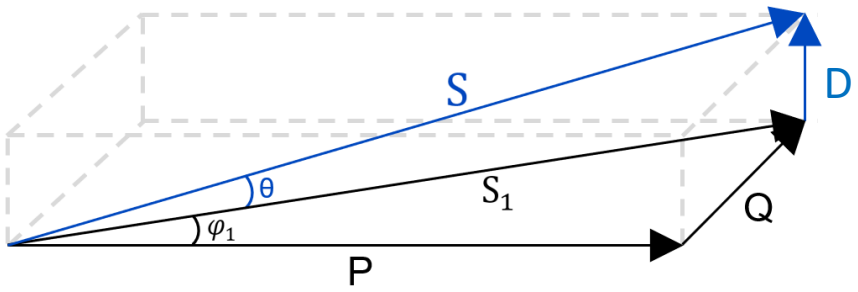

Figure 22 Power vectors of a system with non-linear loads [35].

Where:

$P = V_{RMS} \cdot I_{RMS} \cdot \cos\varphi \quad \rightarrow$ Real Power

$Q = V_{RMS} \cdot I_{RMS} \cdot \sin\varphi \quad \rightarrow$ Reactive Power

$S_1 = V_{RMS} \cdot I_{1\,RMS} \quad \rightarrow$ Apparent Fundamental Power

$D = V_{RMS} \cdot \sqrt{\sum_{n=2}^{\infty} I_{n\,RMS}^2} \quad \rightarrow$ Distortion Power

$S = V_{RMS} \cdot I_{RMS\,(total)} \quad \rightarrow$ Total Apparent Power

Improving the Power Factor implies reducing the angles $\varphi_1$and θ. Approaching φ_1 to 0 means reducing the phase lag between current and voltage. The reduction of θ leads to a beneficial decrease of the harmonic content of current.

The reduction of Power Factor is associated with operation conditions. On the one hand, the load has an impact on Power Factor because the Power Factor declines quickly when the load decreases and reaches its maximum value under full load. On the other hand, raising the line voltage on motors and transformers above the rated voltage will increase the consumption of reactive energy and negatively affect the power factor [37]. It can cause disadvantages on the correct operation of the systems of which the following factors stand out:

- Penalty for power factor below the limit;
- Extra costs associated with Reactive Energy;
- Loss in equipment efficiency;
- Loss in distribution capacity;
- Oversized transformers;
- Large size conductors.

Contrastingly, improving the power factor will add the following benefits [37]:

- Decrease utility power bills;
- Rise system capacity;
- Improve system operating features (Gain Voltage);
- Reduce line losses improving system operating characteristics.

2.4.4. BALANCED AND UNBALANCED SYSTEMS

A balanced system is defined as perfectly sinusoidal in form with the three phases equal in magnitude and separated by 120^0. It is the ideal three-phase energy provided by a distribution system and the voltage system would remain balanced if the impedances of system constituent equipment are linear as well as all loads are balanced. However, the asymmetrical three-phase equipment, the unequal system impedances, the uneven distribution of single-phase loads, the unbalanced faults and bad connections, cause an unbalanced system where different currents on each phase, or at a phase angle slightly outside 120^0 between each phase and so an unbalance 3-phase supply system. This unbalance in voltage will then affect other customers connected on the same supply network, from the PCC downwards. Figure 23 compare side by side a balance and an unbalance system [38].

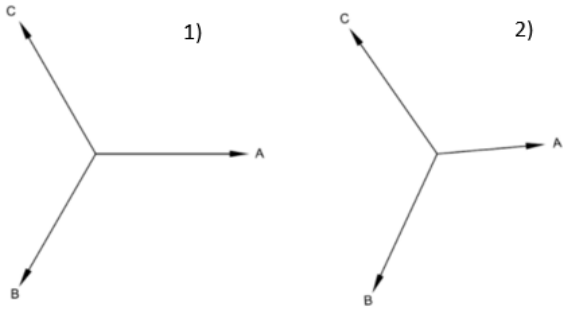

Figure 23 1) Balanced Voltage. 2) Unbalanced Voltage [39].

The voltage unbalance arising at PCC due to a combination of unbalanced three-phase loads may be evaluated by the following expression:

$$Unbalance(\%) = \frac{Max\ deviation\ from\ average\ V\ or\ I}{average\ V\ or\ I} \times 100 \qquad (26)$$

There are no negative and zero sequence voltages in a balanced system, only positive sequence components of balanced three-phase voltage exist. On the contrary, if the system is unbalanced, negative sequence components or zero sequence components or both may exist in the system.

In order to analyse unbalanced networks and system faults, the symmetrical components technique was developed [40]. This powerful tool is based on symmetrical components which are obtained by transforming a three-phase unbalanced system into two sets of balanced phasors and a set of phasors. These sets of phasors are called the positive, negative and zero sequence components [41]. Symmetrical components are a useful way of detailing network elements such as motors or generators [40].

As described in equation 27, the positive ($\vec{I}^{+}$), negative ($\vec{I}^{-}$) and zero ($\vec{I}^{0}$) current sequence components are obtained from current phase quantities $\vec{I}_A$, $\vec{I}_B$ and $\vec{I}_C$ respectively. This equation is also valid for voltage symmetrical component transformation $\vec{V}^{+}$, $\vec{V}^{-}$ and $\vec{V}^{0}$ [41].

$$\begin{bmatrix} \vec{I}^{+} \\ \vec{I}^{-} \\ \vec{I}^{0} \end{bmatrix} = \frac{1}{3} \begin{bmatrix} 1 & \alpha & \alpha^2 \\ 1 & \alpha^2 & \alpha \\ 1 & 1 & 1 \end{bmatrix} \begin{bmatrix} \vec{I}_A \\ \vec{I}_B \\ \vec{I}_C \end{bmatrix} \quad (27)$$

Where α represents the phases displacement and can be defined as $1\angle 120º$.

The zero-sequence component means an unbalance correspondent to current flow in the neutral. In turn, the negative sequence component has a reverse rotation that of the power system resulting in wide eddy currents with serious heating of the rotor. A generator is appointed a continuous negative sequence rating [42].

Power Quality Problems Caused by Nonlinear Loads

Unbalance systems has a negative effect on the right functioning of equipment given its sensitive to oscillation of current and voltage. By this reason, the most important impacts of unbalance systems on system and devices are [43]:

- Increased rms value of the supply current;
- Amplified losses;
- Reduced power factor;
- Poor utilization of distribution system;
- Heating of components;
- Derating of the distribution system;
- Disturbance to the nearby systems;
- Interference in the communication system;
- Mal operation of protection systems such as relays;
- Interference in controllers of many other types of equipment;
- Capacitor bank failure due to overload, resonance, harmonic amplification, and nuisance fuse operation;
- Excessive neutral current;
- Harmonic voltage at the neutral point.

2.4.5. NEUTRAL CURRENT

Three-phase four-wire distribution (3P4W) systems are usually used to supply a large range of loads such as adjustable speeds drives, uninterruptible power supply (UPS) and other electronic equipment. These loads produce harmonics that directly affect the power quality of the system. The harmonic orders take a significant concern for grounded-wye systems with current flowing in the neutral line of a wye configuration [44]. Essentially the triplen harmonics, odd multiples of the third harmonic (h=3, 9, 15, 21, …), have an important influence on the neutral [45].

In an ideal 3P4W system, the current in the neutral given by the sum of three-line current with a balanced sinusoidal three-phase system of currents is equal to zero. This ideal scenario is presented in Figure 24.

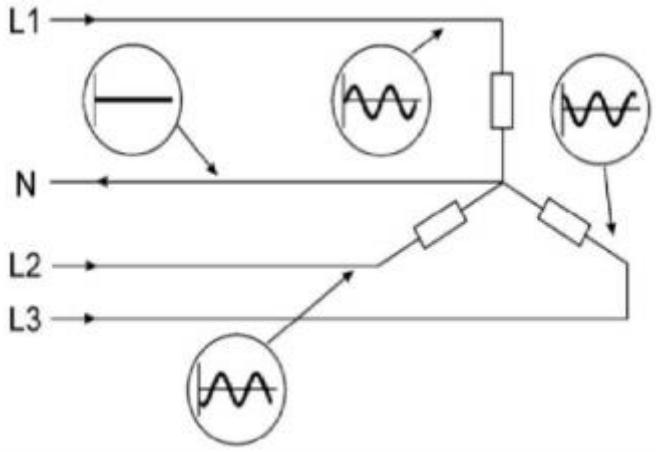

Figure 24 Balanced three-phase loads with none neutral current [45].

The introduction of linear single-phase loads on three-phase power systems induces the non-balancing of the system and consequently the appearance of currents in the neutral. With an unbalanced 3 phase load, the neutral current is not zero, but it is smaller than the phase current. Figure 25 illustrates that. Where nonlinear loads are being supplied, even when the load is well balanced across the phases, there is likely to be substantial current in the neutral conductor [46].

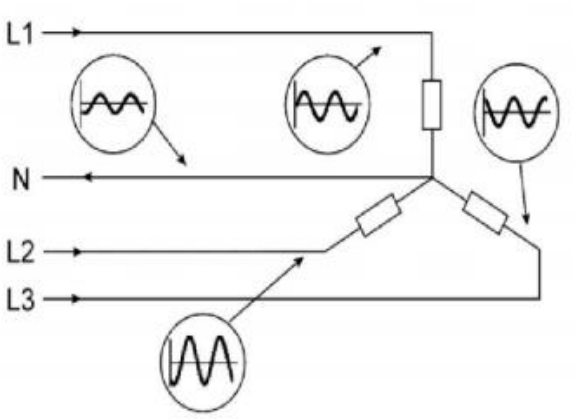

Figure 25 Unbalanced-three phase loads with neutral current [45].

With non–sinusoidal currents, the sum of the three-line currents, even with the same RMS value, may be different from zero, Figure 26 illustrates this case with a non-linear three-phase load. Due to the homopolar harmonics, the neutral current is not zero and can also be larger than the phase current [46].

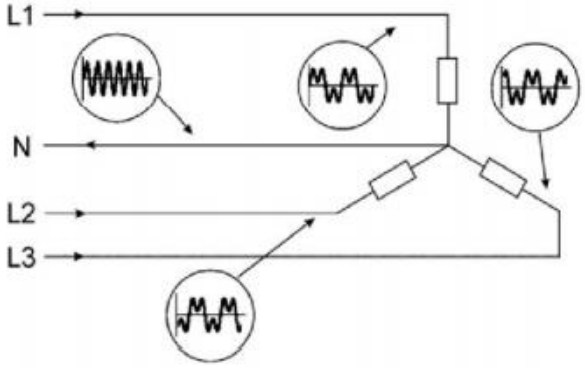

Figure 26 Non-linear three-phase system [45].

With sinusoidal load currents, the neutral current depends only on the system unbalance. When both harmonic distortion and load current unbalance are simultaneously present, the neutral current may contain all harmonics. For these reasons, the excessive neutral current creates overloading of the neutral conductor [47].

Problems of high neutral currents

The excessive current in the neutral conductor that can be present on unbalanced and non-linear loads 3P4W system origin the following anomalies [44]:

- **Overloading of distribution suppliers and transformers**

The distribution system suppliers and transformers may overload and cause additional heat loss.

- **Common mode noise**

The common mode noise induced by the voltage difference between neutral and ground can result in the malfunction of sensitive electronic equipment.

- **Wiring failure**

The course of time and the increasing of loads lead to insufficient neutral conductor size and potential of wiring failure as well as fire hazard.

Neutral Current Compensation

There are different approaches to deal with excess neutral current according to the system under analysis. Some of these approaches are described below [48]:

- **Oversizing neutral wiring**

Oversizing neutral wiring protects the neutral conductor from bursting but does not protect the transformers whereby neutral wiring should always be defined to be the same capacity as the power wiring or larger and if necessary other solutions should be taken to solve the excess neutral current.

- **Passive harmonic filters**

To deal with harmonic currents to the ground, the passive harmonic filters use capacitors, inductors, and resistors where each of which is destined to deflect harmonics of a specific

frequency. This type of filters is only used with static harmonic content not being effective in situations with fast load change.

- **Active harmonic filters**

Active harmonics filters analysed the network through power electronics detecting non-linear loads and dynamically correcting harmonic order by injecting a compensating current into the load. The high-speed process cancels high-frequency output current, while it ultimately determines the precise value of injected load current. Active harmonic filter is intended to work at levels that unceasingly adapt to rapid load variations. With its efficient operation, this type of filters is used for an extensive diversity of industrial environments.

As proposed, the present chapter provides a fundamental study of intralogistics automation systems that allows understanding the main equipment with the most significant energy impact. The energy impact is analysed through an important group of energy parameters that are presented throughout this chapter. The contextualization carried out is an important basis for the perception of the points to be monitored as well as for the acquisition methods of the desired electrical variables.

3. MONITORING OF ELECTRICAL PARAMETERS

Energy monitoring of the intralogistics systems under study requires constant measurement of electrical parameters. For the measurement of these parameters it is necessary to use dedicated equipment, so the measurement methods used as well as the quality of monitoring must be taken into account. For correct monitoring, the management of measuring equipment must also be considered. Thus, this chapter intends to clarify these concepts.

In addition, this chapter proposes a brief description of the measurement equipment to be used in this project, highlighting its main characteristics and the added value of its use in the intended energy monitoring. In order to accomplish the proposed monitoring, it is necessary to integrate the monitoring equipment on the intralogistic systems under study.

3.1. MEASUREMENT METHODS

When we want to know the value of a quantity, defined in the metrology field as a measurable physical quantity, it is necessary to carry out a set of operations. The logical sequence of such operations is called measurement methods. Typically, in the electrical engineering field, measurement methods are classified into indirect and direct [49]:

- **Indirect measurement method**: Method whereby the value of the measured quantity is obtained by measuring other associated quantities. An example of this method is an indirect determination of power based on voltage and current measurement ($P = U.I$).
- **Direct measurement method**: Method in which the value of the measured quantity is obtained immediately as a result of the measurement. This method is employed, for example, when using a Wattmeter for direct power measurement.

Direct measurement methods may also include comparison measurement methods. In this variant, the measured quantity is compared with one or more quantities of the same nature that have a known value, for example, the measurement of resistances using the current comparison method.

Once any measurement is affected by error and in order to identify the relationship between the obtained value and the actual value of a measurement, it is essential to introduce concepts associated with measurement quality such as error, uncertainty, accuracy and significant figures.

True Quantity Value

According to the International Vocabulary of Metrology (VIM) a true quantity Value consists of the meaning of a quantity. Since any measurement is affected by error, a true quantity value is deemed unique and unknowable [50].

Conventional Quantity Value

A conventional quantity value is defined as a quantity value assigned by agreement to a quantity for a given purpose [50]. It is usually assumed as an estimated true value obtained through a reference instrument.

Measurement Accuracy

The accuracy of a given quantity represents an approximation between the measurement result and the true value of the measured quantity [50].

The measurement accuracy is a qualitative concept, so it can only be concluded that one measurement is more accurate than another based on the used equipment characteristics. The smaller the measurement error, the more accurate the measurement is.

Measurement Uncertainty

The measurement uncertainty describes the dispersion of the quantity values being attributed to a measurand [50]. The uncertainty indicates the highest limits, upper and

lower, associated with a quantity measuring. Since it is impossible to know the sign of such errors, uncertainty is always indicated as "±" [49].

When associated with an instrument, the VIM defines measurement uncertainty as: "Component of measurement uncertainty from the instrument measuring used." [50].

Generally, it is possible to know the instrument measurement uncertainty resorting to the specifications given by the manufacturer in the instrument manual. In this way, the upper and lower limits are displayed within which the true value of the measured quantity must lie.

Considering x_m the measured value of the quantity X and δ_m the measure uncertainty:

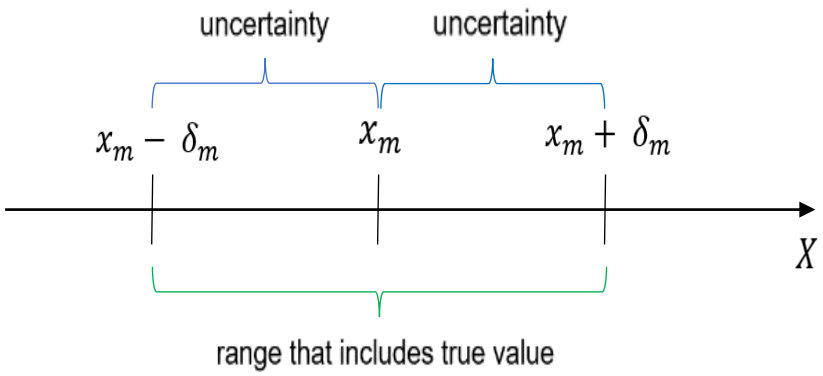

For any measurement, it is important to identify the error sources in order to consider the measurement validity as well as to mitigate the error causes whenever possible. The main uncertainty sources are:

- Measuring instrument;
- Instrument calibration standard;
- Operator performing the measurement;
- Measurement method;
- Environmental conditions (temperature, humidity, electromagnetic interference, etc)

Measurement Errors

The measurement errors refer to the difference between the measured quantity value and the reference quantity value [50]. The errors occurrence, mainly introduced by the uncertainty sources described in the previous topic, are grouped into three categories:

- **Systematic errors**: Part of measurement error that keeps constant in replicate measurements or change in an expected way (International Vocabulary of metrology). The errors normally associated with instrument faults, inconsistencies in the measurement method or environmental conditions.
- **Random errors**: Element of measurement error that keeps uncertain in repeated measurements (International Vocabulary of metrology).
- **Coarse errors**: Although not featured in the International Vocabulary of metrology, this component of measurement errors is commonly defined as errors resulting from the incorrect use of measuring instruments or incorrect results recording.

Significant Figures

When analysing, recording and calculating values associated with a measurement, it is essential to have a knowledge of significant figures. Thus, three rules are presented to consider in addition, subtraction, multiplication, division and taking roots operations [49]:

1^{st} Rule – Figures to Preserve (Addition and Subtraction)

In the result of an addition or subtraction, the figures must be preserved until the first doubtful position. As a rule, if all figures are significant, the figures to the right of the doubtful position must be disposed [49].

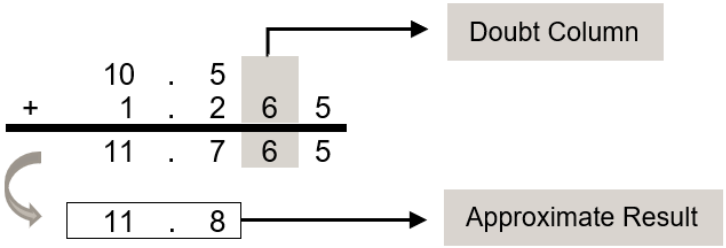

If the calculation involves an exact integer, all significant figures are taken into account.

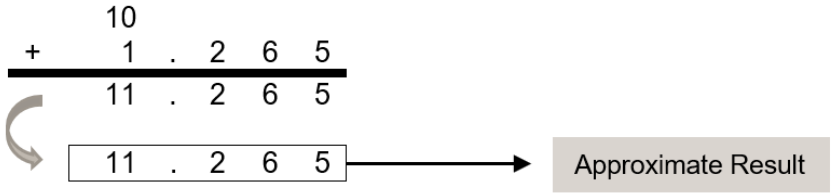

2^{nd} Rule – Figures to Preserve (multiplication, division and taking roots)

In multiplication, division and taking roots, the number of significant figures to be retained must be equal to the value with the lowest number of significant figures [49].

Multiplication:

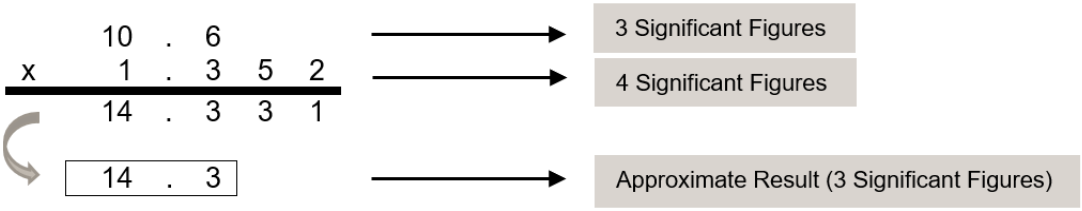

Division:

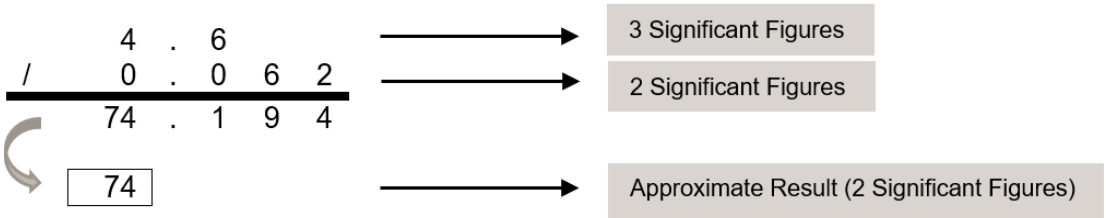

Taking roots:

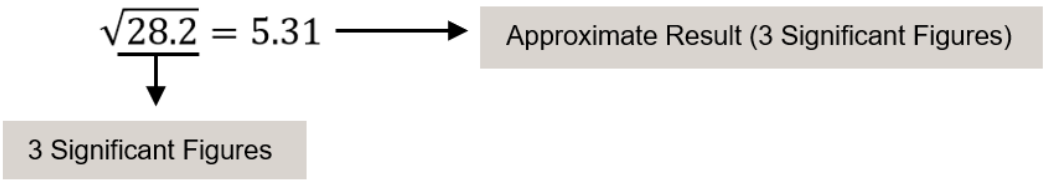

3^{rd} Rule – Rounding results

The rounding results contemplate significant figures take into account that [49]:

- If the leftmost non-significant figure is less than 5 then it does not change the last significant figure.

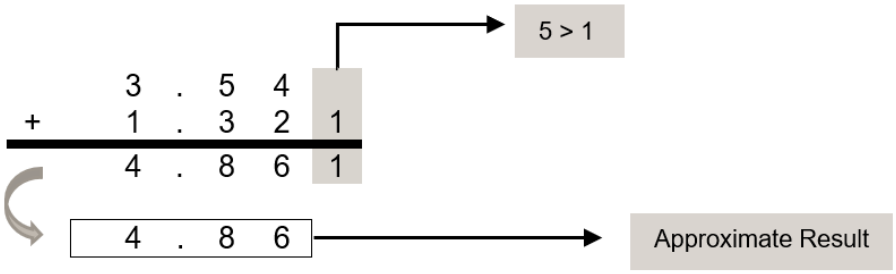

- If the leftmost non-significant figure is higher than 5 then it does not change the last significant figure.

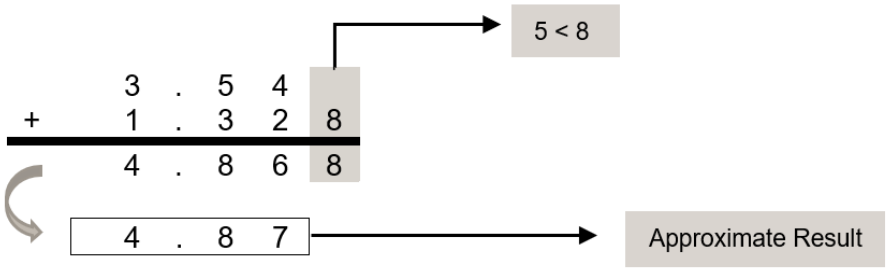

Uncertainty Determination

- **Direct Measurement**

Considering a quantity X directly measured where:

x_T represents its true value;

x_T^* represents its conventional value;

x_m represents its measured value.

Absolute error (δ_x) is described as [51]:

$$\delta_x = | x_m - x_T^* | \quad (28)$$

In turn, the relative error ($\mathcal{E}_x$) is obtained by the equation [51]:

$$\mathcal{E}_x = \left| \frac{\delta_x}{x_T^*} \right| = \left| \frac{x_m - x_T^*}{x_T^*} \right| \quad (29)$$

- **Indirect Measurement**

Whereas the quantity X is achieved using other quantities (y_i), $X = f(y_1, y_2, \dots, y_n)$, to which are associated absolute errors from measurement, $\delta_{y_1}, \delta_{y_2}, \dots, \delta_{y_n}$, it is inferred that these errors will correspond to an absolute error in the measurement of X expressed by [51]:

$$\delta_x = f\left(y_1 + \delta_{y_1}, y_2 + \delta_{y_2}, \dots, y_n + \delta_{y_n}\right) - f(y_1, y_2, \dots, y_n) \quad (30)$$

Developing the function f in Taylor Polynomial, at the point $Y_i + \partial_i$, it is obtained [51]:

$$f\left(y_1 + \delta_{y_1}, y_2 + \delta_{y_2}, \dots, y_n + \delta_{y_n}\right) = f(y_1, y_2, \dots, y_n) + \left(\delta_{y_1}\frac{\partial f}{\partial y_1} + \delta_{y_2}\frac{\partial f}{\partial y_2} + \cdots + \delta_{y_1}\frac{\partial f}{\partial y_n}\right) + \frac{1}{2!}\left(\partial_{y_1}^2\frac{\partial^2 f}{\partial y_1^2} + \partial_{y_2}^2\frac{\partial^2 f}{\partial y_2^2} + \cdots + \partial_{y_n}^2\frac{\partial^2 f}{\partial y_n^2}\right) + \cdots$$

Moving $f(y_1, y_2, \dots, y_n)$ to the left side of the equality,

$$f\left(y_1 + \delta_{y_1}, y_2 + \delta_{y_2}, \dots, y_n + \delta_{y_n}\right) - f(y_1, y_2, \dots, y_n) = \boldsymbol{\delta_x} = \left(\delta_{y_1}\frac{\partial f}{\partial y_1} + \delta_{y_2}\frac{\partial f}{\partial y_2} + \cdots + \delta_{y_1}\frac{\partial f}{\partial y_n}\right) + \frac{1}{2!}\left(\partial_{y_1}^2\frac{\partial^2 f}{\partial y_1^2} + \partial_{y_2}^2\frac{\partial^2 f}{\partial y_2^2} + \cdots + \partial_{y_n}^2\frac{\partial^2 f}{\partial y_n^2}\right) + \cdots$$

Despising the terms of a higher order than the first,

$$\delta_x \approx \sum_{i=1}^{n} \delta_{y_1}\frac{\partial f}{\partial y_i} \quad (31)$$

Bearing in mind that δ_{yi} are the upper error bounds in y_i and that the elements from the addition can be positive or negative, the absolute error of an indirect measurement is expressed as follows [51]:

$$\delta_x \leq \sum_{i=1}^{n} \delta_{y_1} \left|\frac{\partial f}{\partial y_i}\right| \tag{32}$$

The relative error in X derives from the previous expression, since [51]:

$$\varepsilon_x = \left|\frac{\delta_x}{x}\right| = \left|\frac{\delta_x}{f(y_i)}\right| \leq \sum_{i=1}^{n} \left|\frac{\partial f}{\partial y_i}\frac{\delta_{y_i}}{f}\right| = \sum_{i=1}^{n} \left|\frac{\partial f}{\partial y_i}\frac{\delta_{y_i}}{y_i}\frac{y_i}{f}\right|$$

ε_{y_i}

Then:

$$\varepsilon_x \leq \sum_{i=1}^{n} \left|\frac{\partial f}{\partial y_i}\frac{\delta_{y_i}}{f}\right| \varepsilon_{y_i} \tag{33}$$

Application examples of absolute and relative errors in multiplication, division, addition, and subtraction [51]:

- Multiplication

$$P = U \cdot I \longrightarrow \begin{cases} \delta_P \leq |I| \cdot \delta_U + |U| \cdot \delta_I \\ \varepsilon_P \leq \left|I \cdot \frac{U}{U \cdot I}\right| \cdot \varepsilon_U + \left|U \cdot \frac{I}{U \cdot I}\right| \cdot \varepsilon_I = \varepsilon_U + \varepsilon_I \end{cases}$$

- Division

$$R = \frac{U}{I} \longrightarrow \begin{cases} \delta_R \leq \left|\frac{1}{I}\right| \cdot \delta_U + \left|\frac{-U}{I^2}\right| \cdot \delta_I \\ \varepsilon_R \leq \left|\frac{1}{I} \cdot \frac{U}{U/I}\right| \cdot \varepsilon_U + \left|\frac{-U}{I^2} \cdot \frac{I}{U/I}\right| \cdot \varepsilon_I = \varepsilon_U + \varepsilon_I \end{cases}$$

- Addition

$$U = U_1 + U_2 \longrightarrow \begin{cases} \delta_U \leq \delta_{U_1} + \delta_{U_2} \\ \varepsilon_P \leq \left|\frac{U_1}{U_1+U_2}\right| \cdot \varepsilon_{U_1} + \left|\frac{U_2}{U_1+U_2}\right| \cdot \varepsilon_{U_2} \end{cases}$$

- Subtraction

$$U = U_1 - U_2 \longrightarrow \begin{cases} \delta_U \leq \delta_{U_1} + \delta_{U_2} \\ \varepsilon_P \leq \left|\frac{U_1}{U_1-U_2}\right| \cdot \varepsilon_{U_1} + \left|\frac{-U_2}{U_1-U_2}\right| \cdot \varepsilon_{U_2} \end{cases}$$

It is equally important to approach the quality of measurement operations. This matter aims at adapting metrological resources to the company's needs, the correct functioning of measuring instruments and the connection of their measurements to national standards. Only in this way will the company be able to guarantee the quality of measurements.

Measuring instruments management

The measuring instruments management contemplates the necessary actions to guarantee and preserve the range of measuring instruments that meet the company's needs. The measuring instruments management includes the following points [52]:

- Requirement analysis and measuring instruments selection;
- Instrument reception, calibration, or verification and respective decisions;
- Putting into service and monitoring operation.

Requirement analysis and measuring instruments selection

Technical requirements, economic and commercial conditions, and previous evaluations are predominant factors to support the choice of a particular measuring instrument [52].

- **Technical Requirements**: It is important to adapt the instrument characteristics and precision class to the demanded requirements as well as the limitations of putting into service and use. The homogeneity of the company's instrument fleet and the evolution of the measuring instrument must also be considered so that the measuring instruments have identical behaviour and do not become obsolete. In

the case of a specific or complex measuring instrument, it is advisable to create a technical specification that includes the required characteristics, reception, usage, environment and maintenance conditions, calibration and verification requirements.

- **Economic and Commercial Conditions**: This topic deals with purchase options, price, delivery period, warranties, and maintenance or technical assistance contract.

- **Previous Evaluations**: The knowledge acquired with the equipment used is a factor that impacts the choice of new identical equipment.

Instrument reception, calibration or verification and respective decisions

Upon instrument reception, the order must be checked for compliance. If the order is compliant, the equipment must be identified and inventoried.

Before putting the equipment into operation, it must be calibrated or checked. Calibration and verification are essential for validating the indications provided by the measuring instruments. The result of calibration is based on comparing the values obtained by the measuring instrument with the values specified by the standard. In turn, the result of verification defines whether the measuring instrument falls within the regulated error limits that authorized the entry into or continuation of the equipment's operation.

Regardless of the measurement instrument, there must be a periodic and systematic calibration process that allows preventing any degradation in the measurement's quality ensuring their credibility over time.

In order to establish the calibrations, different factors must be taken into account, such as frequency, type of use, expected deviations, calibration uncertainty, wear, economic restrictions, and the nature of the equipment. In the case of verifications, the periodicity is imposed by the metrological control regulations [52].

Putting into service and monitoring operation

After validating the previous topics, proceed to the installation of the measuring instrument, taking care that the installation requirements comply with the defined by the manufacturer. At this phase, the conditions of operation, safety, accessibility and equipment used must also be verified.

During operation, the equipment must operate correctly in order to effectively perform the function for which it is intended. The protection of people and material goods, the qualification of operators and the environmental conditions are essential aspects for the correct use of the measuring instrument [52].

3.2. MEASURING INSTRUMENT

As this project aims to monitor different intralogistics systems with different characteristics and needs, the use of a mobile and versatile instrument with memory capacity allows the collection and analysis of the most important variables of each system. Thus, to carry out the measurements included in the project, the MI 2892 Power Master instrument developed by METREL will be used. Although the equipment has already been purchased by the host company, it has rarely been used, so its use and exploitation in this project is an asset.

The Mi 2892 Power Master is a hand-held power quality analyzer with a user-friendly interface that includes a quick set button and an extensive easy-to-read graphical colour display, as presented in Figure 27, providing a faster data overview for energy analyzing.

Based on equipment characteristics it is important to highlight the following measuring functions and key features [53]:

- 4 voltage channels with support for medium and high voltage systems;
- 4 current channels with support for automatic clamp identification and range selection;
- Power measurements compliant with IEEE 1459;

- Harmonic analysis up to 50th harmonics, THD and TDD measurement;
- Power supply events caption and record;
- Power factor;
- Active, reactive, generated and consumed energy;
- Waveform/inrush displaying, snapshot and recording;
- Power quality analysis according to EN 50160 and IEEE 519;
- Compliance with power quality standard IEC 61000-4-30 Class A;
- Temperature measurement;
- Adjustable alarms;
- Support for microSD memory card up to 32 GB;
- Intuitive navigation and configuration.

Figure 27 Measuring instrument Mi 2892 Power Master [53].

One of the great advantages of the Mi 2892 Power Master is the diversity of records that the equipment offers. In the General Recorder option, recorder specifications can be customized in order to define interval acquisition, start time and duration for the recording

test and activate events or alarms register. In this recording mode, current and voltage values are RMS values obtained based on the defined acquisition interval. Events are associated with swells, dips and voltage interruptions. Its thresholds can be defined in the event setup table. When the thresholds are overtaken, a new register starts with the acquisition of the RMS voltage value every 10 ms. In turn, an alarm can be seen as an event on arbitrary quantity. Alarms are available for voltage, current, frequency, active, nonactive and apparent power, harmonics and interharmonics, unbalance, flickers and signalling. For each alarm is defined the quantity, the phase, the trigger slope, the threshold value and the minimum duration. When the defined phase crosses the threshold value according to the defined trigger slope for a minimum duration value, the voltage and current waveforms are recorded during a time interval of 200 ms. For both events and alarms, their occurrence is logged in a table form.

3.3. SOLUTION INTEGRATION IN INTRALOGISTICS SYSTEMS

The intralogistics systems to be monitored have different connection configurations with different cable sections and current ranges. Furthermore, it is pretended that the monitorizations have minimal impact on the normal system functioning. Thus, the monitoring to be carried out requires the use of flexible structure ammeter clamps, capable of different current ranges and adaptable to three-phase systems with and without neutral.

The A1227 Flexible Current Clamps developed by METREL meet the required needs, as they are flexible clamps capable of embracing the cables and configurable according to three current ranges 30A, 300A and 3000A. These ammeter clamps can be connected directly to the monitoring instrument, in this case the Mi 2982 Power Master, and the instrument will have the function of powering them. At reference conditions, the A1227 has an accuracy of +/- 1%, linearity of +/- 0,2% and noise of 0,12A, 0,3A and 3A for the 30A, 300A and 3000A current ranges respectively. Reference conditions include a frequency between 45 Hz and 65 Hz, temperature from 15 °C to 25 °C. Figure 28 illustrates the correct application of the clamp around a conductor considering the current direction [54].

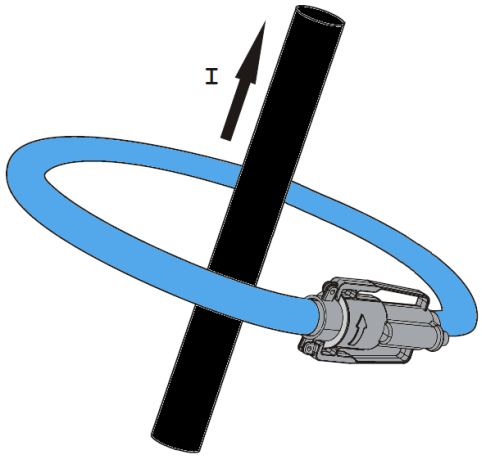

Figure 28 A1227 Flexible Current Clamp [54].

3.4. DATA PROCESSING

Although the measuring instrument has real-time data storage, analysis and presentation capacity, it can be complemented with PowerView 3.0 software. PowerView 3.0 is an integral part of the measurement system and is a strong tool for downloading, analyzing and printing recorded data for Metrel's Power Quality Analyzers such as the Mi 2892 Power Master. The software allows the simultaneous presentation of multiple data records and their respective correlation. It is also capable of real-time scope and instrument remote access over the internet connection. With PowerView 3.0, the user can generate graphs and tables for analysis as well as export or copy data to other applications in order to carry out more detailed analysis [55]. For this project, as a complement, the Microsoft Excel tool will be used.

As intended, this chapter initiates with the introduction of measurement methods including the clarification of concepts associated with measurement quality, which focus true and conventional quantity values, measurement errors, accuracy, uncertainty and significant figures. Regarding measuring equipment, this chapter highlights the actions necessary to guarantee and preserve the measuring equipment. The present chapter also introduces the monitoring solution to be used in the project, the Metrel Mi 2892 Power Master. In order to minimize the impact on the normal system operation, the integration of this solution in intralogistic systems relies on the use of flexible current clamps A1227. At a higher level, the collected data can be processed and analysed using the software PowerView 3.0 presented at the end of the chapter.

4. MEASURING PROCESS

Considered as an intermediate stage between the choice of monitoring equipment and the monitoring to be performed, this chapter assumes as essential since it intends to validate the selected equipment and define the monitoring points according to the characteristics of each intralogistic system under study.

4.1. EQUIPMENT VALIDATION

The first step after receiving the monitoring equipment was to validate the equipment compliance. Physically, the Metrel MI 2892 and the respective A1227 current clamps were in an excellent state of conservation. On a functional level, all keys, display, power supply and communication ports were operational. Additionally, the correct recording of data on the memory card and the detection of current clamps by the monitoring equipment were validated.

With regard to current clamps, in addition to their physical compliance, the calibration certificates were also verified. The last certificate of 2018, as shown in annex 1, indicates that the current clamps obtained a positive result in the calibration performed. Since the last record is already beyond the recommended period of twelve months, a new calibration has been requested. According to the certificate of this new calibration, contained in annex 2, carried out in August of the present year, the compliance of the monitoring equipment and the respective current clamps for the three measurement ranges is validated.

4.2. TEST REGISTER

Given the number of tests to be carried out and the vast number of data to be collected, the Python application "Test Register" was developed. The Test Register is intended to assist in the registration of all tests performed. For each register, generic information is requested, such as equipment to be monitored, measuring instrument, connection and frequency. Then, important characteristics of each movement are requested, including a description of the load, type of movement, number of repetitions, detected anomalies and possible notes. After filling in the requested information, the application allows the user to make a temporal register of the test to be performed. To start the time recording, the user should press the “Start Test” button. At that moment the time and date are recorded. In addition to the test start time, the user can record the start and end times of the movement under test. To do so, the user should press the “Start Mov” and “Finish Mov” keys respectively. By pressing the “Finish Test” key, the user ends the test. At that moment, the requested inputs are recorded in an Excel database, followed by a cleaning of variables, enabling the user to start a new test. The code snippet responsible for executing these tasks is shown in Figure 29.

```
    df2 = pd.DataFrame({"Start Test":SeriesSSS,"Start Mov
Time":SeriesTSS, "Finish Mov Time":SeriesTFF, "Finish
Test":SeriesFFF, "Equipment":SeriesAA, "Measuring
Instrument":SeriesBB, "Connection":SeriesCC,
"Frequency":SeriesDD, "Load":SeriesEE, "Type":SeriesFF,
"Repetitions":SeriesGG, "Anomalies":SeriesHH, "Notes":SeriesII})
    df2.to_excel(path,index=False)
    entry1.delete(0,END)
    entry2.delete(0,END)
    entry3.delete(0,END)
    entry4.delete(0,END)
    entry5.delete(0,END)
    entry6.delete(0,END)
    entry7.delete(0,END)
    entry8.delete(0,END)
    entry9.delete(0,END)
```

Figure 29 Sending test data to excel database and cleaning inputs.

During the test, the user can choose to quit the registration using the “Quit” key. The program logic described throughout this paragraph is summarized in the block diagram in appendix A. Moreover, Figure 30 presents a graphical representation of the input data in the application and the respective data registered in the database.

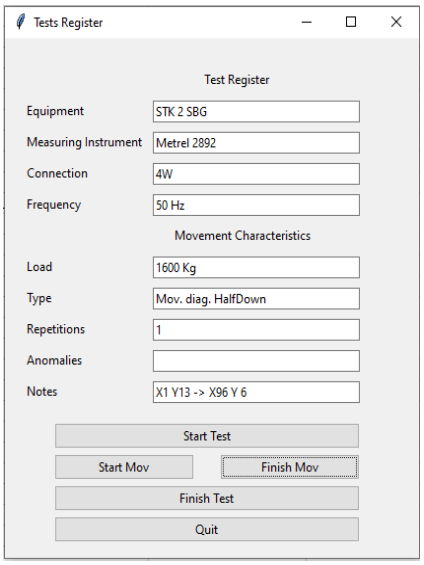

Start Test	Start Mov Time	Finish Mov Time	Finish Test	Equipment	Measuring Instrument	Connection	Frequency	Load	Type	Repetitions	Anomalies	Notes
2021-06-08 15:10:24	2021-06-08 15:10:24	2021-06-08 15:11:04	2021-06-08 15:23:29	STK 2 SBG	Metrel 2892	4W	50 Hz	none	mov. X	1		X1 Y1 -> X96 Y1
2021-06-08 15:11:32	2021-06-08 15:11:32	2021-06-08 15:12:09	2021-06-08 15:23:29	STK 2 SBG	Metrel 2892	4W	50 Hz	none	mov. Y Up	1		Y1 -> Y13
2021-06-08 15:12:28	2021-06-08 15:12:28	2021-06-08 15:13:07	2021-06-08 15:23:29	STK 2 SBG	Metrel 2892	4W	50 Hz	none	mov. diag. Down	1		X96 Y13 -> X1 Y1
2021-06-08 15:13:29	2021-06-08 15:13:29	2021-06-08 15:14:08	2021-06-08 15:23:29	STK 2 SBG	Metrel 2892	4W	50 Hz	none	mov. diag. Up	1		X1 Y1 -> X96 Y13
2021-06-08 15:14:27	2021-06-08 15:14:27	2021-06-08 15:15:04	2021-06-08 15:23:29	STK 2 SBG	Metrel 2892	4W	50 Hz	none	mov. Y Down	1		Y13 -> Y1
2021-06-08 15:16:11	2021-06-08 15:16:11	2021-06-08 15:16:48	2021-06-08 15:23:29	STK 2 SBG	Metrel 2892	4W	50 Hz	none	mov. Y Up	1		Y1 -> Y13
2021-06-08 15:17:00	2021-06-08 15:17:00	2021-06-08 15:17:39	2021-06-08 15:23:29	STK 2 SBG	Metrel 2892	4W	50 Hz	none	mov. diag. Down	1		X1 Y13 -> X96 Y1
2021-06-08 15:19:13	2021-06-08 15:19:13	2021-06-08 15:19:50	2021-06-08 15:23:29	STK 2 SBG	Metrel 2892	4W	50 Hz	none	mov. Y Up	1		Y1 -> Y13
2021-06-08 15:20:14	2021-06-08 15:20:14	2021-06-08 15:20:53	2021-06-08 15:23:29	STK 2 SBG	Metrel 2892	4W	50 Hz	none	mov. diag. Down	1		X96 Y13 -> X1 Y1
2021-06-08 15:28:49	2021-06-08 15:28:49	2021-06-08 15:29:28	2021-06-08 15:35:22	STK 2 SBG	Metrel 2892	4W	50 Hz	1600 kg	mov. X	1		X1 Y1 -> X96 Y1
2021-06-08 15:30:27	2021-06-08 15:30:27	2021-06-08 15:31:06	2021-06-08 15:35:22	STK 2 SBG	Metrel 2892	4W	50 Hz	1600 kg	mov. diag. Down	1		X96 Y13 -> X1 Y1
2021-06-08 15:31:13	2021-06-08 15:31:13	2021-06-08 15:31:54	2021-06-08 15:35:22	STK 2 SBG	Metrel 2892	4W	50 Hz	1600 kg	mov. diag. Up	1		X1 Y1 -> X96 Y13
2021-06-08 15:32:08	2021-06-08 15:32:08	2021-06-08 15:32:46	2021-06-08 15:35:22	STK 2 SBG	Metrel 2892	4W	50 Hz	1600 kg	mov. Y Down	1		Y13 -> Y1
2021-06-08 15:32:54	2021-06-08 15:32:54	2021-06-08 15:33:32	2021-06-08 15:35:22	STK 2 SBG	Metrel 2892	4W	50 Hz	1600 kg	mov. Y Up	1		Y1 -> Y13
2021-06-08 15:34:41	2021-06-08 15:34:41	2021-06-08 15:35:20	2021-06-08 15:35:22	STK 2 SBG	Metrel 2892	4W	50 Hz	1600 kg	mov. diag. Half Down	1		X1 Y13 -> X96 Y6

Figure 30 Test Register inputs and excel database.

4.3. MONITORING POINTS

For all systems under analysis: stacker crane, conveyors circuit and RGV system, the chosen monitoring point refers to the system's power supply point from the installation's electrical network. Before the introduction of the monitoring equipment, a previous analysis of the electrical diagram of each chosen point was carried out. Based on the analysis carried out, it was concluded that the monitoring equipment is capable of monitoring the currents and voltages at each point. It was also verified that physically the introduction of monitoring equipment into the system would not imply any intervention with a significant impact on its normal functioning.

Given the specificity of the systems in question for each point, different monitoring configurations are necessary. The purpose of this subchapter is to clarify the monitoring points used for each system.

4.3.1. STACKER CRANE

The stacker crane is fed through a four-wire configuration that includes three phases and neutral. To these lines, the grounding line is added. Beyond the system feed configuration, the use of a thermomagnetic circuit breaker for nominal currents of 250 A, designated in figure 31 as +CAB-Q7, to which a differential protection block is coupled, stands out.

The circuit breaker trip curve can be adjusted in order to set the thermal and magnetic protections. The thermal and magnetic adjustment dials are on the front of the trip unit. For this system, the thermal protection pickup, Ir, is regulated to 160 A whereas the magnetic protection pickup, Im, is adjusted to 1250 A. In turn, the differential current is defined to 300 mA.

Considering the characteristics of the system, to monitor the phase voltages, a claw with direct connection to the voltage inputs of the monitoring equipment must be connected to each circuit-breaker pole. The Metrel has five voltage inputs which also include neutral and earth connections. In turn, the reading of currents is not carried out directly, requiring the

use of A1227 current clamps responsible for measuring the currents per phase and sending this information to the respective current input of the monitoring equipment. The Metrel Mi 2892 allows the reading of four currents simultaneously so that phase currents and neutral current can be monitored. Figure 31 is intended to convey a visual notion of monitoring equipment integration in the system based on its electrical diagram.

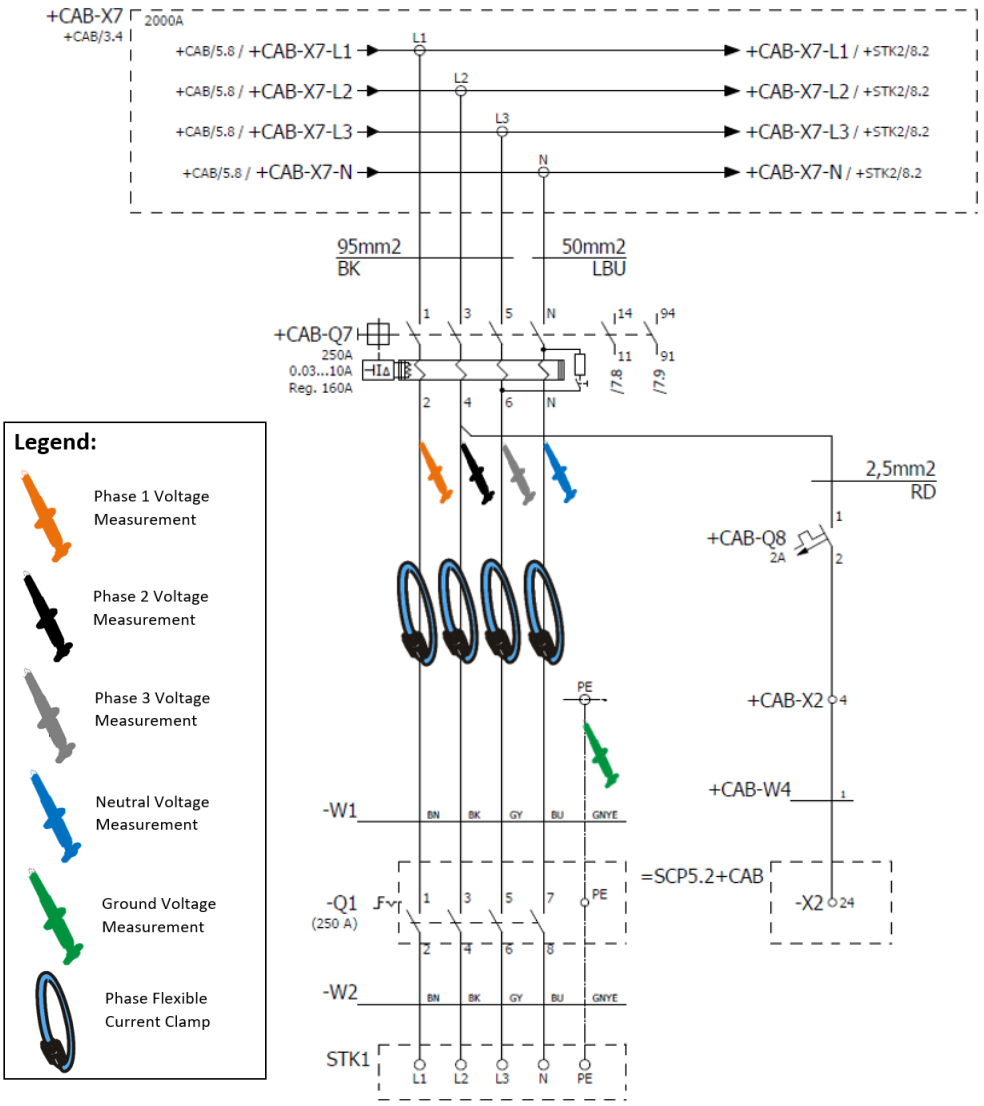

Figure 31 STK Monitoring Point.

4.3.2. CONVEYORS

The analysed conveyors circuit highlighted in Figure 32, is inserted at the intersection point of three pallet entries. The first conveyor in this area is a linear movement conveyor responsible for forwarding the pallets from two entry points. Then, the second conveyor includes a rotating platform because it can receive pallets from the aforementioned conveyor and an entry point. The third conveyor included in the monitored area is a linear conveyor with the function of forwarding the pallets of the previous conveyor to the next decision point. This conveyors circuit was strategically selected as it is a critical area for pallet entry into the system. A long downtime in this area means that it is not possible to introduce new pallets, which affects the entire system.

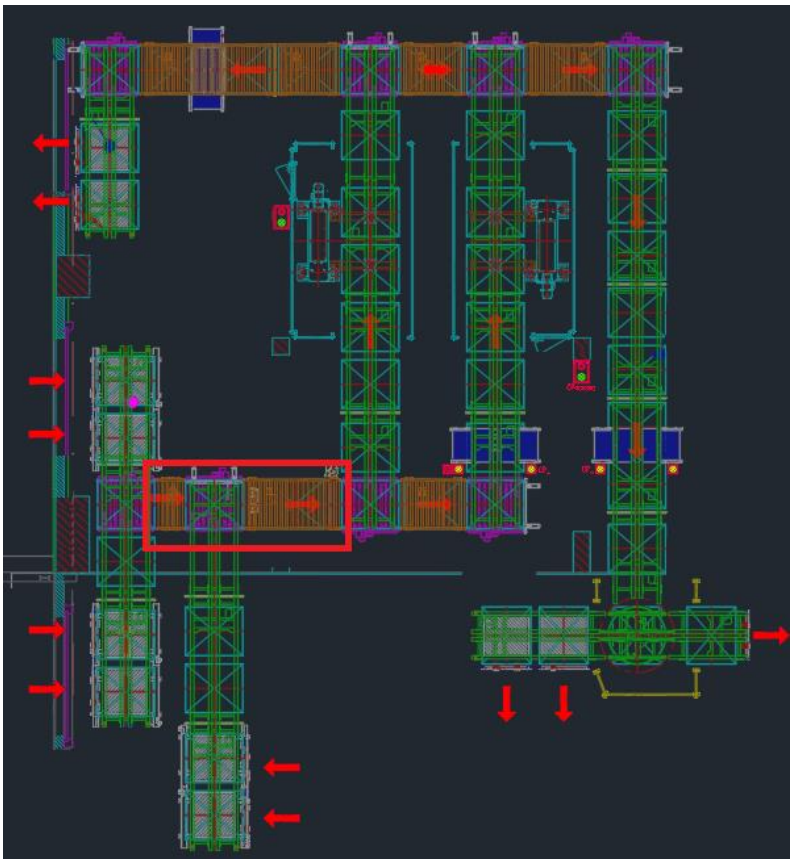

Figure 32 Selected Conveyors Circuit.

The conveyor feed is based on a branched system in which the mains feed is routed to a circuit breaker. Then, at the circuit breaker output, the circuit is branched in order to supply different conveyors circuits. The system under analysis has the particularity that each conveyor area is made up of a small group of conveyors, that is, as a rule, each conveyor is not fed individually. Based on the electrical diagram of the system present in figure 32, the connection point to the network is carried out by the -Q15 circuit breaker, which in turn supplies three conveyor areas. The conveyors circuit to be analysed includes a magnetothermal circuit breaker for 16 A rated currents to which a 300 mA differential block is coupled. No breaker parameters are adjustable. The area described is a pallet entry area consisting of three conveyors in series.

Given the characteristics of the point to be monitored, a claw with direct connection to the three-phase voltage inputs of the monitoring equipment must be coupled to each circuit-breaker pole. Grounding must also be included. For indirect reading of currents, each phase cable must be embraced by a flexible current clamp A1227. Each current clamp is connected to the respective phase current input of the monitoring equipment. The addition of monitoring equipment is visually clarified in Figure 33 based on the electrical system schematic

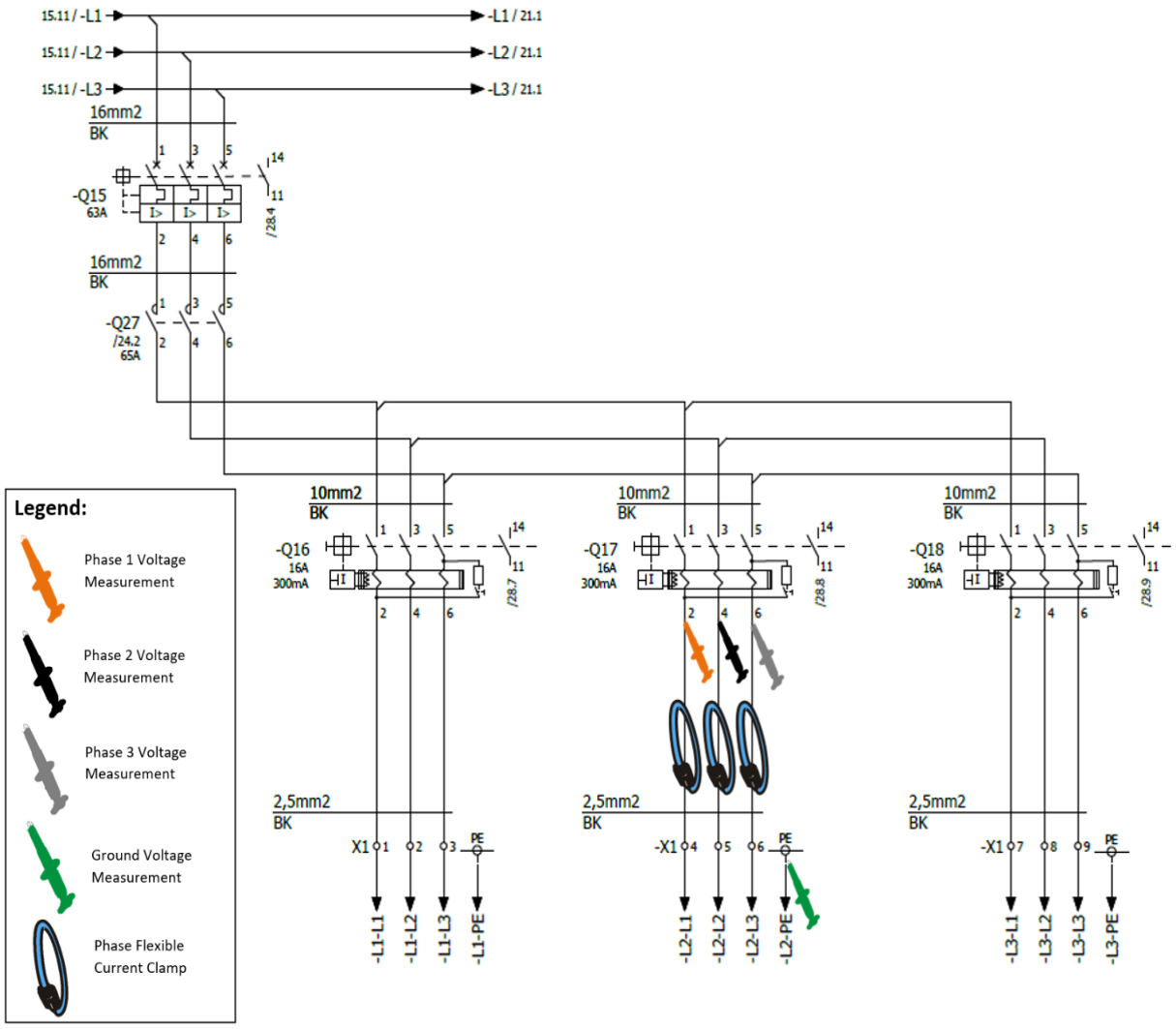

Figure 33 Conveyors Monitoring Point.

4.3.3. RGV SYSTEM

Given the length of the RGV loop and the 31 vehicles inserted in it, the system is divided into three zones with independent feeds. Circuit breakers Q38, Q39 and Q40 present in Figure 34 are responsible for supplying zone one, two and three. The three circuit breakers listed have upstream a main circuit breaker, Q37, responsible for making the connection point between the RGV system and the installation's electrical network. The main circuit breaker dimensioned for rated currents of 200 A has the particularity of being the only circuit breaker in the system to which a regulated differential block for currents up to 3 A

is associated. In a first approach, the desired monitoring point concerns the output of the Q37 circuit breaker, making it possible to analyze the energy dynamics of the entire system.

If relevant, each zone can be monitored. Since there is only one monitoring equipment available and given its limited number of voltage and current inputs, it is not possible to monitor more than one zone at the same time. For the defined monitoring, three claws responsible for transmitting the voltage signal to the monitoring equipment inputs must be added to the poles of the Q37 circuit-breaker. In turn, to monitor the currents of each phase, each cable must be surrounded with a current clamp A1227.

Figure 34 shows the electrical diagram of the point to be monitored, to which a graphical representation of the elements necessary for monitoring has been added.

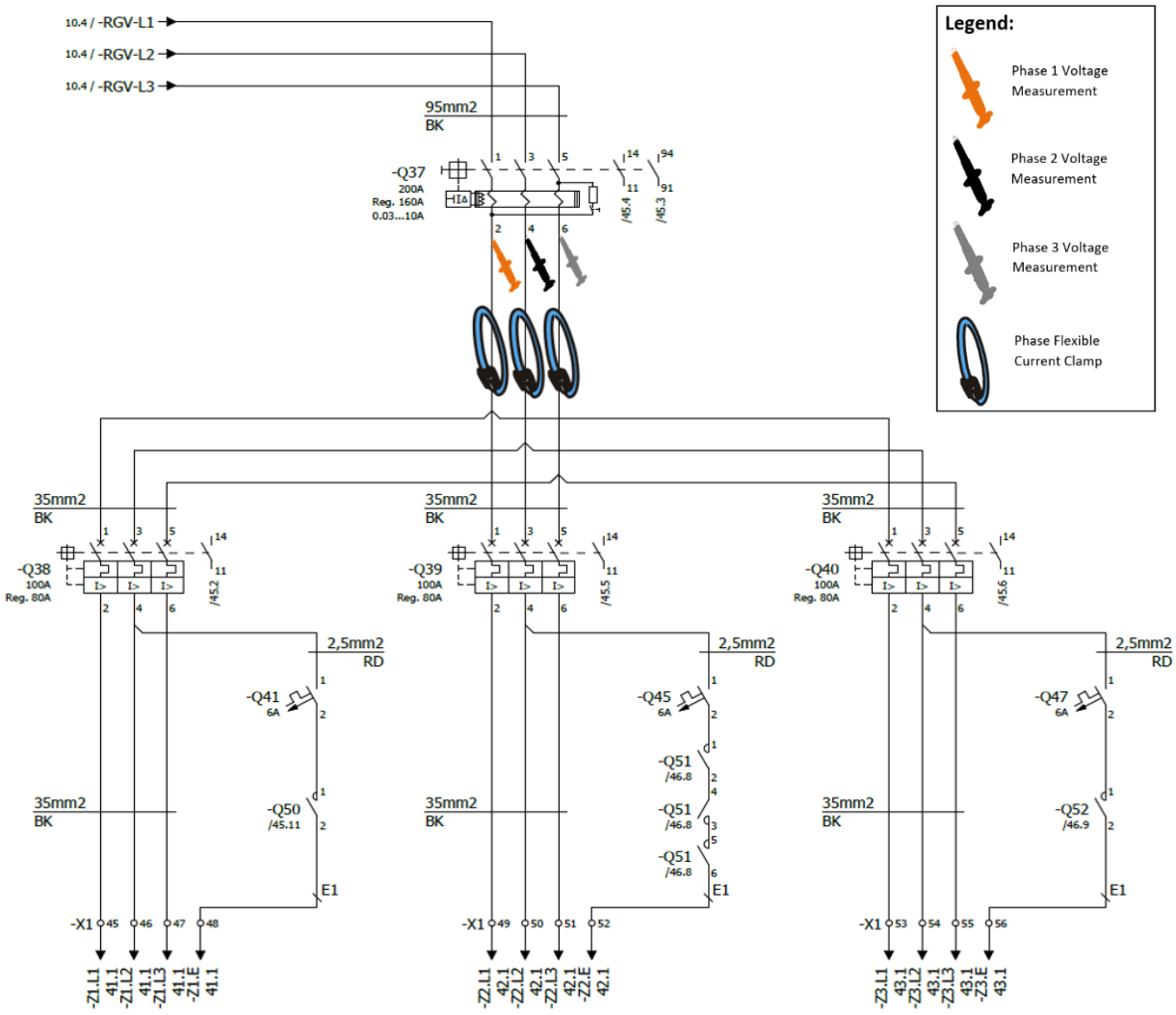

Figure 34 RGV System Monitoring Point.

The fourth chapter starts with a physical and operational validation of the monitoring equipment, highlighting the validation of the equipment's compliance and the respective current clamps. The application developed for the project is also introduced in order to help record the tests performed. Finally, after an electrical analysis of each of the systems under study, the point to be monitored in each system is presented, which includes a graphical representation of the introduction of the monitoring equipment in the respective monitoring points. Thus, it fulfils the objectives defined for this chapter.

5. ENERGY MONITORING TESTS AND ANALYSIS

Since tests were performed for three different systems, this chapter presents a section dedicated to each system. In each section, it is intended to clarify the tests performed and analyze the results obtained. Whenever possible, the contribution of monitoring carried out in the design, operation and maintenance of the intralogistics systems under study will be contextualized. Then, it was validated that the functionalities and respective configurations of the monitoring equipment matched the needs of the tests to be carried out. For that, small records were accomplished to analyze the measurement ranges, current direction, phase order and recording modes. PowerView 3.0 software was also installed and used to import the recorded data, making it possible to establish a first approach to the software with real data.

Before starting the energy monitoring tests, the physical feasibility of integrating the monitoring equipment at each previously defined monitoring point was verified. Then, it was validated that the functionalities and respective configurations of the monitoring equipment matched the needs of the tests to be carried out. For that, small records were executed to analyse the measurement ranges, current direction, phase order and recording modes. PowerView 3.0 software was also installed and used to import the recorded data, making it possible to establish a first approach to the software with real data.

Whenever necessary, the tests and interventions on the systems were supervised by elements responsible for ensuring the security and integrity of the systems.

5.1. STACKER CRANE

The first step in starting the monitoring tests on the stacker crane was to incorporate the monitoring equipment at the previously defined point. As seen in Figure 35, for this system the voltage and current of each phase including the neutral were monitored.

For correct monitoring, the current clamps were defined in the monitoring equipment for the range of 300 A. However, the current clamp used for measuring the neutral was configured for the range of 30 A because in the initial analysis the current in the neutral was never higher to 5 A.

Figure 35 Introduction of monitoring equipment at the stacker crane feed point.

Considering the purpose of analysing the energy behaviour of the STK and how this behaviour changes depending on the movement performed, movements were individually monitored according to the travelling axis, X, and the hoisting axis, Y, in the ascending and descending directions, with and without load. The load used was composed of two pallets with identical shape and weight, totalling 1600 kg. Diagonal movements under identical conditions were also analysed.

In order to frame the energy monitoring carried out with the movement in progress, variables already available in the PLC were registered. For the acquisition and recording of

these variables, it was necessary to use the PLC Analyzer Pro 5 software. First, in order to establish communication with the PLC, the computer's IP address was changed to a valid IP address within the automaton network. Then, in the software configuration, the PLC IP address was added as well as the data acquisition interval, in this case, 200 ms. After a successful connection to the PLC, a variable table was defined in which the name, memory address and type of each variable to be monitored were indicated. Since the tests focused on the STK movement, the variables that indicate the distance between the actual and final position and the STK velocity were always taken as a reference in the data analysis. As exemplified in Figure 36, the variables recording of an acquisition by the PLC Analyzer allows to evaluate the dynamics of the STK movement and, at the same time, perform a useful time recording for synchronization with data from energy monitoring. Whenever necessary, the relevant data from both the PLC Analyzer and the monitoring equipment were exported and aggregated in an excel document, being subsequently processed and presented in tables or charts.

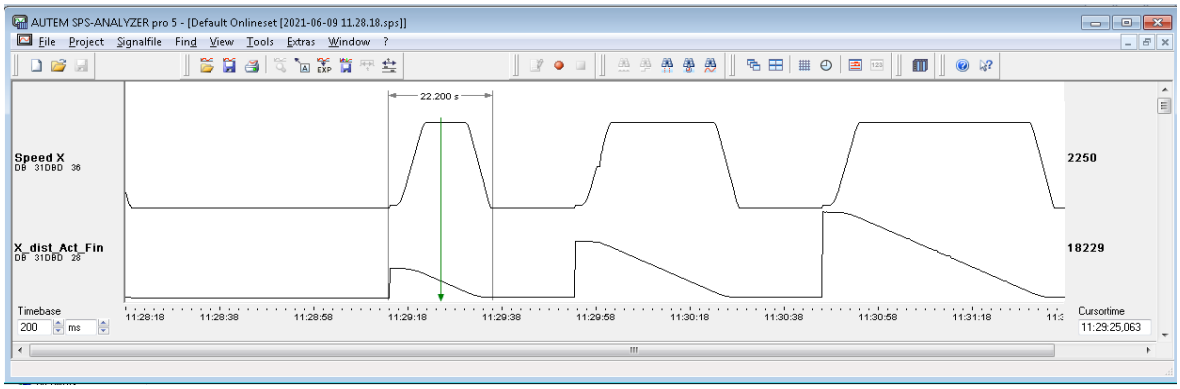

Figure 36 Stacker crane movement data obtained through PLC Analyzer software.

5.1.1. TRAVELLING MOVEMENT

The stacker crane, for each complete travelling movement lasting 40 seconds, travels along approximately 108 meters reaching a maximum speed of 4 m/s.

Regarding the phase voltages, these are correctly out of phase with each other, as shown in Figure 37, with stable RMS values in a range between 237 and 241 volts.

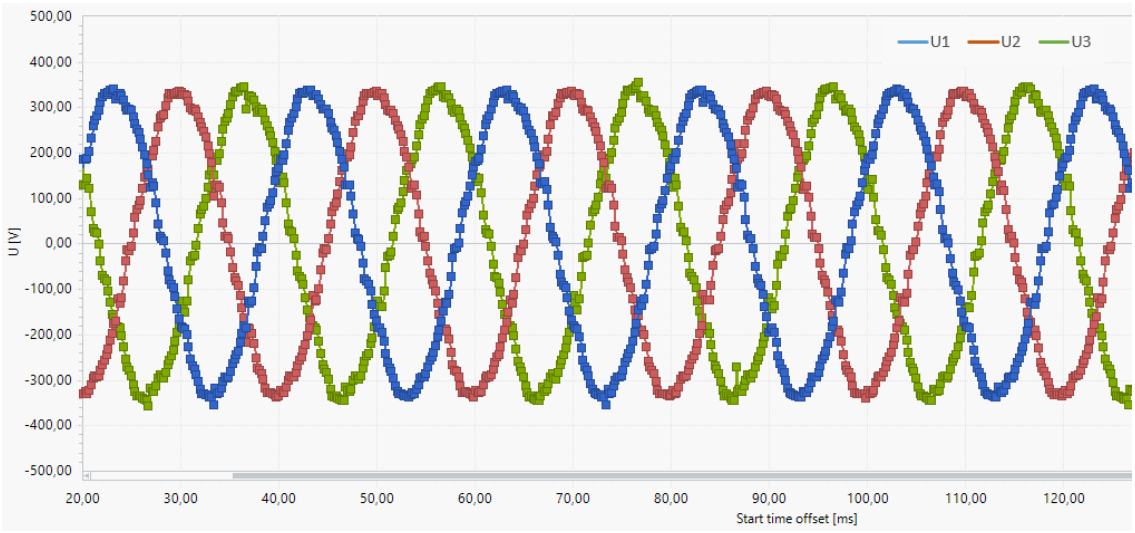

Figure 37 Phases Voltage Waveform.

As for the phase currents and based on the phase diagram, shown in Figure 38, captured at maximum speed, it is concluded that the currents are 120º out of phase with each other and slightly delayed when compared to the respective phase voltage, which corresponds to the correct operation.

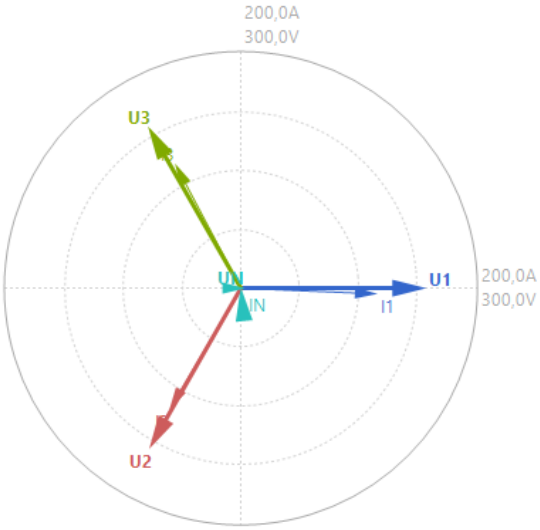

Figure 38 Voltage and Current Phases Diagram.

In turn, the voltage and current in the neutral throughout the movement present RMS values in the order of 13 V and 1,7 A respectively.

As for the current associated with the travelling movement, this was monitored, highlighting the different current requirements throughout the movement, as shown graphically in appendix B. Given the inertia associated with starting the movement as well as the need to quickly reach maximum speed, along the STK acceleration ramp there is a high current consumption which represents about 57,42% of the total current consumed. However, after reaching the maximum speed, the STK only requires the current necessary to maintain its movement at the desired speed. Finally, in the deceleration curve, the current requirements tend to zero, with the energy resulting from the deceleration being dissipated by a braking resistor.

The power factor was also monitored according to the same time basis as shown in appendix C. This comparison allows to verify that during acceleration the required current increases to values close to the rated current, which increases the power factor. However, for constant speed movement, the current requirement is considerably lower with the motor running below its best performance. Consequently, the power factor decreases.

The travelling movement was performed on the stacker crane with and without load. The difference in consumed active power between the complete execution of the two movements is 16,79 kW, being the movement with load the movement with the highest consumption as shown in Figure 39. Although there is a slight increase in consumption, the effort to move the stacker crane resides in the weight of the equipment and not in the load to be moved.

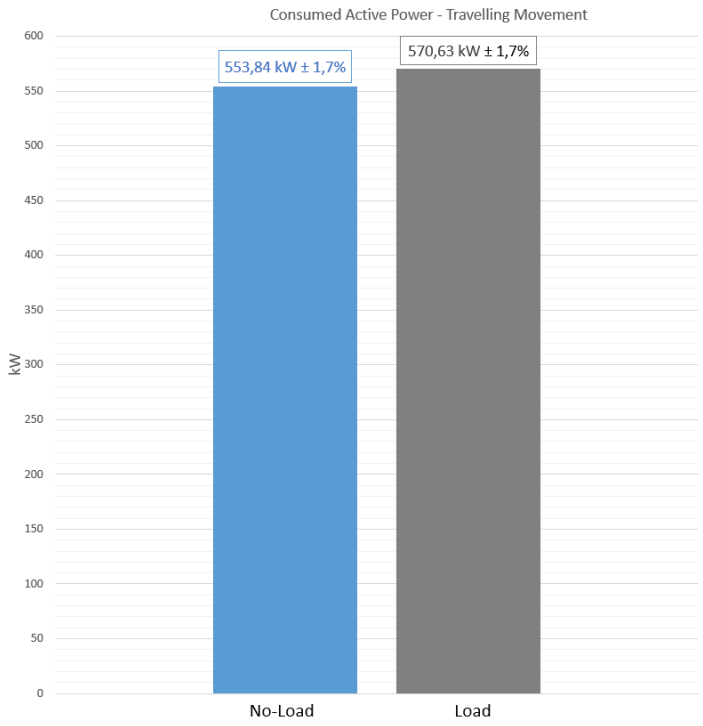

Figure 39 Analysis of consumed active power for travelling movement.

With the purpose to understand the impact of maximum speed on current consumption for movements on the X axis, the current was monitored for movements with maximum speeds of 2000, 3000 and 4000 mm/s. Logically, the decrease in speed leads to each movement being performed for a longer time, as shown in Figure 40. As only the maximum speed of the movement was changed and not its acceleration, the current consumption profiles for each movement have a similar start. However, the movement with lower maximum speed first reaches its maximum speed, thus decreasing the peak current consumption and increasing the time during which it is consuming. Appendix D graphically describes a temporal relationship between the current consumption for the three defined speeds where it is possible to infer that at the maximum speed of 2000 mm/s current consumption has a peak of 6 seconds and a movement duration of 58 seconds while the movement with the highest maximum speed corresponds to a peak of 10 seconds and a duration of 32 seconds.

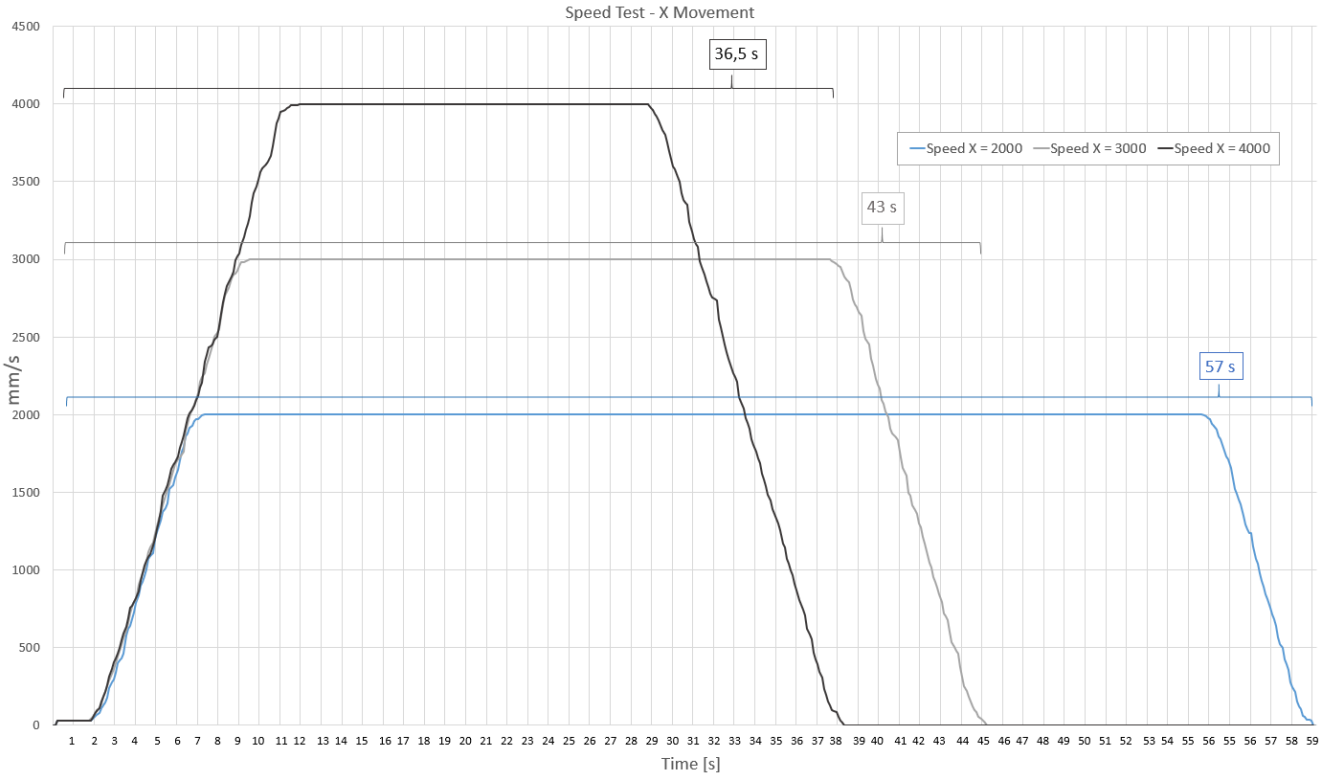

Figure 40 Speed curves for travelling movement with different maximum speeds.

To verify the speed at which the system has the lowest consumption, a consumption analysis was performed for each speed. Based on the graphic results present in Figure 41, it is verified that the definition of 2000 mm/s as the maximum movement speed reduces 19,61% of consumption compared to the second speed and 35,40% when compared to the higher speed. That is, the decrease in speed significantly affects the decrease in current demand, which results in lower active current consumption. Similarly, and as described in Figure 42, the increase in maximum speed induces a proportional increase in the reactive current generated.

According to the monitoring carried out, the temperature of the travelling motor ranged between 44,40 ºC and 46,70 ºC for ambient temperatures from 19,60 ºC to 20,00 ºC.

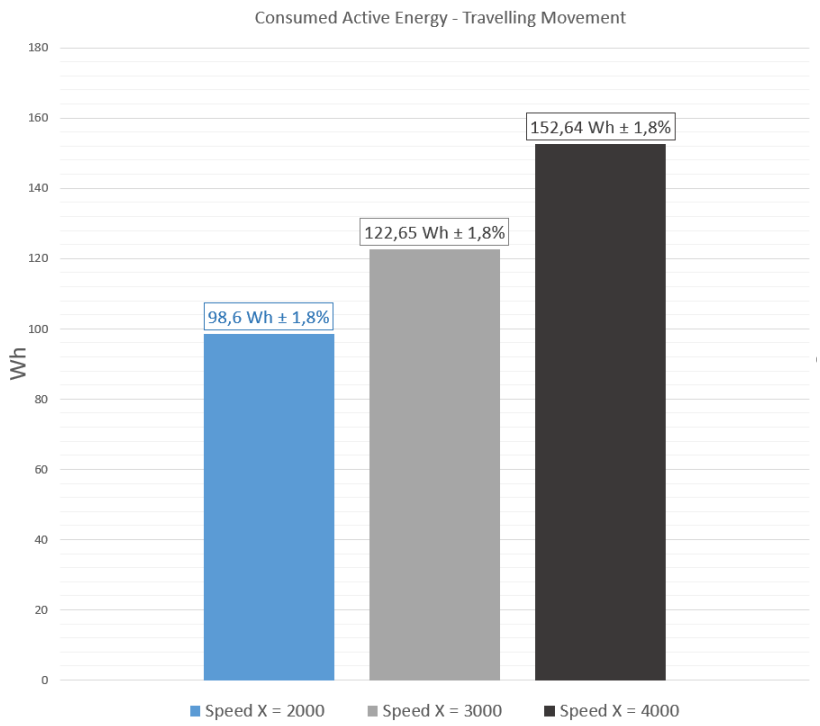

Figure 41 Consumed active energy for travelling movement with different speeds.

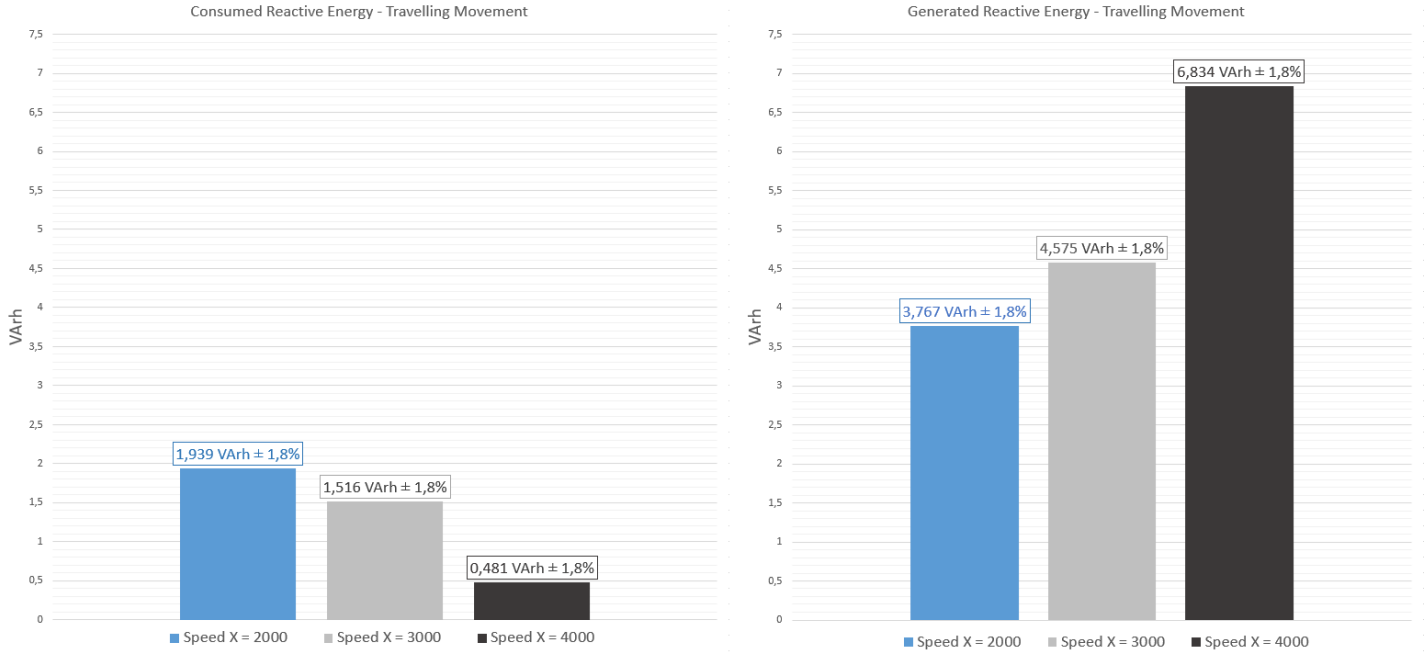

Figure 42 Consumed and generated reactive energy for travelling movement with different speeds.

5.1.2. HOISTING MOVEMENT

While for the travelling movement its direction does not have a significant impact on the energy dynamics of the system, the same does not occur for the hoisting movement. Upward and downward movements have different behaviour and are therefore analysed separately.

First, the upward movement was monitored, for which an analysis of speed and current consumption with and without load was carried out on the same time basis. Using appendix E, it is possible to verify that the acceleration ramp corresponds to the current demand ramp by the STK. When the maximum speed is reached, a slight peak occurs in the current curve, which tends to stabilize in the subsequent moments. As this is an upward movement and since the maximum speed is constant throughout it, the hoisting motor maintains its current demand in order to generate the necessary torque to move the platform and load at the desired speed. Regarding the power factor and according to appendix F, it remains stable and at high values, which indicates a good ratio between active and reactive energy associated with this movement.

In terms of consumption, when comparing the movement with and without load it is verified that the movement with load has a consumption of active power 39,56% higher than the consumption without load. This relationship is graphically shown in Figure 43.

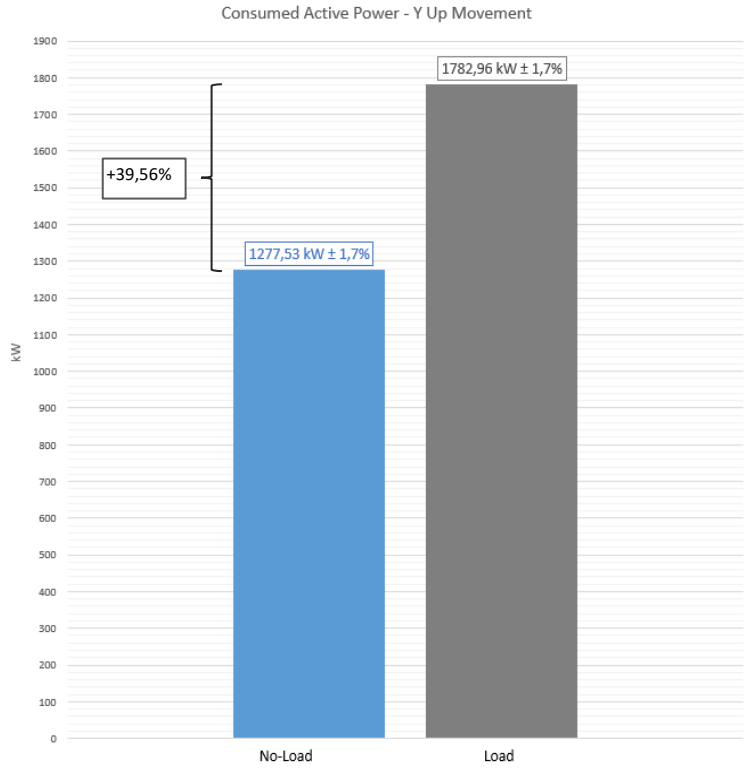

Figure 43 Consumed Active Power for hoisting movement with and without load.

Relative to the downward movement on the Y axis, the STK motor starts to function as a generator, as the STK no longer exerts force on the platform and starts to regulate its descent at the desired speed. As the Y axis speed drive has a regenerative module, the current generated in the STK during the movement is returned to the network. According to Figure 44 considering the same acceleration ramp and the same maximum speed, the movement with and without load presents a similar current generation curve, varying only in the amount of current generated per instant of time. While no-load movement at maximum speed generates about 30 A, loaded movement generates 49 A. After 33 seconds from the beginning of the movement, there is a slight increase in current for both movements resulting from the increase in deceleration to end the movement.

The consumption and generation of active power graphically described in Figure 45 allow to conclude that the energy generated by movement is much higher than that consumed. As for the comparison of the generated energy between the movement with and without load, the movement with load represents 85,27% more active power generation than the movement without load. For this movement, the presence of load translates into added value for energy generation.

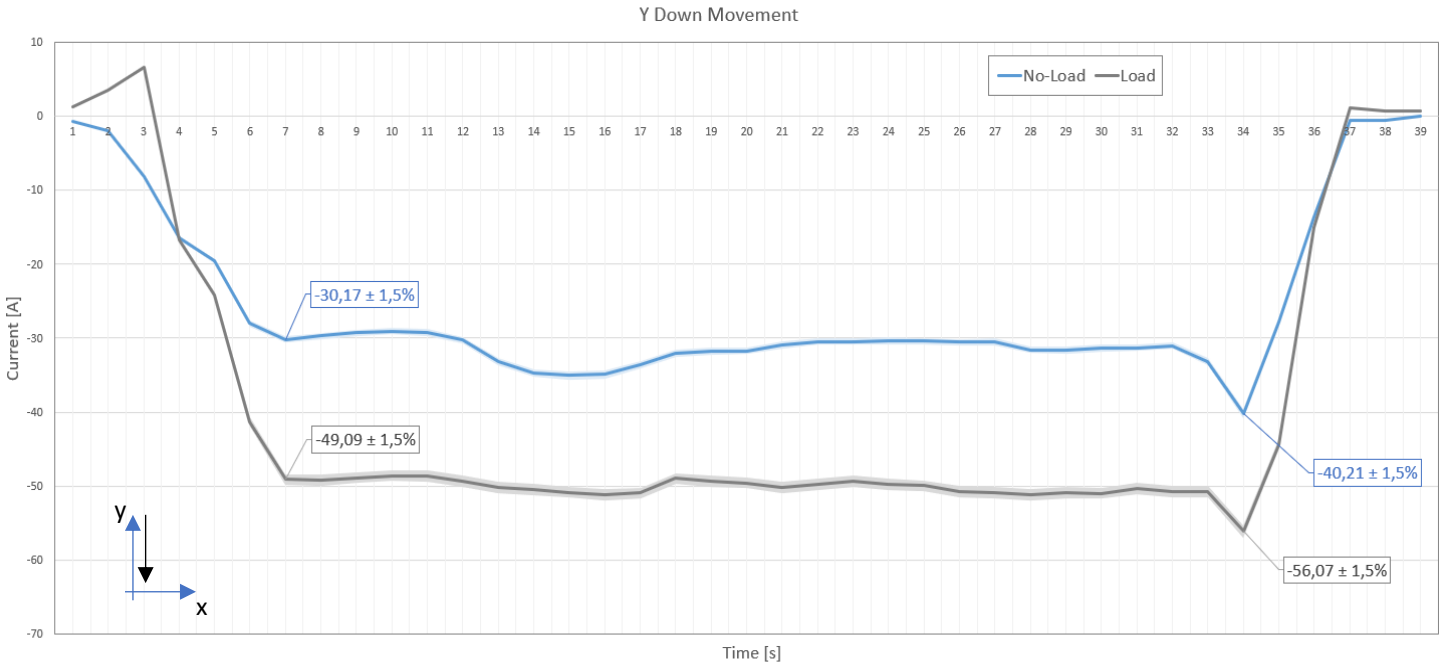

Figure 44 Current analysis of downward movement with and without load.

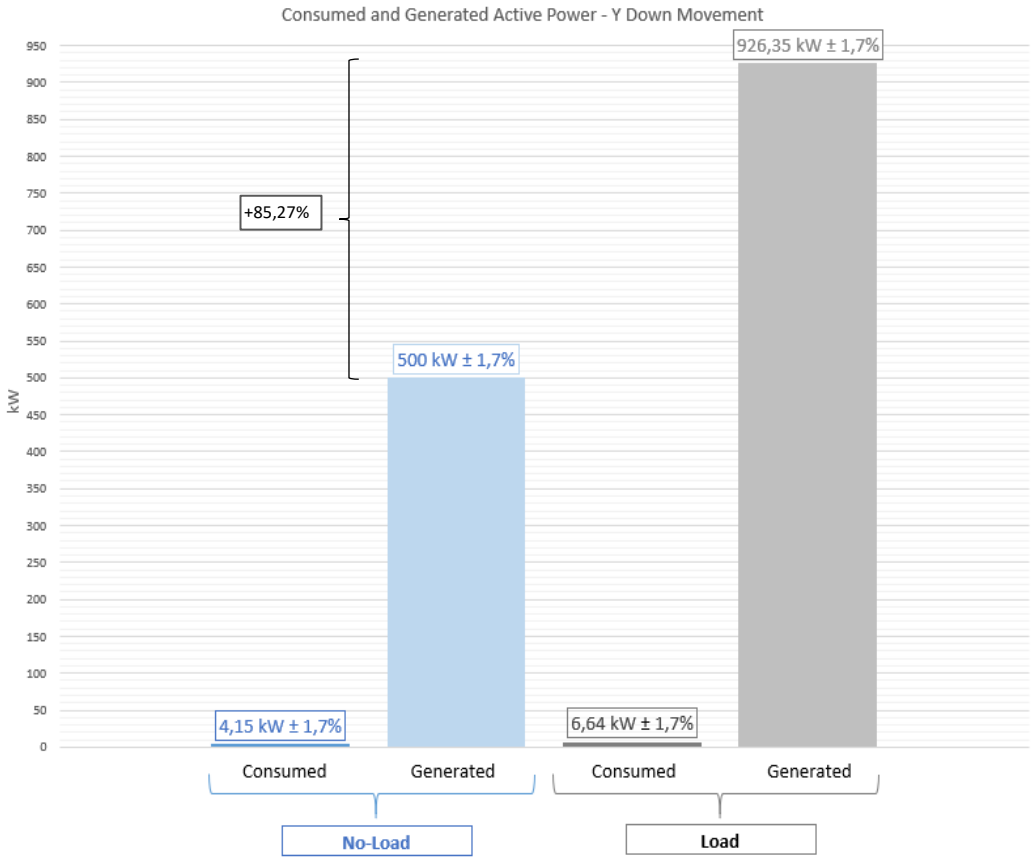

Figure 45 Consumed and generated active power for downward movement with and without load.

Similar to the test performed for the travelling movement, the maximum movement speed of the downward movement without load was changed to 440, 660 and 880 mm/s in order to understand the impact of the maximum speed on the amount of energy returned to the network. The current monitoring described in Figure 46 for the three defined speeds shows that decreasing the maximum speed increases the movement time and slightly reduces the maximum current generated by each instant of time.

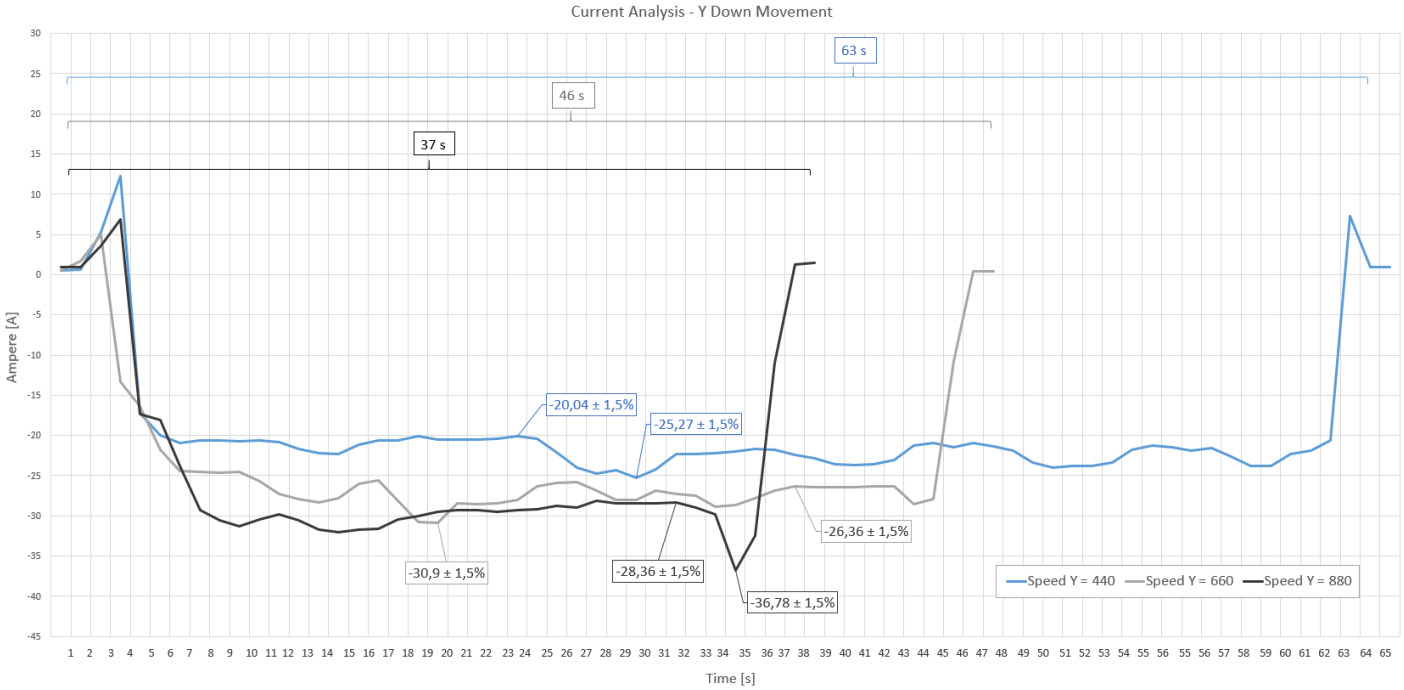

Figure 46 Current analysis for velocity changes in downward movement along the Y axis.

Although the movement at 440 mm/s presents a lower value of maximum generated current, the graph in Figure 47 indicates that the total active power generated for this movement is 1,85% higher than with intermediate speed and 6,48% higher with faster movement.

Based on the results obtained, it is concluded that active power generation benefits from the reduction of maximum speed, however, the weight of the load has a greater impact regarding power generation.

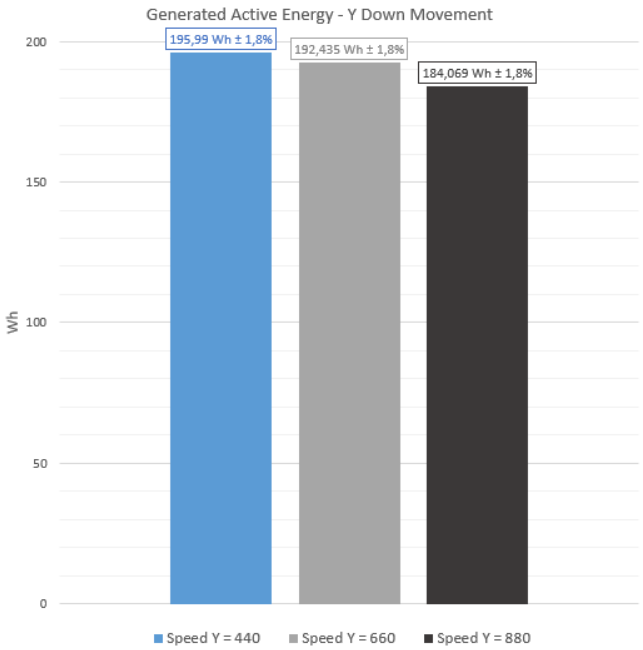

Figure 47 Generated active energy for unloaded downward movements at different speeds.

5.1.3. DIAGONAL MOVEMENT

The diagonal movements stand out because in the same movement there are variations in the STK travelling and hoisting axis to reach the target position. In this study, diagonal movements were performed with and without a load in up and down diagonal directions between the ends of the rack, in this case, between the positions with coordinates X1_Y1 and X96_Y13.

It is noted that the storage area associated with the STK has 96 coordinates in length, X axis, and 13 in height, Y axis. As the motors of both axes demand power from the same supply point, the total current and voltage demand of the entire STK is monitored at the monitoring point.

As for the upward diagonal movement, the current at the input of the circuit was monitored, so the shape of the graph in Figure 48 is identical to that of the travelling movement, to which the linear consumption of current from the hoisting movement is

added. The peak value of 224,67 A for the loaded movement and 184,80 A for the unloaded movement is justified by the stated reason.

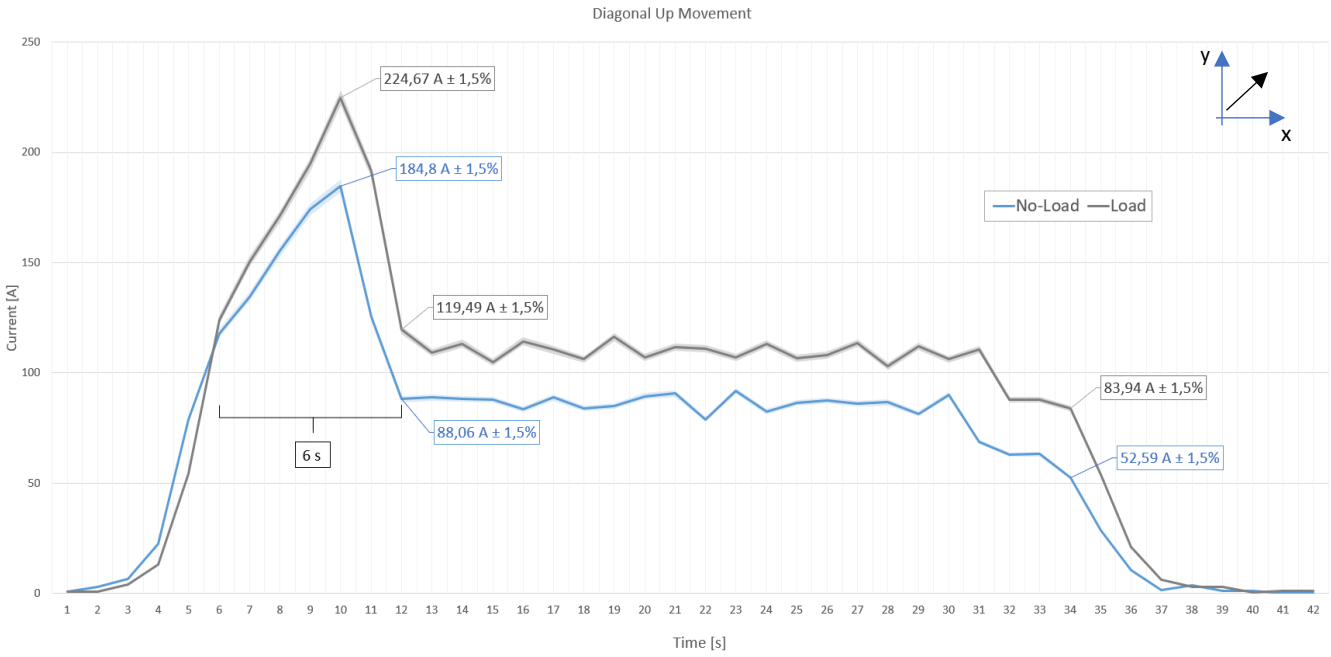

Figure 48 Current analysis of diagonal upward movement with and without load.

Regarding the downward diagonal movement and since the movement along the Y axis has the particularity of returning energy to the network, the current resulting from the internal dynamics of the machine is monitored at the STK supply point. As can be seen in figure 49, at the beginning of the movement and as the movements along the X and Y axis simultaneously start, the energy that starts to be generated by the downward displacement of the load is not able to meet the current requirement of the travelling axis. After 7 seconds, each axis stabilizes its speed so that the travelling axis consumes only the current necessary to maintain its movement and the hoisting axis has reached its maximum generation. Thus, the system can supply the current needs in the hoisting axis and return the excess current to the network. The dynamics of consumption and generation of active power for diagonal movements with and without load is compared in Figure 50, allowing to infer power needs and excesses at different moments of the movement. In an ideal scenario, this type of movement could present a behaviour capable of being adjusted to the needs and, in this way, increasing the efficiency of the movement.

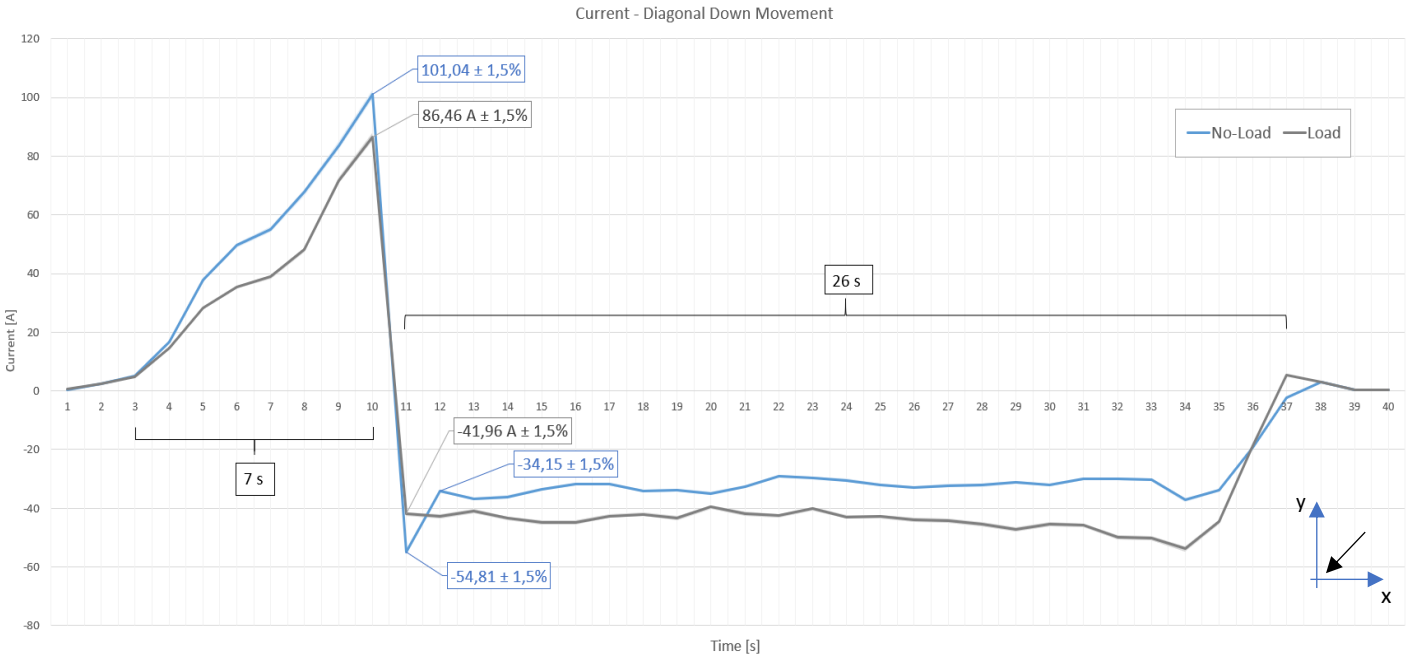

Figure 49 Current analysis of diagonal downward movement with and without load.

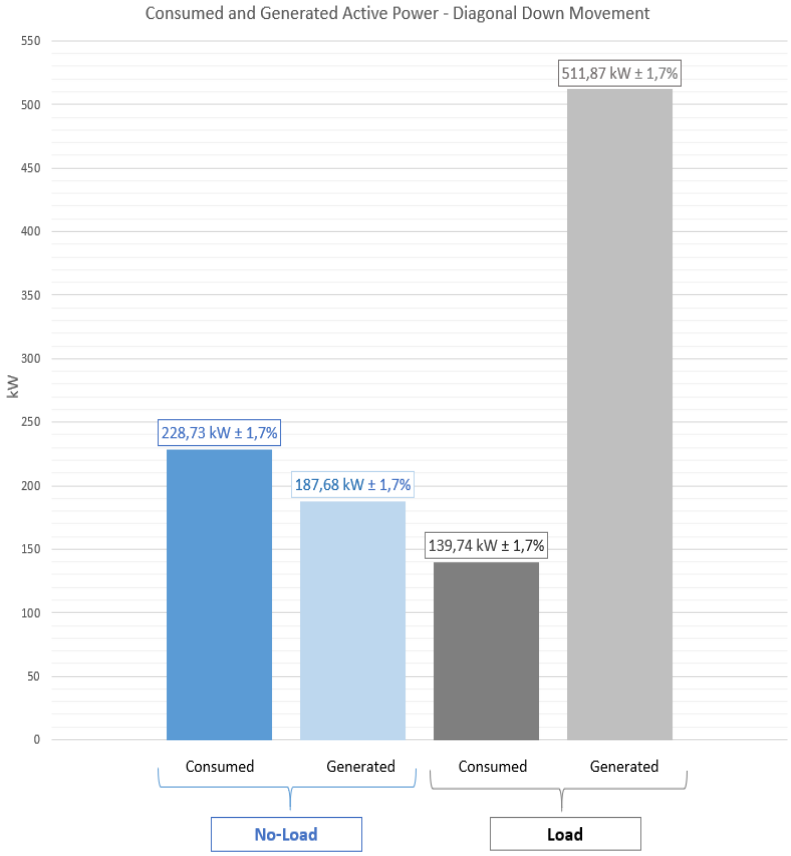

Figure 50 Consumed and generated active power for diagonal downward movement with and without load.

5.1.4. OPTIMIZATION MODULES

As shown in the previous sub-chapter, the STK movement has huge potential in terms of optimizing movement with a view to increasing energy efficiency. Although the present study has focused on the maximum speed variation for consumption perception, other variables such as the acceleration ramp, the beginning and end of movement per axis without simultaneity and the use of energy dissipated in the movement braking are important factors for an efficient optimization of each movement.

In this perspective, Figure 51 presents four optimization models useful for different movement scenarios. For each scenario, the axis with the longest movement is taken as master so that the optimization does not affect the requested cadence.

In the first scenario, the X axis as master starts its movement reaching its maximum speed. As necessary, the Y axis initiates the hoisting movement so that the energy generated from the X axis deceleration is used to feed the upward movement.

For the second scenario, and as verified in the tests carried out, the use of low speeds for downward movements on the Y axis exploits the energy generation that can be used to feed the X axis consumption.

Regarding the third movement and as previously analysed, in the case where an axis needs a certain amount of time to execute its movement, reducing the speed of the other axis so that they finish simultaneously reduces the current consumption of the system.

For the last scenario, four, it is validated that if the longest movement to perform is the downward movement of the Y axis, the fact that the X axis starts with a slow acceleration ramp and a lower maximum velocity leads to the Y axis being able to feed all the movement of the X axis.

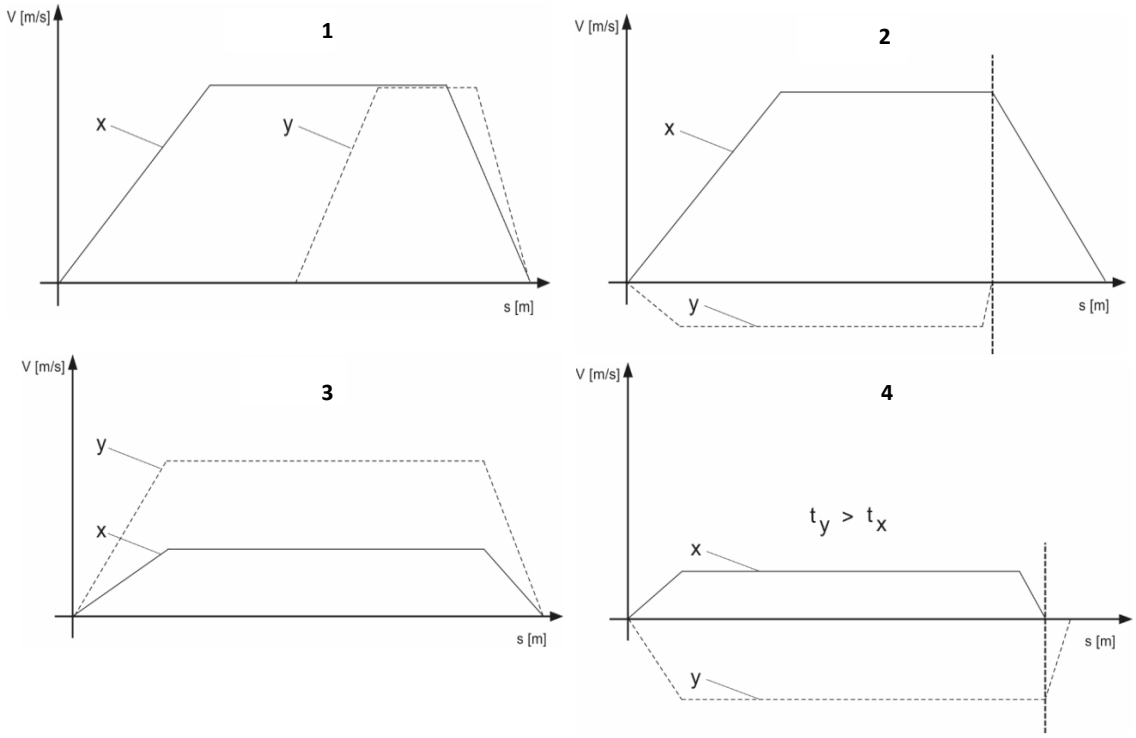

Figure 51 Energy optimization models for Stacker crane movement.

5.1.5. CONSUMPTION ANALYSIS - CONTINUOUS OPERATION

In order to analyze the continuous consumption of STK as well as to explore the added value of using the generative module that integrates the Y-axis speed drive, a STK monitoring was realized with a duration of 6 days, 8 hours, 46 minutes and 24 seconds. According to data obtained and shown in Table 2, the consumption of total active energy was 570394,220 Wh and in the same period 106888,068 Wh was returned to the main power network, representing an interesting energy return of 18,739%. It is also notorious that the generation movement produces a significant reactive component.

Table 2 Consumption analysis of stacker crane continuous operation.

Total Time	
6	days
8	hours
46	minutes
24	seconds

Consumed Total Active energy:	570394,220	Wh
Consumed Total Fundamental Reactive energy:	25647,719	Varh
Generated Total Active energy:	106888,068	Wh
Generated Total Fundamental Reactive energy:	23013,008	Varh
Percentage of energy recovered	18,739	%

5.1.6. ANOMALY DETECTION

In addition to the analysis of the STK design and operation, the monitoring performed was useful in detecting anomalies during the normal system operation. The graph introduced in Figure 52, composed of current values every 1 second for the three phases, clarifies that a problem occurred in the STK affects phases one and two with an extremely high current peak. With a case in the data from the monitoring, it was concluded that it was a short circuit between phases 1 and 2. After a physical validation of the equipment, the maintenance technician validated that the insulation of the phase cables was traced being the copper wires of each cable in contact.

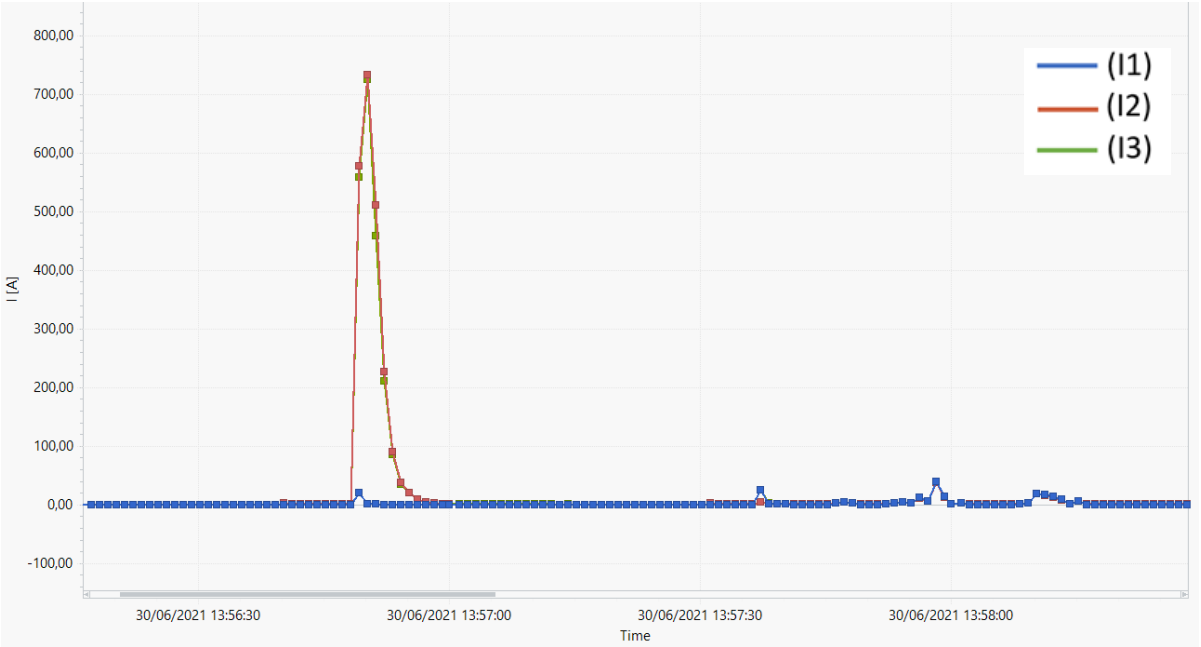

Figure 52 Anomaly detection in stacker crane power system.

5.2. CONVEYORS CIRCUIT

Although the analysed conveyor circuit consists of three conveyors with independent motors, the total current consumption falls within a low range, having been the circuit's power circuit breaker dimensioned for 16 A rated currents. Accordingly, the MI 2892 Power Meter used to monitor the system was configured for its lowest current range, that is, 30 A.

Since the conveyor circuit stands out for carrying out repeated movements along an axis, the tests realized on this circuit focused on the current analysis of the movements and the analysis of their continuous operation.

Based on a set of circuit phase currents monitoring lasting one minute, when the circuit initiates a new pallet transfer order, it performs an identical current demand pattern, as visually represented in Figure 53 for three movements. The movement initializes with the start of the first conveyor causing the pallet to move. When the pallet enters the second conveyor, this conveyor starts its movement and the pallet transitions from the first to the second conveyor. After the pallet moves from the first conveyor to the second, the first one ends the movement. Likewise, the transition of the pallet from the second to the third occurs. In the transitions of pallets between conveyors, there is an overlap between the motor consumption, with a slight increase in the current demand.

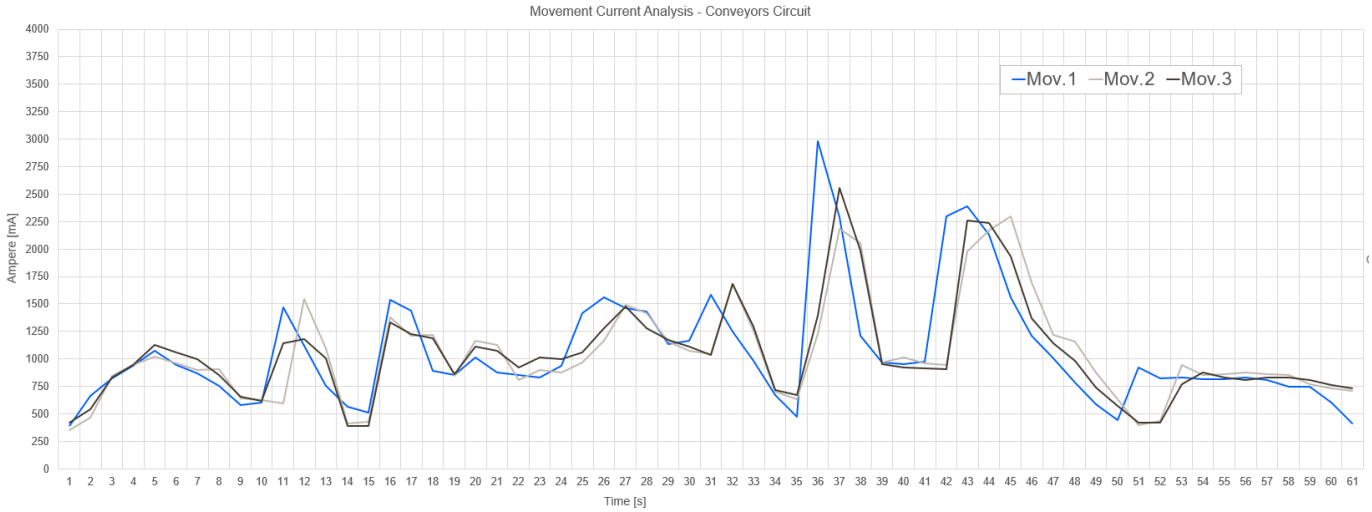

Figure 53 Current consumption by conveyors movement.

In order to validate the current consumption and behaviour of the conveyors circuit under study, continuous monitoring was carried out, comprising three records with an acquisition rate of 200 ms. The total monitoring time was converted from ms to days, hours, minutes and seconds form, making a total of 2 days, 22 hours, 32 minutes and 38 seconds. Based on the records made, it was validated that the maximum current value required by the conveyor circuit is between 3574,62 mA and 3503.84 mA. In turn, the total active energy consumed was 7,341 Wh and the total reactive energy was 2,4117 Varh, which is associated with a margin of error of 1.8% for both values. Thus, it is concluded that the power factor of the circuit is 0,950 with an error margin of 0,02. Table 3 aims to summarize this information.

Table 3 Energy consumption analysis of conveyors circuit.

Consumed Total Active energy:			7,341	Wh		
Consumed Total Fundamental Reactive energy:			2,41172	Varh		
Power Factor:			0.950			
	Register 1		**Register 2**		**Register 3**	
Max Current:	3529,23	mA	2840,73	mA	3117,97	mA
Min Current:	292,75	mA	273,32	mA	248,73	mA

To complement the study of the conveyor circuit, an analysis of the utilization time and the respective number of uses for each record was prepared. As shown in Table 4, in total, the conveyor circuit started operating 1090 times with a usage percentage of 34.93%.

Table 4 Analysis of time and number of conveyors circuit uses.

Registers	Monitoring Time (s)		Utilization Time (s)		Nº Uses
1ª	1860		760		14
2ª	226325		80555		931
3ª	25773		7402		145
Total:	253958	seconds	88717	seconds	1090
Use %:			34,93%		

The data obtained from the monitoring carried out allow the conclusion that typically a conveyor circuit performs a high number of movements in which each one lasts a short period of time being the utilization rate considerably low. The increased use of the conveyors circuit is directly limited by the pallet inputs and the saturation of decision points upstream and downstream.

5.3. RGV SYSTEM

Monitoring of the RGV System started with the monitoring of phase voltages and currents at the output of the main circuit breaker identified as Q37. Due to the lack of space for placing the current transformers at the Q37 output, the CTs were placed in the connection upstream of the circuit breaker. The placement of the CTs as represented in figure 54 had no impact on the results obtained. Then the Metrel MI 2892 was configured for the second measuring range because this is the closest range to the 160 A rated current set at the main circuit breaker.

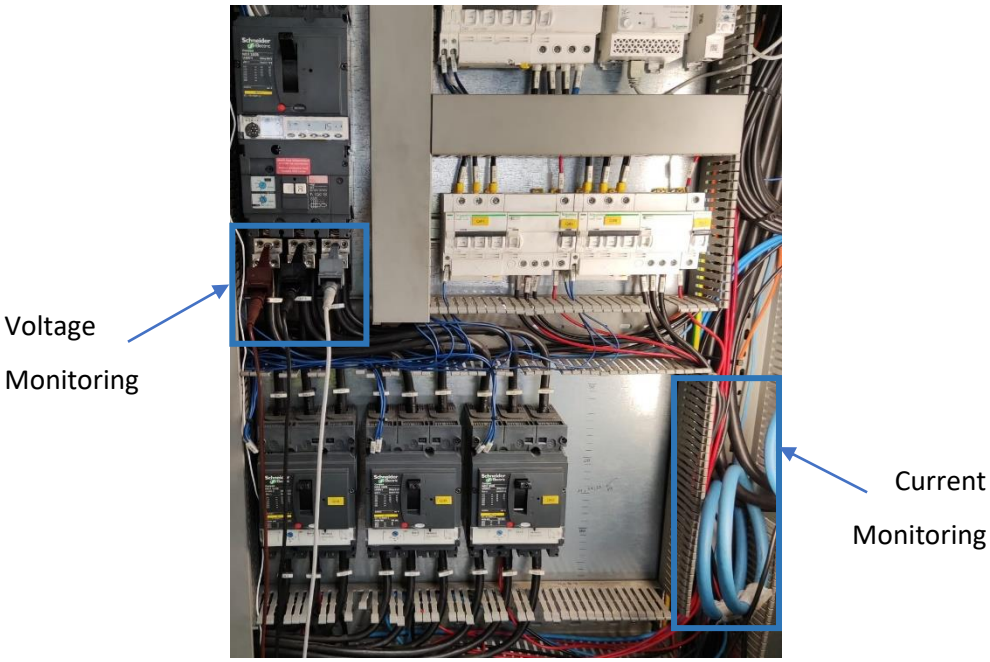

Figure 54 Addition of monitoring equipment to the RGV system.

During the analysis of the RGV system, the need arose to monitor each of the loop's power sections. For that, the equipment used for monitoring currents and voltages were placed at the respective monitoring points. Figure 55 exemplifies the addition of CTs downstream of the circuit breaker responsible for feeding the second section of the loop. An identical process was carried out for the first and third sections.

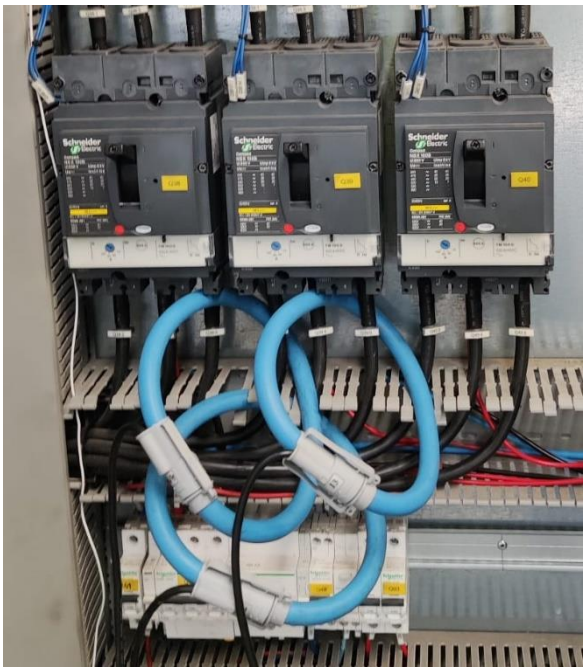

Figure 55 Addition of current transformers for monitoring the second loop feed section.

Regarding the monitoring of the total system, data acquisition was performed at an acquisition rate of 1s in 8 days, 20 hours, 50 minutes and 41 seconds. This monitoring allowed the conclusion that the average current of the system is approximately 23,19 A, as well as the maximum current of 76,52 A. In turn, the total active energy consumption of the system was 2729,921 kWh.

As the vehicles inserted in the system present dynamic movements in which the number of vehicles per section is not linear, for each section monitoring was carried out at different intervals and acquisition rates, as described in Table 5. The section with the highest current values was the section associated with circuit breaker Q39. According to three monitoring lasting 7 hours, 52 minutes and 51 minutes performed at acquisition rates of 1s, 200 ms, and 10 ms respectively, it was found that the maximum current in the section was approximately 56 A at a rate of 1 second. When compared to the maximum current obtained in the main circuit, the maximum current value in the section is only 25% lower. It is verified that the current distribution of the main circuit breaker for each section is not linear. So, the sizing of the system must consider not only the selectivity of the circuit breakers but also the requirements associated with the dynamic consumption of each section

Table 5 Current monitoring power of section two.

Section:	2 (Q39)								
Acquisition rate:	1 s			200 ms			10 ms		
acquisition interval:	7 hours			52 minutes			51 minutes		
Phase:	L1	L2	L3	L1	L2	L3	L1	L2	L3
Max Current:	28,36	27,01	27,94	56,26	53,87	56,4	30,99	29,54	30,38

During the implemented monitoring, constant interruptions in the system caused by the main circuit breaker were detected. For this reason, the main circuit breaker tripping curve was validated so that an overload in a section would first cause the section breaker to trip. Monitoring equipment was also re-introduced into the main circuit. After a new trip, it was concluded that the cause of the trip was not associated with overcurrent or overvoltage. Additionally, it was detected that one or more phase currents oscillated moments before the interruption. Thus, and in order to monitor the residual currents of each monitoring point, the four CT started to surround the three-phase conductors as exemplified in Figure 56 for sections 39 and 40.

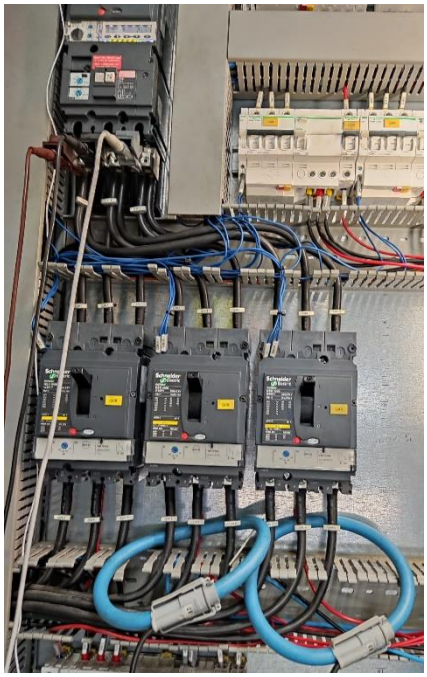

Figure 56 Residual current monitoring in the RGV system.

Considering that the Q37 circuit breaker is configured to withstand residual currents up to 3 A with a time tolerance of zero seconds, in addition to monitoring the normal operation

of the circuit an alarm has been configured in the monitoring equipment to register the current values as soon as a residual current was greater than 3 A.

Based on the normal recording of 1 second present in Figure 57 performed by the monitoring equipment, it is verified that a new anomaly appeared, since the residual current in section Q39 and in the main system Q40 suddenly increased above 3 A causing an interruption in the system.

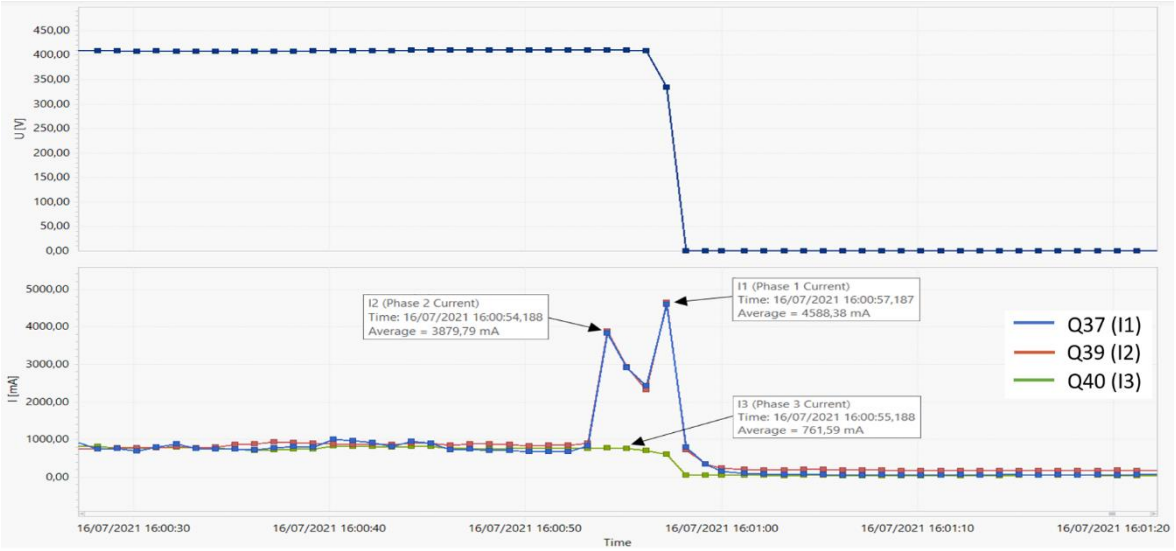

Figure 57 Anomaly detection at 1 second acquisition rate.

If the residual current exceeded 3 A, it means that the alarm conditions defined in the monitoring equipment were met. Thus, the anomalous moment was recorded at a rate of 200 ms, which includes the currents waveform, and at an acquisition rate of 10 ms. These records have a small pretrigger that allows recording the moments before the event that causes the alarm occurrence. The first register, shown in figure 58, allows detecting that at a rate of 200 ms there is a discrepancy between the normal operation in section 3 (Q40) and section 2 which presents an anomalous behaviour. Furthermore, the record at the 10 ms acquisition rate, visible in Figure 59, shows that the main circuit spontaneously increases its residual current due to the residual current coming from section 2. It is then concluded that an anomaly in section 2, such as a short circuit, leads to the interruption of the system's operation.

To validate the conclusion obtained, a physical analysis of section two was carried out, and a short circuit was detected between a phase of the collector that feeds the RGV and the ground.

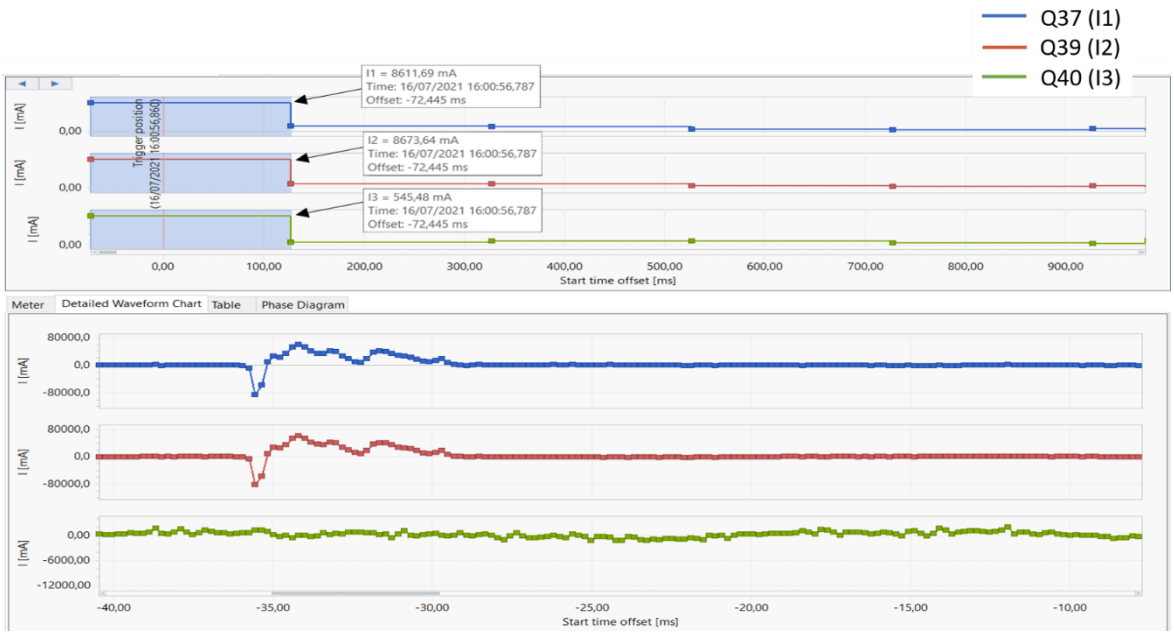

Figure 58 Anomaly detection at 200 ms acquisition rate with waveform record.

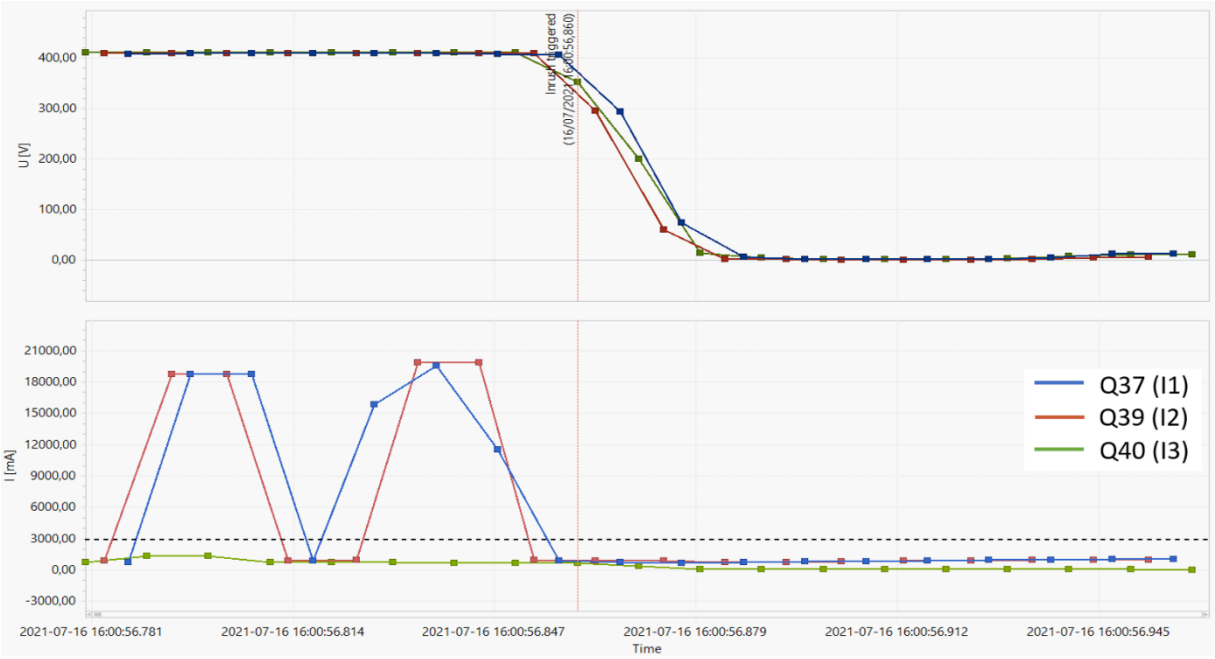

Figure 59 Anomaly detection at 10 ms acquisition rate.

During normal operation, it was found that abrupt increases in residual currents occur simultaneously in two sections, as shown in Figure 60. This phenomenon happens because the RGV collector has two brushes that are internally connected to the same point. When the RGV transits between sections, the collector has the first brush in one section and the second in another, interconnecting two sections, which causes instantaneous oscillations.

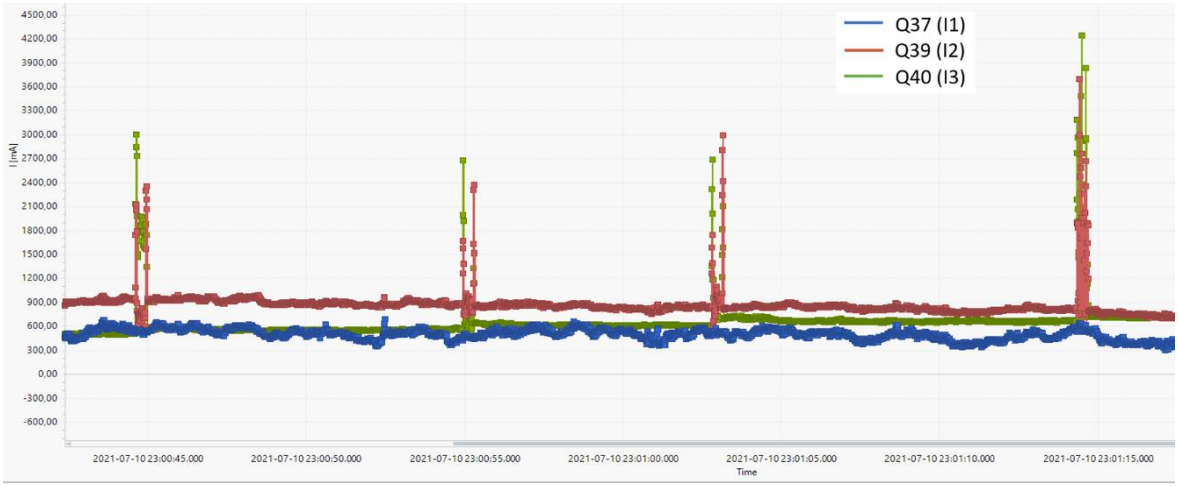

Figure 60 Abrupt increases in residual currents at RGV section transition.

Figure 61 demonstrates the current values for sections two and three and the main system according to samples collected at 10 ms, which allow us to verify that the resulting oscillations between sections at no time have an impact on the main system. Thus, for these cases, the main circuit-breaker does not detect any anomaly with the system operating in its entirety.

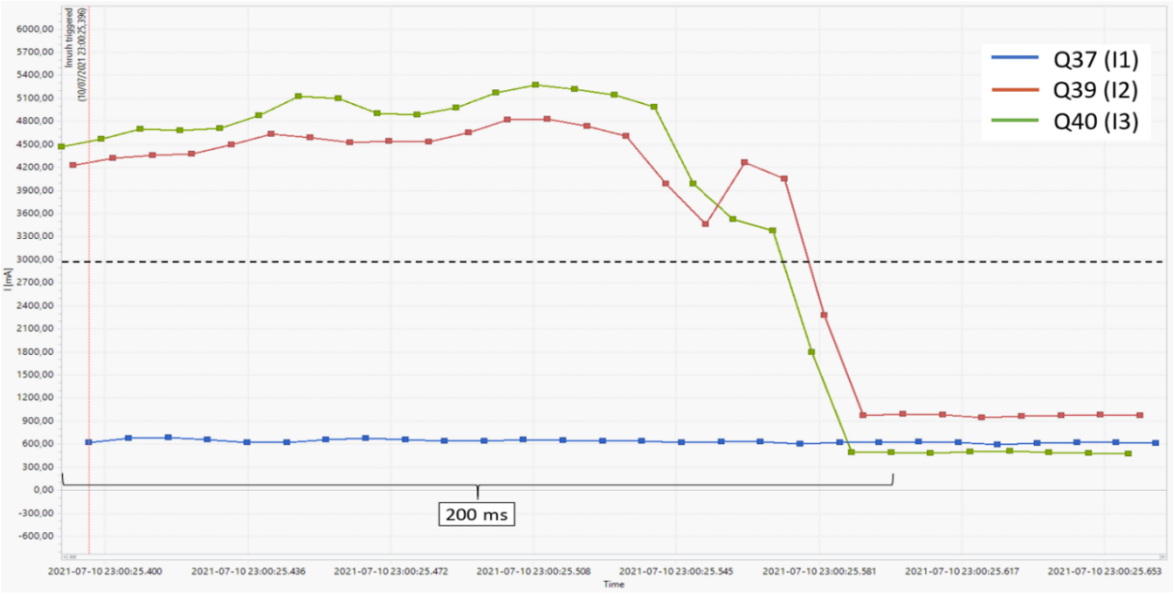

Figure 61 Comparison of residual currents between sections and main circuit in the RGV section transition.

6. MARKET SOLUTIONS FOR ENERGY MONITORING

After an analysis of the main intralogistics systems developed and commercialized by the company, it was possible to carry out a cohesive survey of the monitoring needs of each system. Thus, this chapter begins with the evaluation and comparison of market solutions, detecting those that best suit the systems in question. To complete the purpose of the chapter, a hypothetical intralogistic system will be considered as a reference for which the best suited energy monitoring solutions and what monitoring equipment will be chosen. Thus, it is intended to clarify what is the solution with the lowest acquisition cost.

6.1. EQUIPMENT ANALYSIS AND COMPARISON

The analysis process started with a market search for energy monitoring solutions. This first step allowed to identify a large number of brands with identical monitoring solutions. Therefore, it was decided to restrict the number of brands to be analysed, with the selected brands being Siemens AG and Janitza Electronics. The choice for Siemens AG was based on the partnership between it and Korber Supply Chain as the main supplier of equipment for the intralogistics systems developed. Janitza Electronics was chosen because it is specialized in the development of monitoring solutions containing a broad catalogue of energy and power quality measurement products. Another decisive factor was the fact that the host company already had contact with representatives of both brands, which facilitated the provision of information and the preparation of budgets.

6.2. EQUIPMENT COMPATIBILITY WITH THE SOLUTION

Based on the catalogue analysis of the above-mentioned brands, this subchapter intends to present the energy monitoring equipment that best fits the needs of intralogistics systems, highlighting their advantages.

6.2.1. JANITZA UMG 96-RM

The Janitza UMG 96RM, illustrated in Figure 62, is a front mounting multifunctional power analyzer able to measure, monitor and check the electrical characteristics in 3 or 4-phase energy distribution networks. This equipment has a measurement accuracy of 0,2% for currents and voltages and power class 0.5S (…/5A) [56].

The UMG 96RM provides up to 4 digital inputs for pulse, logic and state monitoring inputs. It also provides up to 6 digital outputs for pulse, switch, threshold value and logic outputs. In terms of channel inputs, the equipment under analysis has up to 4 input channels that can be used as analog, thermistor and residual current inputs. As for power quality analysis, this equipment allows a detailed acquisition of the energy data and load profile being able to monitor up to the 40th harmonic and detect current and voltage distortions. To perform continuous data acquisition the UMG 96RM has a memory of up to 256 MB. In order to guarantee an easy connection with the energy management system, PLC or SCADA, the Janitza UMG 96RM presents different versions for the Modbus (RTU), Profibus DP, Profinet, TCP/IP and M-Bus communication protocols. There are versions that have more than one communication protocol [56].

Figure 62 Janitza UMG 96-RM [57].

6.2.2. JANITZA UMG 96-PA

The Janitza UMG 96-PA is a modular energy measurement device (MID) that can be mounted in the cabinet front panel. This unit features an intuitive color graphical display through which the user can navigate a set of submenus dedicated to the illustration of measured values in numeric form, as a bar graph or line graph. For data acquisition, this unit has an 8 MB memory in which it records the minimum and maximum values acquired. As for communication, the UMG 96-PA has only one RS485 interface designed to use the Modbus RTU protocol [58].

The UMG 96-PA can be inserted into three and four conductor networks and is capable of monitoring three currents and three voltages simultaneously. The power quality analysis performed by this equipment allows the acquisition of current and voltage waveforms per phase, harmonics analysis up to 40th harmonic, detection of current and voltage distortions and the measurement of positive, negative and zero sequence component. This equipment has a measurement accuracy of 0,2% for currents and voltages and power class 0.2S (…/5A) [58].

Extension of functions can be performed by add-on modules. The add-on module UMG 96-PA-RCM-EL enables monitoring a fourth current and adds two inputs to the equipment that can be selected as 0-2 mA analogue inputs or as RCM measuring inputs with detection of cable breaks and additional temperature measurement. This module also provides an Ethernet interface. The Janitza UMG 96-PA on the left side and the add-on module UMG 96-PA-RCM-EL on the right side are graphically represented in Figure 63 [59].

Figure 63 Janitza UMG 96-PA and add-on module Janitza UMG 96-PA-RCM-EL [57].

6.2.3. JANITZA UMG 20 CM

The Janitza UMG 20 CM, presented in Figure 64, is a branch circuit monitoring device with residual current monitoring. With an accuracy of 1% for current and voltage and active energy class 1, the UMG 20CM has available 20 channels for phase or residual current inputs. This equipment can be used for three and four conductor networks and has available four voltage inputs to monitor the phase and neutral voltages in the main branch [60].

As for the power quality, the UMG 20 CM can analyses harmonics up to 63rd harmonic, register crest factor, total harmonic distortion and minimum and maximum values. The logging of values is aided by a small 769 kB memory. This unit features two digital outputs and an RS485 interface with Modbus RTU communication [60].

The UMG 20 CM allows alarm management through GridVis software monitors.

Figure 64 Janitza UMG 20 CM [57].

6.2.4. JANITZA UMG 801

The all-in-one power analyzer Janitza UMG 801 provides energy management, power quality monitoring and residual current monitoring. Available for three and four conductor networks, the UMG 801 can be extended up to 10 current measurement modules. The 800-CT-8-A modules offers eight current measurement channels and can be easily integrated into the main unit through a click bus system achieving up to 92 current measurement

channels. In addition, with the 800-CON transfer modules, measuring points up to 100 m can be connected [61].

The UMG 801 provides 4 digital inputs, 4 digital outputs, 1 analog output and 4 multifunction channels that can be used optionally and flexibly for RCM, temperature or current measurement. In terms of measuring accuracy, this equipment has an accuracy of 0.2% for current and voltage and active energy class 0.2S. The UMG 801 is able to register harmonics up to 63rd harmonic for current measurement and 127th harmonic for voltage measurement. It is also capable to perform 10 ms acquisitions, register waveforms, and detect distortion and transients. This unit supports a large data register due to its 4 GB memory [62].

The Janitza UMG 801 energy measurement device provides diverse communication protocols being them Modbus RTU, Modbus TCP/IP and OPC UA. Via OPC UA this equipment enables direct data transmission to higher-level systems like Enterprise Resource Planning (ERP) systems eliminating the need for costly integration. It has also available one RS485 and two Ethernet Interfaces [62].

Figure 65 shows the Janitza UMG 801 and its expansion modules. From left to right is presented the UMG 801 unit followed by 800-CT-8-A module and then the 800-CON module.

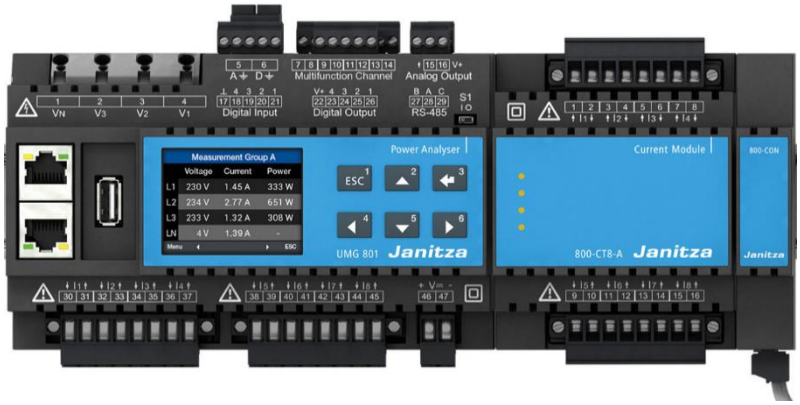

Figure 65 Janitza UMG 801 and its expansion modules [57].

6.2.5. JANITZA UMG 806

The modular universal measurement device Janitza UMG 806, introduced in Figure 66, has the essential characteristics for complete energy monitoring. This equipment can be integrated into three or four conductor networks being capable to monitor up to four voltages and currents. Four more analog current inputs can be monitored with the addition of the UMG 806-EI1 expansion module in the main unit. This equipment also offers one analog input for residual current or temperature monitoring [63].

The Janitza UMG 806 provides a register of harmonic current up to the 31st harmonic, unbalance and distortion factor for current and voltage. It is a measurement device with an accuracy of 0,2% for current and voltage and active energy class 0.5S. The unit has only one digital output and any digital input. However, the expansion module UMG 806-ED1 with four digital inputs and two outputs can be added. To support the data registers this unit has a 4 MB memory [64].

In terms of communication, the UMG 806 uses the Modbus RTU protocol. The communication options can be expanded with the UMG 806-EC1 expansion module that allows an easy integration of Modbus RTU devices into an Ethernet architecture through the Modbus gateway function [64].

The expansion modules can be used to extend the functionality of the basic device, although the basic device only supports one extension module per module type.

Figure 66 Janitza UMG 806 [57].

6.2.6. SIEMENS 7KM PAC 4200

The power meter Siemens 7KM PAC 4200 is a feature-packed power monitoring device that is suitable for use as a standalone device monitoring over 200 parameters or as part of industrial control. With an accuracy of 0,2% for voltage and current and active energy class 0.2S, the PAC 4200 is able to analyse and register the average value of voltage and current, power factor, distortion factor, phase angle and harmonics up to 64th harmonic for current and voltage. Although the base unit cannot monitor more than three current simultaneously, an expansion module can be added making it possible to measure quantities such as neutral current, residual current and temperature [65].

With regard to the integrated communication interfaces, the PAC 4200 has an Ethernet interface destinated to Modbus TCP protocol. This unit can also work as a gateway for integrating Modbus RTU slaves into an Ethernet network. There are two additional modules that can be integrated into the main unit in order to establish PROFINET or PROFIBUS communications [65].

Although different types of expansion modules are available, the PAC 4200 can only integrate two additional modules.

As shown in Figure 67 the PAC 4200 is a panel-mounted instruments with a graphic display through which the user can navigate to access different monitoring data.

Figure 67 Siemens 7KM PAC 4200 [65].

6.2.7. ET 200SP ANALOG INPUT MODULE – AI ENERGY METER

The AI Energy Meter is developed to suit the scalable SIMATIC ET 200SP peripheral system for interfacing process signals to a central control unit. This equipment aims at creating transparency about the energy requirements of individual components of a production plant at the machine level.

Contrary to the equipment described above the AI Energy Meter does not have any expansion modules, but different versions. The basic version, AI Energy Meter ST, monitors systems up to three phases recording voltages, currents, phase angles, power, frequencies and power factors [66]. In turn, the high feature version, AI Energy Meter HF, beyond the quantities measured by the basic version it also monitors neutral current, operating hours, limits and power quality data for voltages and currents. The power quality data monitored by AI Energy Meter HF include harmonic analysis up to 63rd harmonic, active power factor for phase and distortion factor for current and voltage. This equipment does not have any input for residual currents [67]. The residual currents are obtained by calculation.

The AI Energy Meter is available for PROFINET and PROFIBUS communications, however it depends on the interface module in use by SIMATIC ET 200SP. More energy values from measuring instruments can be transmitted to the modular SIMATIC ET 200SP system which supports up to 64 modules. Figure 68 exhibit an AI Energy Meter and a SIMATIC ET 200SP peripheral system.

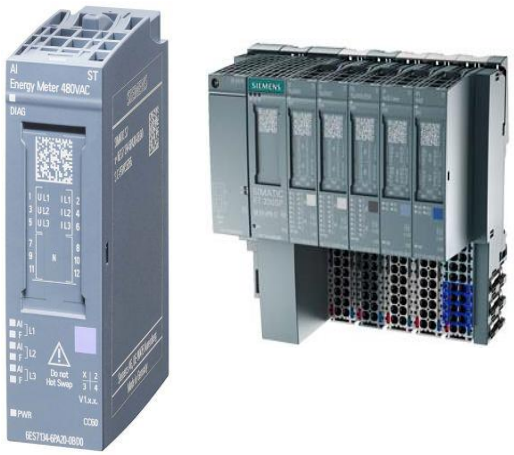

Figure 68 AI Energy Meter and SIMATIC ET 200SP [67].

6.2.8. CURRENT TRANSFORMERS

All energy monitoring equipment described requires current transformers in order to carry out the acquisition of current value at a given time. A current transformer (CT) has the function of transforming a current from a higher value into a proportionate current to a lower value. Accordingly, the high current that flows through the electrical networks is safely monitored.

The current transformers studied in this project are intended for monitoring phase and residual currents. Only moulded case current transformers were considered, because in the systems under analysis the investment in flexible current transformers such as Rogowski coils would not be justified.

Moulded case current transformers for phase currents monitoring

Moulded case current transformers are applied to record high currents. These current transformers are used for mounting on conductor rail. However, the primary conductor must be disconnected during installation. Moulded case current transformers are the most common and cost-effective form of current transformers. Janitza presents two types for this form of current transformers, the type ASK for primary currents up to 100 A and the type CTB for primary currents from 100 A to 2500 A. The type ASK and CTB are graphically demonstrated in Figure 69 as (a) and (b) respectively. The Janitza ASK and CTB current transformers have precision class 1 and secondary currents of 5A [68].

(a) (b)

Figure 69 CT type ASK (a) and CT type CTB (b) [68].

In turn, Siemens also provides two series of moulded case current transformers. The series 4NC5 has a wide range of current transformers in order to monitor from low primary currents to high primary currents. According to the monitoring needs the 4NC5 series features secondary currents of 1 or 5 amps and different accuracy classes. The current transformers suitable for the energy monitoring equipment presented have secondary currents of 5A and accuracy class 1 [69].

The series 7KT12 has the particularity of monitoring three conductors simultaneously. These current transformers are only designed to monitor 60, 100 and 150 A primary currents with 5 A secondary currents and accuracy class 1 [69].

Figure 70 visually clarifies the difference between 4NC5 current transformers (a) and 7KT12 current transformers (b).

Figure 70 CT 4NC5 (a) [70] and CT 7KT12 (b) [71].

Residual current transformer

After an analysis of Siemens current transformers, it was verified that Siemens does not present viable solutions for monitoring the residual currents of the systems under analysis. Therefore, the most suitable equipment for the needs of the systems under analysis is the Janitza CT-AC RCM 110N displayed in Figure 71 [72].

The CT-AC RCM has a compact construction designed to increase the sensitivity of residual current detection. With a transformation ratio of 700/1 and an interval diameter from 35

mm to 210 mm, this equipment monitors primary residual currents up to 1000 mA that can be raised to 21000 mA in specific conditions [72].

Figure 71 CT-AC RCM [68].

6.3. CHOOSING THE MOST SUITABLE SOLUTION

An analysis of Siemens and Janitza monitoring equipment allows concluding that while Siemens with solutions such as the AI Energy Meter centralizes information in a processing unit, Janitza presents solutions external to the system's processing. These two approaches are relevant to apply in different intralogistics systems.

Siemens monitoring solution is the best option to add to new systems, given the easy integration of monitoring equipment with the processing units currently used through PROFINET communications. Currently, the processing units are commonly connected to scalable SIMATIC ET 200SP peripheral system. Thus, it is only necessary to introduce an AI Energy Meter followed by signal processing. Furthermore, as other variables related to the systems are already monitored, such as temperatures, speeds and distances, the joint processing of all data allows for a more complex analysis of the intralogistics system.

On the other hand, older systems do not have the type of communication and data processing mentioned above, so the integration of a monitoring solution in these systems

can be complex. In these cases, the Janitza monitoring solution simplifies data transmission and processing by providing information at the highest levels such as ERP systems or energy analysis software. As an example, the architecture presented in Figure 72 describes a monitoring system with a Modbus network. At the top of the system, a gateway establishes the connection between the Modbus network and an ethernet network with internet access for sending data to data processing and presentation systems.

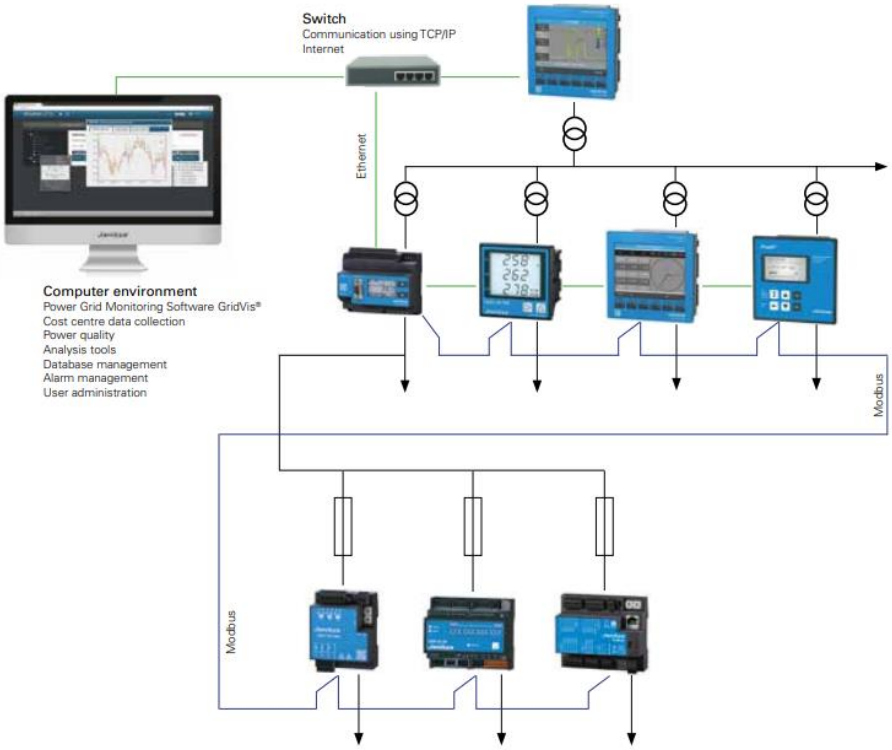

Figure 72 Example of Janitza Monitoring Architecture [57].

For an evaluation between the two types of energy monitoring solutions, a hypothetical architecture of an intralogistic system will be taken as reference. As depicted in Figure 73, this architecture includes a customer-supplied power cabinet, three STKs, a conveyor system with five areas and an elevator, and an RGVs loop with three feed segments JB1, JB2 and JB3. It is assumed that the system respects the current project configuration, being constituted by PROFINET communications and Siemens PLCs.

Figure 73 Hypothetical architecture of an Intralogistic System.

The first energy monitoring solution made up of Siemens equipment allows linear integration with the system's processing units via PROFINET. Thus, in the cabinet responsible for receiving the energy supplied by the customer, a Siemens 7KM PAC 4200 would be added with two expansion modules. One module for adding current input channels and the other for adding ethernet interface. It would be also necessary to include three current transformers 4NC5432-2CH21 for rated currents of 1000 A and a current transformer 4NC5112-2CB21 for neutral currents up to 50 A. All current transformers have accuracy class 1. For each stacker crane, an AI Energy Meter HF would be involved to which three current transformers 4NC5121-2CC21 dimensioned for a rated current of 150 A and one CT 4NC5112-2CB21 for a rated current of 50 A would be associated. To the SCP10 responsible for feeding the five conveyor areas and an elevator, five AI Energy Meter ST would be added in order to monitor the conveyor areas and one AI Energy Meter HF for elevator monitoring. The feed conveyors system is a three-conductor system so a 7KT1200 current transformer would be used. This CT is intended for monitoring three rated currents of 50 A. Regarding the RGVs loop, SCP11, the three feed segments must be monitored as well as the main supply. Given the relevance of energy monitoring in this system, an AI

energy meter HF would be included for each monitoring point. As the power supply system is a three-phase system without neutral, for each AI Energy Meter three current transformers 4NC5121-2CC21 would be coupled for rated currents of 150 A. The AI Energy Meter obtains the residual currents by calculation, so it is not necessary to add any CT for residual currents.

It was assumed that no system had an ET 200SP. Therefore, an ET 200SP with its ethernet bus adapter and base units would be taken into account for the cabinet of each STK, for the SCP10 and for the SCP11.

As for the energy monitoring solution consisting of Janitza equipment, the communication between equipment is realized through the Modbus protocol. The communication with the highest levels requires a gateway to interconnect the Modbus network with the ethernet network as clarified in figure 47. Some devices are already adapted to perform the gateway function. However, others require an external gateway.

For this solution, a Janitza UMG 96-PA would be added to the customer supply energy cabinet. The UMG 96-PA would be complemented with a 96-PA-RCM-EL expansion module in order to allow the monitoring of a greater number of currents as well as to enable the connection to an ethernet network. For current monitoring, three CTB 41.35 current transformers sized for 1000 A rated currents would be deployed. Since each STK is dimensioned equally, for each STK a UMG 806 would be used. Three CTB 31.35 current transformers for measuring phase currents dimensioned for 200 A, one ASK 21.3 for neutral current up to 75A and one CT-AC RCM 110N for residual currents would be associated with this equipment. In turn, the SCP 10 cabinet would require two energy monitoring devices. One to monitor the elevator and another to analyze the branched conveyor feeding system. To monitor the elevator, equipment equal to those used in the STK would be installed, as well as the same current transformers for phase, neutral and residual currents. The Janitza UMG 20 CM monitoring equipment can be configured to monitor 15 phase currents and 5 differential currents. Thus, with only one monitoring unit it would be possible to monitor the five conveyor areas. Each area requires three ASK 21.3 for phase current monitoring and one CT-AC RCM 110N for residual current. As the Janitza UMG 20 CM equipment has only a Modbus communication interface, it would be connected directly to the UMG 806

inserted in the same cabinet. The UMG 806 would be responsible for the gateway function. Lastly, in the SCP11 cabinet responsible for feeding the loop of RGVs, four UMG 806 would be included. In this way, the main power feed and each of the feed sections would be monitored. Given the system to be monitored, for the main feed and for the feed sections, the residual current transformers would be configured to monitor currents up to 3 A. To monitor each phase current, a CTB 31.35 current transformer would be used. Since the UMG 806 units are not based on an ethernet network, the four units would be connected in series through a Modbus network and one of them would include an ethernet module with the gateway function. All current transformers indicated for the solution under analysis have accuracy class 1.

After checking the equipment needs for each solution, quotes were requested from representatives of both brands. Based on the values provided, it was concluded that the purchase of equipment for the hypothetical architecture is 67% cheaper with Siemens solution than with Janitza solution.

7. CONCLUSIONS

7.1. MAIN CONCLUSIONS AND CONTRIBUTIONS

The present project, as a pioneer in the monitoring of the intralogistic systems in question, fulfilled its objectives, allowing the acquisition of knowledge of energy dynamics useful in the design and operation analysis as well as in anomalies detection and prevention.

The monitoring performed for the stacker crane emphasized the energy impact of this system on an automated warehouse. The analysis of STK movements according to the movement axes allowed the identification of the STK behaviour and which movements could increase the system's energy efficiency. Within this framework of thought, the energy generated during the downward movements of the stacker crane stands out given the enormous potential of using this energy to feed the system. This process represents a significant reduction in energy demand from the electrical network. The suggested models for movement optimization seek to conciliate the generated and consumed energy maximizing the system's efficiency.

Regarding conveyors, these are the system with the lowest energy impact. However, its presence in critical positions such as inputs, outputs and interconnection points make conveyors essential in the flow of materials throughout the automated warehouse. The introduction of monitoring equipment in this system is a useful tool in anomalies detection and prevention avoiding unexpected interruptions with operational, temporal and financial consequences.

Based on the monitoring dedicated to the RGV system, the validation of the variable current demand in each section according to the RGVs movements stands out. Detecting the cause of unwanted system outages was also helpful. Since section circuit breakers are not designed for residual current detection, any short circuit that causes a spontaneous increase in residual current will first be detected by the main circuit breaker. Thus, the selectivity of circuit breakers for this type of current is not valid. As verified, the

introduction of equipment in each section would allow the detection of anomalies indicating which section and the respective phases are associated with the problem. In this project, it was not possible to monitor more than one section simultaneously because the monitoring equipment only has four current and voltage inputs. Furthermore, the current clamps used are not entirely dedicated to monitoring residual currents, which introduces uncertainty to the values obtained through the monitoring carried out.

The use of Metrel MI 2892 to carry out the monitoring included in this project allowed for a clearer notion of the real requirements of each system. In this way, the monitoring solutions suggested for the hypothetical architecture meet the requirements of each system. For the described solutions, communication with the logical units of intralogistics systems was also taken into account, allowing for further data processing and presentation of useful information to the user.

Finally, the analysis of the acquisition cost of equipment for monitoring solutions demonstrated that the cost of integrating monitoring solutions is quickly amortized by its advantages. The fact that it helps the dimensioning by avoiding oversizing the electrical installation or detecting anomalies without the need for travel and intervention by a specialized technician are some examples of this.

7.2. SUGGESTIONS FOR FUTURE WORK

Based on the results obtained in this project and due to its temporal limitation, it is suggested that future work be carried out in different areas that have relevant interest for energy monitoring of the intralogistic systems analysed.

One of the suggested works would aim at choosing, installing and configuring a monitoring solution like those described in sub-chapter 6.3 in order to monitor all the systems of an automated warehouse with impact on its energy efficiency. In turn, another suggestion for future work would be directed to the development of ecological operation modes in which an algorithm based on the flow of requests would allow to adjust movement parameters such as maximum speed and acceleration ramps without ever affecting the necessary cadences. Thus, all movements would not be performed at maximum speed, but according to the best relationship between time available and energy efficiency.

Bibliography

[1] J. Qin, Y. Liu, and R. Grosvenor, “A Categorical Framework of Manufacturing for Industry 4.0 and beyond,” *Procedia CIRP*, vol. 52, pp. 173–178, 2016, doi: 10.1016/j.procir.2016.08.005.

[2] European Council, “Euco 169/14,” *Eur. Counc.*, no. October, pp. 1–15, 2014.

[3] T. Javied, J. Bakakeu, D. Gessinger, and J. Franke, “Strategic energy management in industry 4.0 environment,” *12th Annu. IEEE Int. Syst. Conf. SysCon 2018 - Proc.*, pp. 1–4, 2018, doi: 10.1109/SYSCON.2018.8369610.

[4] M. Meißner and L. Massalski, “Modeling the electrical power and energy consumption of automated guided vehicles to improve the energy efficiency of production systems,” *Int. J. Adv. Manuf. Technol.*, vol. 110, no. 1–2, pp. 481–498, 2020, doi: 10.1007/s00170-020-05796-8.

[5] Fernandes, A. Baptista, F. J. G. Silva, R. D. S. G. Campilho, and G. F. L. Pinto, “Intralogistics and industry 4.0: Designing a novel shuttle with picking system,” *Procedia Manuf.*, vol. 38, no. 2019, pp. 1801–1832, 2019, doi: 10.1016/j.promfg.2020.01.078.

[6] J. Dyntar, “Application of Agent-Based Supply Chain Modelling in Intralogistics System Design and Optimisation,” *8th Int. Days Stat. Econ.*, pp. 374–384, 2014.

[7] N. Hafner and F. Lottersberger, “Intralogistics systems - optimization of energy efficiency,” *FME Trans.*, vol. 44, no. 3, pp. 256–262, 2016, doi: 10.5937/fmet1603256H.

[8] A. Rücker, J. Rief, and J. Fottner, “Development of a Method for the Energy Efficiency Determination of Stacker Cranes in Automated High-Bay Warehouses,” *FME Trans.*, vol. 48, no. 4, pp. 753–760, 2020, doi: 10.5937/fme2004753R.

[9] R. Ortt, C. Stolwijk, and M. Punter, “Implementing Industry 4.0: assessing the current state,” *J. Manuf. Technol. Manag.*, vol. 31, no. 5, pp. 825–836, 2020, doi:

10.1108/JMTM-07-2020-0284.

[10] M. V. Guedes, “O motor de indução trifásico,” *Fac. Eng. da Univ. do Porto*, 1994, [Online]. Available: https://paginas.fe.up.pt/maquel/AD/MI_sel&aplic.pdf. (accessed Feb. 02, 2021)

[11] Integrated Publishing, “AC Motor Theory.” .

[12] S. J. Chapman, *Electric Machinery Fundamentals*, Fourth. New York: McGraw-Hill, 2005.

[13] B. C. Neves and M. J. Gonçalves, “MELEC - Motores de Indução Trifásicos.”

[14] A. E. Fitzgerald, C. Kingsley, and S. D. Umans, *Electric Machinery Fundamentals - 6th ed*. 2003.

[15] R. R. Lawrence, “Alternating Current Machinery,” *Science*, vol. 41, no. 1057. pp. 505–505, 1915, doi: 10.1126/science.41.1057.505.

[16] S. Eurodrive, “Frequency Inverters.” Available: https://www.sew-eurodrive.pt/products/inverter_technology/frequency_inverters.html. (accessed Mar. 03, 2021)

[17] VariableFrequencyDrive.org, “Variable Frequency Drive Working Principle.” Available: http://www.variablefrequencydrive.org/vfd-working-principle.

[18] Government of Canada’s digital presence, “Principles of Operation - AC VFD Drives,” 2015. Available: https://www.nrcan.gc.ca/energy-efficiency/energy-star-canada/about/energy-star-announcements/publications/variable-frequency-drives/principles-operation-ac-vfd-drives/15433. (accessed Apr. 04, 2021)

[19] C. Hartman, “What is a Variable Frequency Drive?,” 2020. Available: https://vfds.com/blog/what-is-a-vfd/. (accessed Apr. 04, 2021)

[20] Philip, “What is a Programmable Logic Controller (PLC)?,” 2021. Available: https://en.m.wikibooks.org/wiki/Introductory_PLC_Programming. (accessed Apr. 04, 2021)

[21] Autem, “PLC Analyzer pro 6,” 2021. Available: https://www.autem.de/products/plc-analyzer-pro-6/. (accessed Aug. 08, 2021)

[22] IEEE Std 1159, *IEEE Recommended Practice for Monitoring Electric Power Quality*, vol. 2019. 2019.

[23] M. I. Muhamad, N. Mariun, and M. A. M. Radzi, “The effects of power quality to the industries,” *2007 5th Student Conf. Res. Dev. SCORED*, no. December, 2007, doi: 10.1109/SCORED.2007.4451410.

[24] J. Afonso and J. Martins, “Qualidade da energia eléctrica,” *Robótica Automação, Control. Instrumentação*, pp. 66–71, 2004.

[25] FLUKE, “What are voltage sags, dips, swells and transients?,” 2021. Available: https://www.fluke.com/en-my/learn/blog/power-quality/what-are-voltage-sags-dips-swells-and-transients-2 (accessed Mar. 03, 2021).

[26] Continental Control Systems, “Current Crest Factor,” 2021. https://ctlsys.com/support/current_crest_factor/. (accessed Apr. 04, 2021)

[27] Pinyol Ramon, “Harmonics : Causes , Effects and Minimization,” *Salicru White Pap.*, no. August, pp. 1–32, 2015.

[28] R. Neelam, “Harmonics: Definition, Types and Causes | Electrical Engineering.” https://www.engineeringenotes.com/electrical-engineering/harmonics/harmonics-definition-types-and-causes-electrical-engineering/32482 (accessed Mar. 03, 2021).

[29] F. Oladipo, O. A. O, and A. Adedayo, “Harmonic Analysis and its Mathematical Philosophy,” *Int. J. Sci. Eng. Investig.*, vol. 4, no. 41, pp. 30–31, 2015.

[30] D. Chapman, “Harmonics Causes and Effects,” *Copp. Dev. Assoc.*, 2001, [Online]. http://www.leonardo-energy.org/sites/leonardo-energy/files/Cu0119_AN_Causes%5Cnand%5Cneffects%5Cnof%5Cnharmonics_v2.pdf%5Cnfile:///Users/tortades/Dropbox/Investigacio?n/Biblioteca%5CnPapers/Library.papers3/Articles/2001/Chapman/2001%5CnChapman.pdf%5Cnpape. (accessed Mar. 03, 2021)

[31] R. C. Dugan, M. F. McGranaghan, S. Santoso, and H. W. Beaty, “Electrical Power Systems Quality,” 2004. doi: 10.1007/978-3-319-51118-4_1.

[32] A. Jordan and D. Hogan, “PFC Harmonic Current Emissions – Guide to EN61000-3-2 : 2014,” *EPSMA*, pp. 1–19, 2018.

[33] R. T. Sataloff, M. M. Johns, and K. M. Kost, “Total Harmonic Distortion and Effects in Electrical Power System,” *Assoc. Power Technol.*, no. Figure 1, pp. 1–4.

[34] AEMC Instruments, “Understanding Power & Power Quality Measurements,” no. 800, pp. 1–8.

[35] L. Wuidart, “Understanding Power Factor,” *Power*, pp. 1–5, 2003, [Online]. Available: http://www.thierry-lequeu.fr/data/AN824.pdf. (accessed May 05, 2021)

[36] A. Kalair, N. Abas, A. R. Kalair, Z. Saleem, and N. Khan, “Review of harmonic analysis, modeling and mitigation techniques,” *Renew. Sustain. Energy Rev.*, vol. 78, no. February, pp. 1152–1187, 2017, doi: 10.1016/j.rser.2017.04.121.

[37] A. Bhatia, “Power Factor in Electrical Energy Management,” vol. 144, pp. 1–41, 2012.

[38] Abu Dhabi Distribution Company, Al Ain Distribution Company, and Abu Dhabi Supply Company for Remote Areas (RASCO), “Limits for Voltage Unbalance in the Electricity Supply System,” no. 10, pp. 1–7, 2005.

[39] Voltage Disturbance, “Voltage Unbalance.” http://voltage-disturbance.com/voltage-quality/voltage-unbalance/. (accessed May 05, 2021)

[40] K. J. L. Jr., “Class Notes, Chapter 4: Introduction To Symmetrical Components,” *MIT OpenCourseWare*, p. 17, 2011, [Online]. Available: http://ocw.mit.edu. (accessed May 05, 2021)

[41] A. Amberg and A. Rangel, “Tutorial on Symmetrical Components,” *Selinc.Cachefly.Net*, no. 1, pp. 1–6, 2014, [Online]. Available: https://selinc.cachefly.net/GHRC/1_Tuesday/SymmetricalComponents/LWP0010-02_TutorialSymmetrical-Pt2_AA_20120725.pdf. (accessed Apr. 04, 2021)

[42] E. Csanyi, “What is negative sequence current and how does it affect generator work,” 2019. Available: https://electrical-engineering-portal.com/negative-sequence-current-generator-work. (accessed Apr. 04, 2021)

[43] M. P. Kazmierkowski, *Power Quality: Problems and Mitigation Techniques*, vol. 9, no. 2. 2015.

[44] D. Sreenivasarao, P. Agarwal, and B. Das, “Neutral current compensation in three-phase, four-wire systems: A review,” *Electr. Power Syst. Res.*, vol. 86, pp. 170–180, 2012, doi: 10.1016/j.epsr.2011.12.014.

[45] E. F. Fuchs and M. A. s. Masoum, *Power Quality in Power Systems and Electrical Machines*. 2008.

[46] A. Fatehy and N. Ahmed, “The Analysis of Magnification of Neutral Current in the Presence of Power Quality Problems,” no. June, pp. 15–18, 2015.

[47] K. Nikum, R. Saxena, and A. Wagh, “Neutral Current Problem and Mitigation Techniques : An Overview,” pp. 62–68.

[48] Scheider Electric, “A high 3rd harmonic current can cause a high neutral current,” 2018. Available: https://www.se.com/ww/en/faqs/FA212226/.(accessed Mar. 03, 2021)

[49] F. Alves, “ABC da Metrologia Industrial,” no. 2, p. 56, 2003.

[50] JCGM, “International Vocabulary of metrology - Basic and general concepts and associated terms (VIM),” p. 108, 2012, doi: 10.1016/j.tetlet.2017.07.069.

[51] M. Alves, F. Pereira, and A. Viana, “Instrumentos e Métodos de Medição,” p. 71, 2014.

[52] P. Cabral, “Metrologia Industrial uma função de Gestão de Qualidade.”

[53] Metrel, “MI 2892 Instruction manual,” no. 20. 2020.

[54] Metrel, “Flex current clamps A 1227 User Manual,” 2020.

[55] Metrel, “How to do ... with PowerView3 . 0 Instruction tips,” no. 20. pp. 1–128, 2020.

[56] Janitza, “Power Analyser UMG 96 RM - User manual and technical data,” pp. 1–95, 2021.

[57] Janitza, “Power – Simply Save Catalogue 2021,” pp. 1–451, 2021.

[58] Janitza, “Power Analyzer UMG 96-PA,” pp. 1–104, 2020.

[59] Janitza, “RCM modules for the UMG 96-PA and UMG 96-PQ device series,” pp. 1–54, 2021.

[60] Janitza, “Power Analyser UMG 20 CM Operating instructions and technical data,” pp. 1–64.

[61] Janitza, “800-CT8-A current measuring module 800-CON Transfer modules,” pp. 1–60, 2020.

[62] Janitza, “Modular Power Analyzer UMG 801 User Manual and technical specifications,” pp. 1–114, 2020.

[63] Janitza, “Power Analyser UMG 806 and modules,” pp. 1–8, 2020.

[64] Janitza, “Modular Power Analyzer UMG 806 User manual and technical data,” pp. 1–82, 2020.

[65] Siemens, “Power Monitoring Device SENTRON PAC4200 Manual,” pp. 1–224, 2019.

[66] Siemens, “Analog input module AI Energy Meter 400VAC ST Manual,” pp. 1–107, 2017.

[67] Siemens, “Analog input module AI Energy Meter 480VAC / CT HF Manual,” pp. 1–271, 2019.

[68] Janitza, “The Janitza Current Transformer Range,” pp. 1–63, 2018.

[69] Siemens, “Measuring Devices and Power Monitoring,” pp. 37–40, 2016.

[70] Siemens, “4NC5121 Data sheet,” [Online]. Available:

http://www.papersearch.net/view/detail.asp?detail_key=10000715. (accessed Sept. 09, 2021)

[71] Siemens, “7KM Measuring Devices Manual Module I(N), I(Diff), Analog,” pp. 1–46, 2020.

[72] Janitza, “Feadthrough residual current transformers Technical data Dimension diagrams,” 2021.

Appendix A.

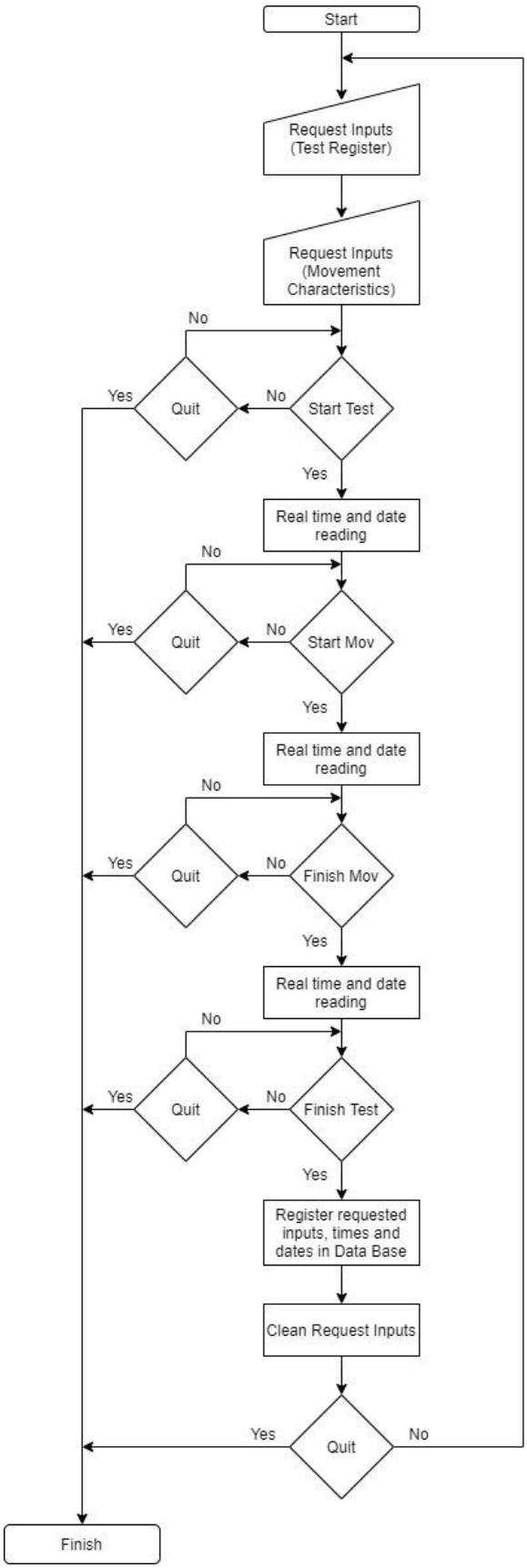
Start
Request Inputs (Test Register)
Request Inputs (Movement Characteristics)
No
Yes
Quit
No
Start Test
Yes
Real time and date reading
No
Yes
Quit
No
Start Mov
Yes
Real time and date reading
No
Yes
Quit
No
Finish Mov
Yes
Real time and date reading
No
Yes
Quit
No
Finish Test
Yes
Register requested inputs, times and dates in Data Base
Clean Request Inputs
Yes
Quit
No
Finish

Appendix B.

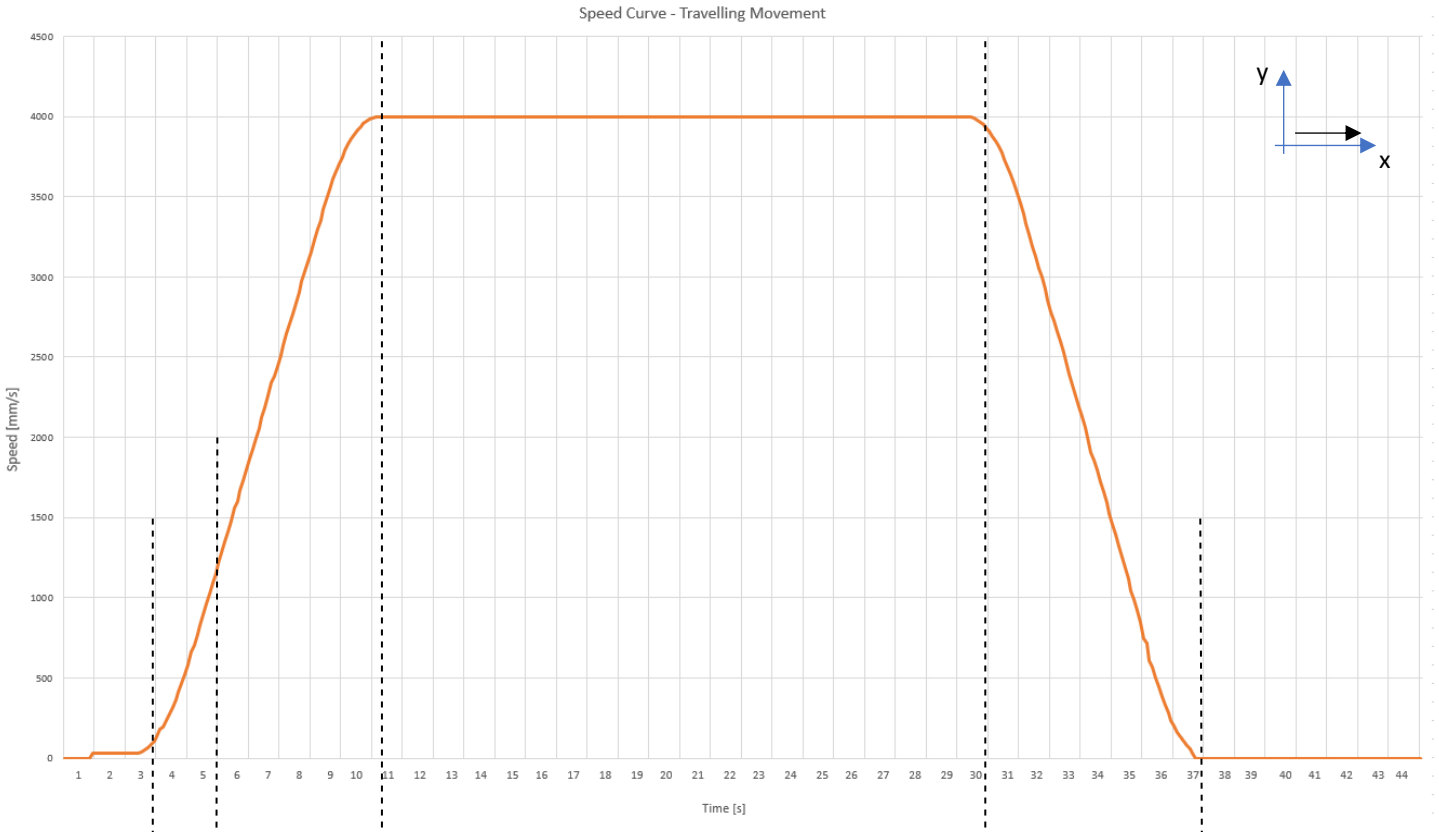
Speed Curve - Travelling Movement
Speed [mm/s]
Time [s]
y
x

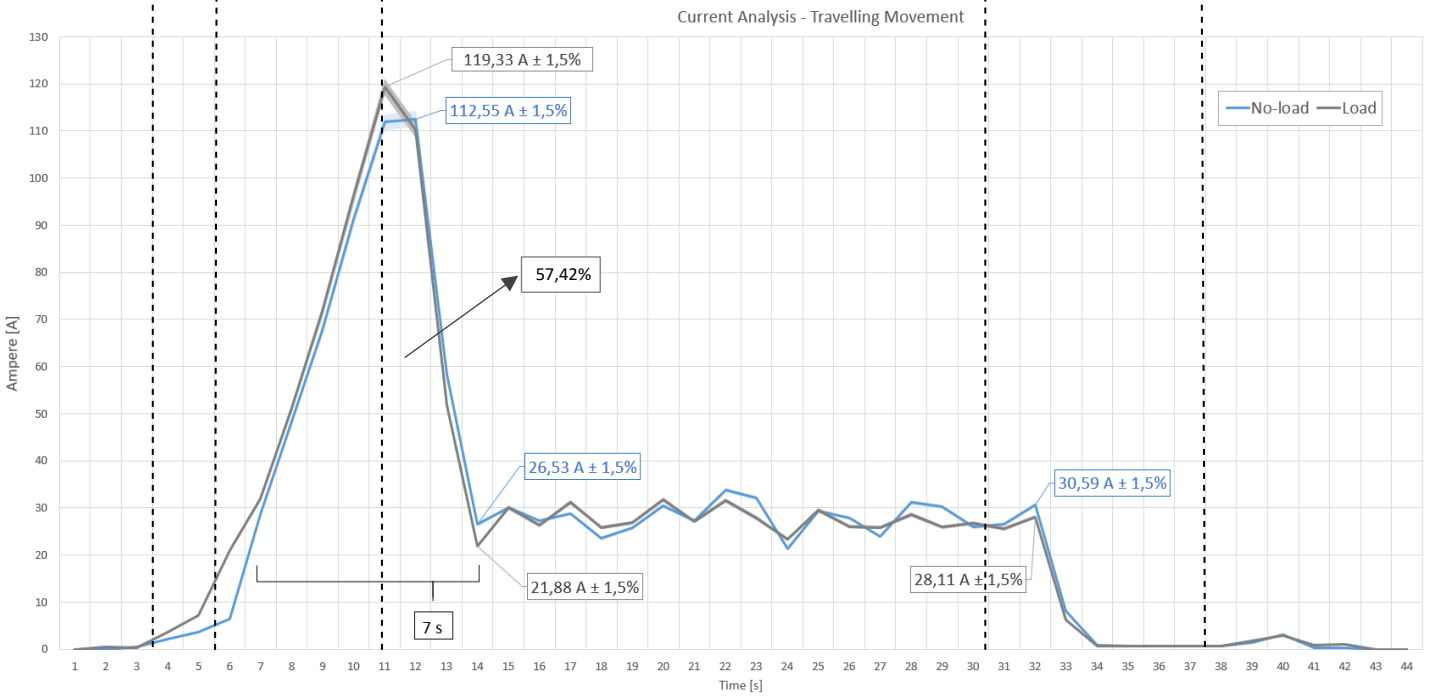
Current Analysis - Travelling Movement
Ampere [A]
Time [s]
119,33 A ± 1,5%
112,55 A ± 1,5%
57,42%
26,53 A ± 1,5%
21,88 A ± 1,5%
7 s
28,11 A ± 1,5%
30,59 A ± 1,5%
No-load
Load

Appendix C.

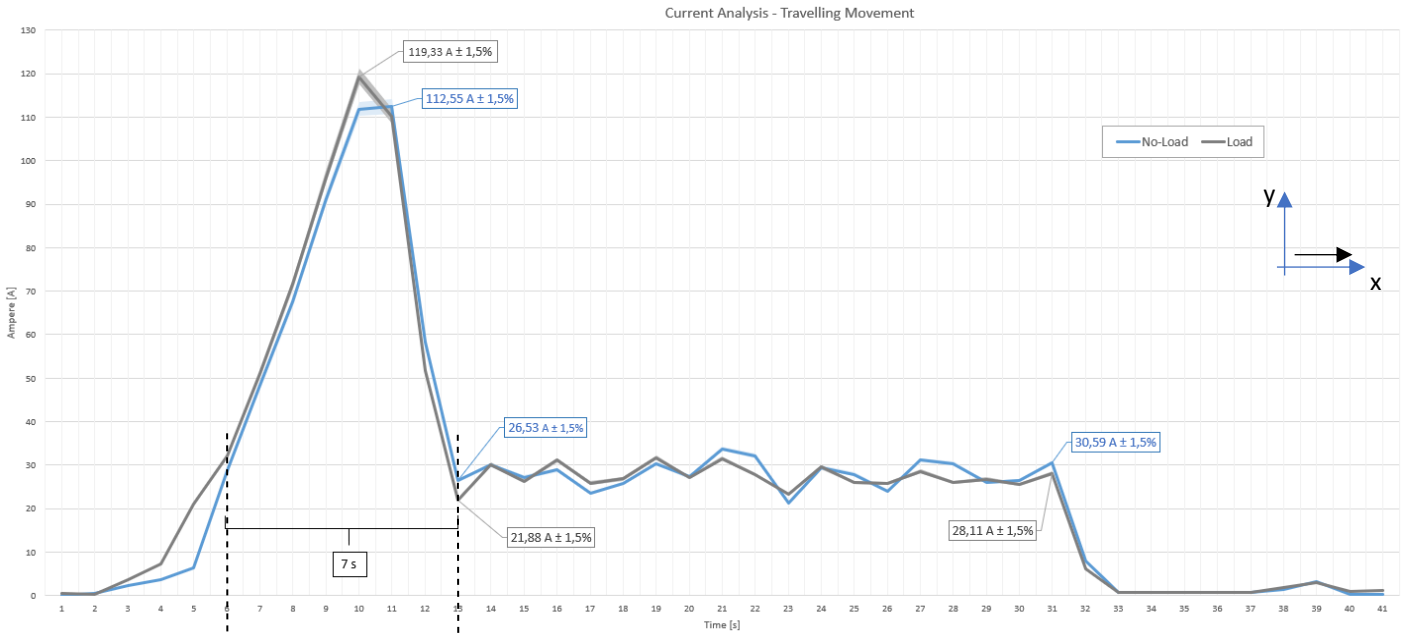
Current Analysis - Travelling Movement
119,33 A ± 1,5%
112,55 A ± 1,5%
No-Load
Load
y
x
26,53 A ± 1,5%
30,59 A ± 1,5%
21,88 A ± 1,5%
28,11 A ± 1,5%
7 s
Ampere [A]
Time [s]

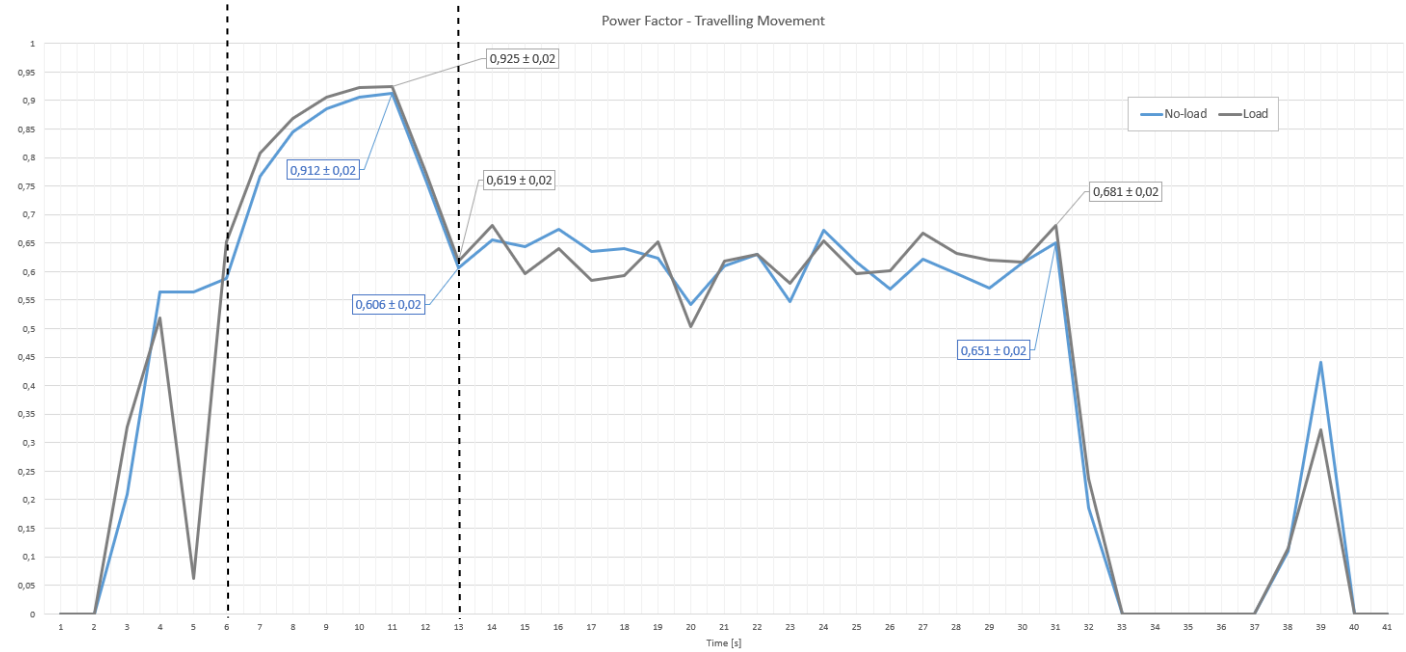
Power Factor - Travelling Movement
0,925 ± 0,02
No-load
Load
0,912 ± 0,02
0,619 ± 0,02
0,681 ± 0,02
0,606 ± 0,02
0,651 ± 0,02
Time [s]

Appendix D.

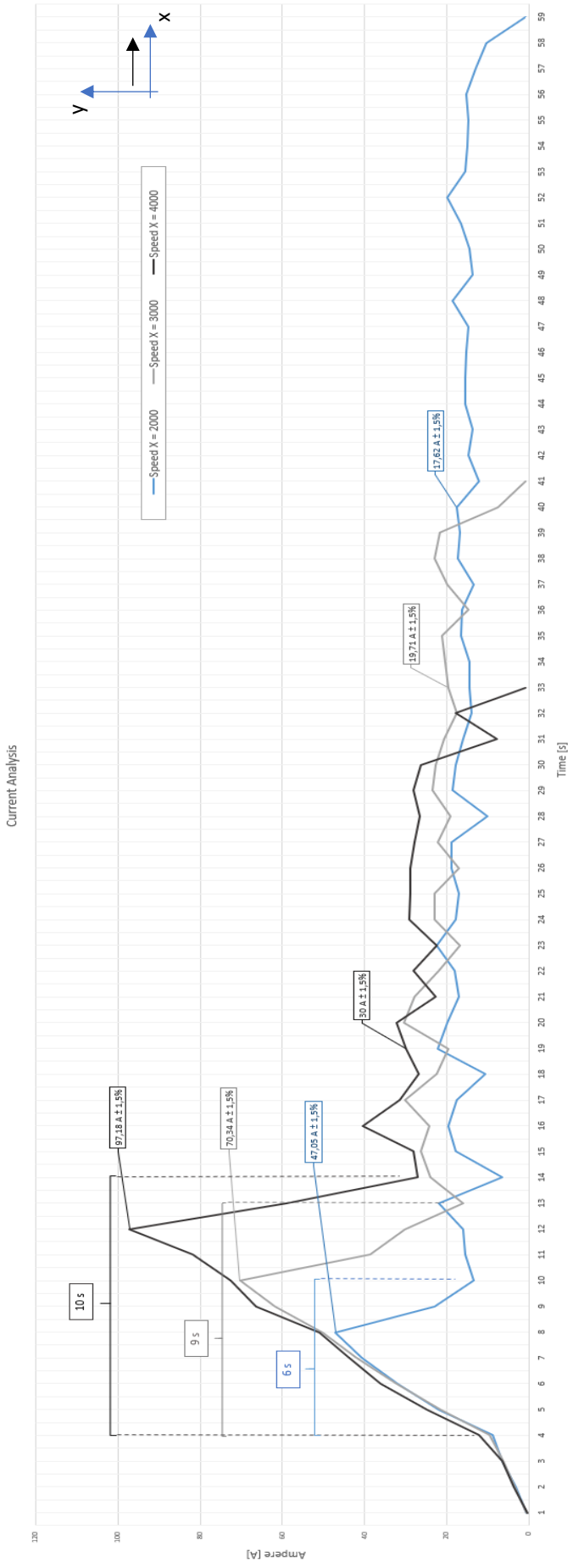
Current Analysis
Ampere [A]
Time [s]
Speed X = 2000
Speed X = 3000
Speed X = 4000
97,18 A ± 1,5%
70,34 A ± 1,5%
47,05 A ± 1,5%
30 A ± 1,5%
19,71 A ± 1,5%
17,62 A ± 1,5%
10 s
9 s
6 s
x
y

Appendix E.

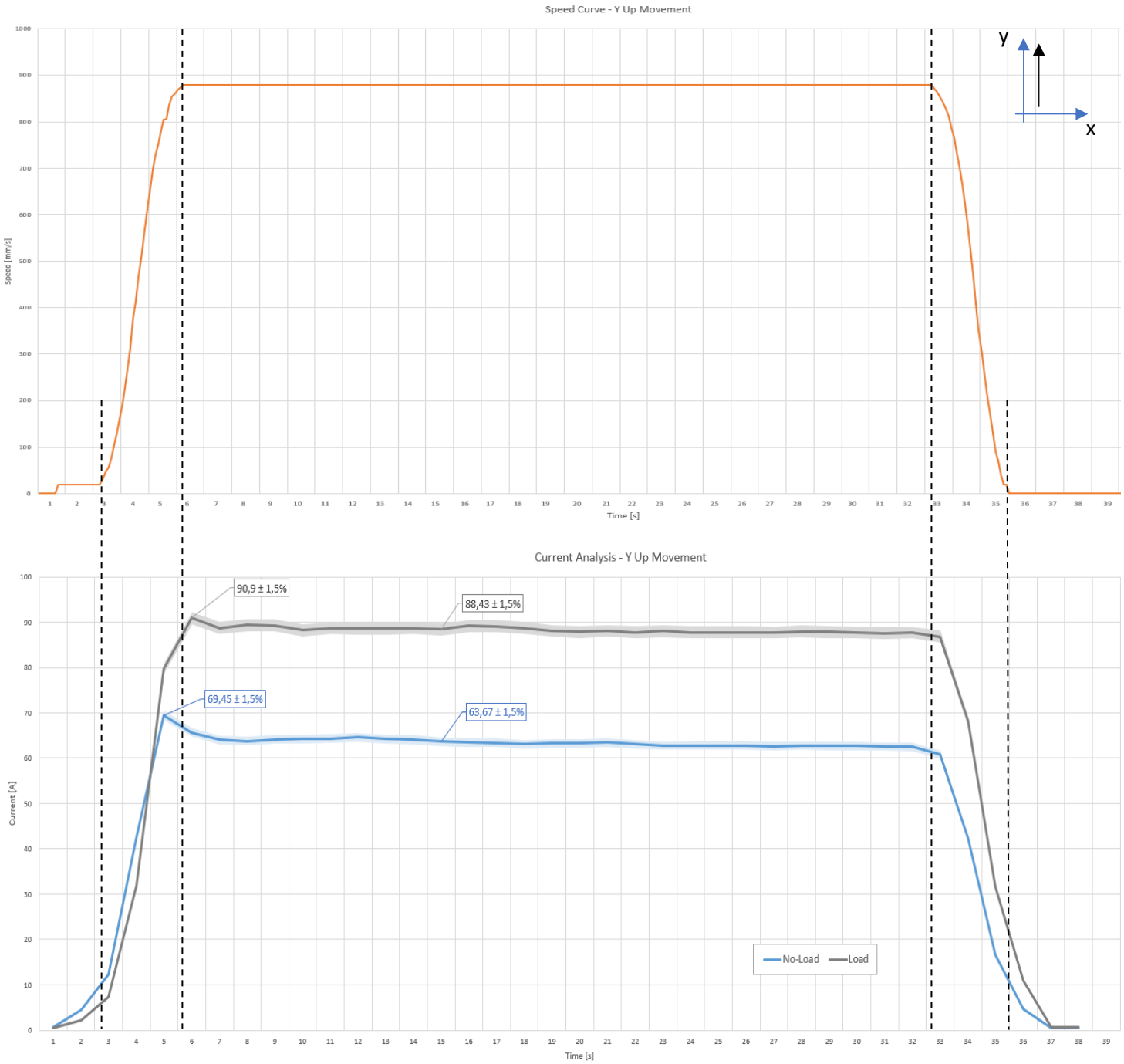
Speed Curve - Y Up Movement
Speed [mm/s]
Time [s]
y
x
Current Analysis - Y Up Movement
Current [A]
Time [s]
90,9 ± 1,5%
88,43 ± 1,5%
69,45 ± 1,5%
63,67 ± 1,5%
No-Load
Load

Appendix F.

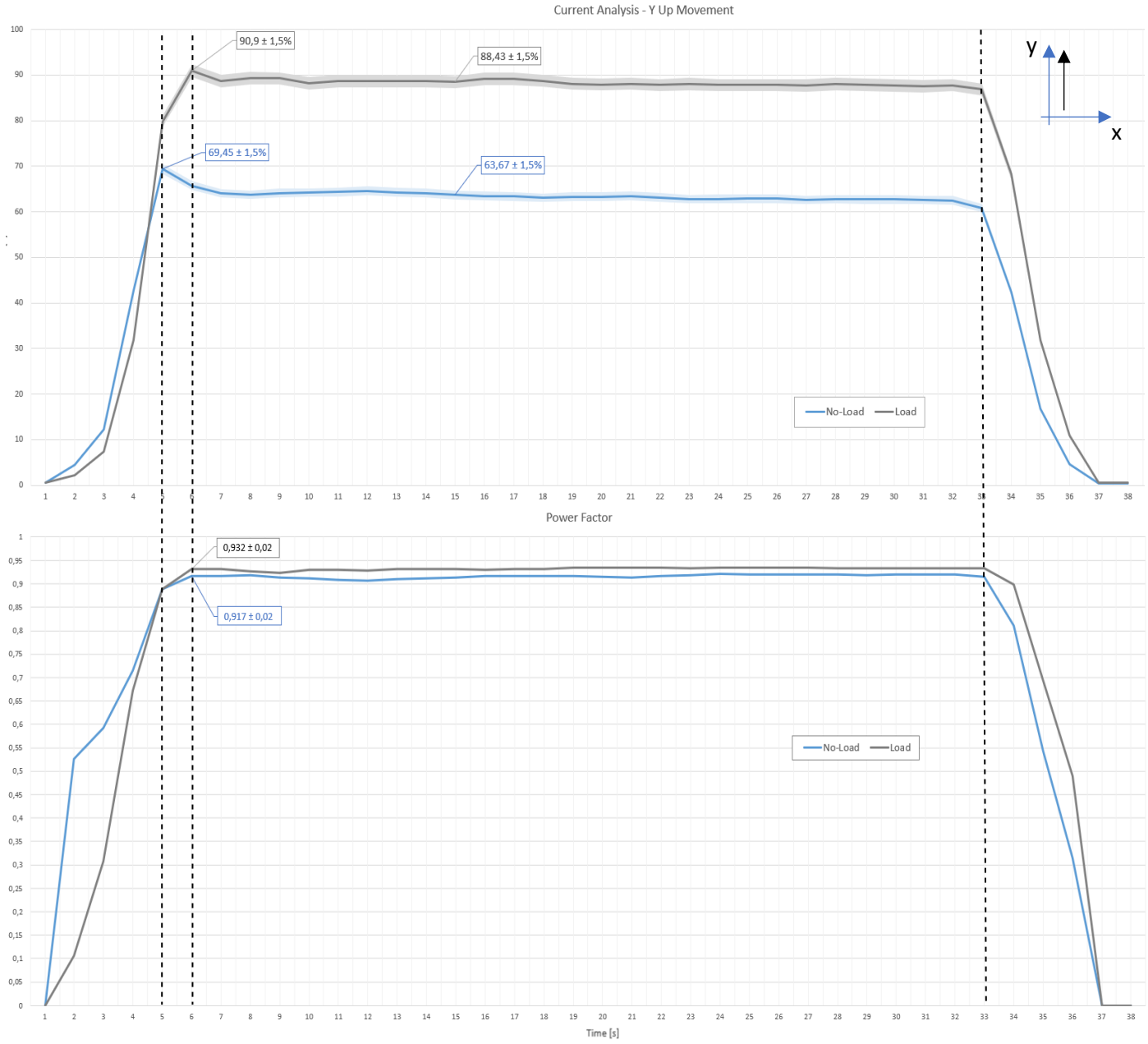
Current Analysis - Y Up Movement
90,9 ± 1,5%
88,43 ± 1,5%
69,45 ± 1,5%
63,67 ± 1,5%
y
x
No-Load
Load
Power Factor
0,932 ± 0,02
0,917 ± 0,02
No-Load
Load
Time [s]

Annex 1.

Metrel Certificate of Calibration Practices

The Metrel Quality System is certified by BVQI according to Quality standard ISO 9001 : 2008, Certificate No. SL21120Q. The Metrel hereby certifies that the above instrument was calibrated in accordance with applicable Metrel calibration procedures during the manufacturing process. These processes are ISO 9001 controlled and are designed to assure that the instrument will meet its published specification.

The Metrel further certifies that the measurement standards and instruments used during the calibration of this instrument are traceable to the (inter)national standards.
The policies and procedures at this facility comply with EN ISO/IEC 17025.

Environmental conditions: Temperature: 23 °C ± 5 °C
Relative humidity: 10 % to 75 %

Calibration Procedure: "Name of Model / Type"

Uncertainty: The reported expanded uncertainty of measurement is stated as the standard uncertainty of measurement multiplied by coverage factor k = 2, which for a nominal distribution corresponds to a coverage probability of approximately 95%. The standard uncertainty of measurement has been determined in accordance with EA Publication EA-4/02.

Edo Reven
Chief Executive Officer

Janko Mole
Head of Calibration Laboratory

Calibration certificate

Model: Current measuring Flexible clamps A1227 Date: 19.1.2018

Serial No.: 18030408 Performed By:Gregor Župevc Signature

Date Placed In Service: _____ Due Date: _____*

Metrel Recommended Cal Interval: 12 months

* The due date may be established (by the customer) by adding the "Recommended Cal Interval" to the "Date Placed In Service."

No.	Function	Input	Low limit	Reading	Uncertainty	High limit
1	Outlook			*Pass*		
2	Range 30 A	3 A	2,774 A	**2.987 A**	0,024 A	3,226 A
	Range 30 A	15 A	14,63 A	**14.98 A**	0,08 A	15,37 A
	Range 30 A	30 A	29,45 A	**30.03 A**	0,16 A	30,55 A
	Range 300 A	200 A	196,0 A	**200.0 A**	1,0 A	204,0 A
	Range 3000 A	1000 A	972,0 A	**999.9 A**	7,3 A	1028,0 A

The measurements have been executed using standards which the traceability to (inter)national standard is guaranteed. The reported expanded uncertainty of measurement is stated as the standard uncertainty of measurement multiplied by coverage factor k = 2, which for a nominal distribution corresponds to a coverage probability of approximately 95%. The standard uncertainty of measurement has been determined in accordance with EA Publication EA-4/02.

All results in accordance with technical specification.

Reference instruments:

No.	Instrument	Type	Certificate No.	Due
1	Calibration System	9100, Wavetek	17C01256	31.7.2018

Annex 2.

catim
centro de apoio tecnológico à indústria metalomecânica

Certificado de Calibração

LaborMet **- LABORATÓRIO DE METROLOGIA**

Data: 2021-09-27 **Certificado Nº: LMGE20215012168/10** **PÁGINA 1 DE 4**

DESCRIÇÃO:

Equipamento: Analisador de Energia
Marca: METREL
Modelo: MI 2892
Nº Serie: 15340077
Ref.Int.: 4369

Acessórios: 4 Sondas amperimétricas
Marca: METREL
Modelo: A 1227
Nº Série: 15391351 / 15330293/ 15330319 / 18030408
Ref.Int.:

PRINCIPAL EQUIPAMENTO UTILIZADO:

Padrão	CATIM Nº	Rastreabilidade
FLUKE 5500A/COIL	99.70005	FLUKE (RvA)

OPERAÇÕES EFECTUADAS:

- Calibração realizada segundo os procedimentos internos, MGE-P01.00 2016-02-13, Rev.A11, MGE-P10.00 2015-04-22, Rev.A04 do Laboratório de Metrologia - Grandezas Eléctricas.

- Todas as medições foram efectuadas em ambiente controlado a 23 °C ± 2 °C e 45 % hr ± 15 % hr, nas instalações do CATIM Porto.

Avaliação de conformidade, perante critério de aceitação indicado.
Erro Máximo Admissível (EMA) = Especificação do fabricante: Regra de Decisão: |Erro| + Incerteza expandida ≤ |EMA|

(#) O resultado está dentro do EMA definido por uma margem menor que a incerteza expandida de medição; não sendo possível garantir conformidade com base no nível de confiança declarado. No entanto, o resultado indica que a conformidade é mais provável do que a não conformidade.

EXAME VISUAL:

Equipamento em bom estado de conservação.

A incerteza expandida apresentada, está expressa pela incerteza-padrão multiplicada pelo factor de expansão k = k', o qual para uma distribuição-t com vef = v'ef graus de liberdade efectivos corresponde a uma probabilidade de expansão de aproximadamente 95%. A incerteza foi calculada de acordo com o documento EA-4/02.

O IPAC é um dos signatários do Acordo de reconhecimento mútuo da EA e do ILAC para calibrações.

Data da calibração: 2021-09-22

Técnico

(Altino Martins)

Responsável Técnico

(Rogério Vitorino)

IPAC acreditação M0003 ISO/IEC 17025 Calibração

ilac-MRA

catim
centro de apoio tecnológico à indústria metalomecânica

Certificado de Calibração

LaborMet - LABORATÓRIO DE METROLOGIA

RESULTADOS:

Função/Gama	Leitura no Padrão		Leitura no Equipamento	Erro	Incerteza Expandida	k'	v'ef	EMA	Avaliação de Conformidade
Tensão Alternada									
Fase L1-N									
136 V	5,00000 V	50,00 Hz	5,02 V	0,0200 V	0,0066 V	2,0	1550	0,14 V	CONFORME
	10,0000 V	50,00 Hz	10,02 V	0,020 V	0,010 V	2,1	25	0,14 V	CONFORME
	30,0000 V	50,00 Hz	30,01 V	0,010 V	0,016 V	2,0	1317	0,14 V	CONFORME
	100,000 V	50,00 Hz	100,01 V	0,010 V	0,066 V	2,0	1052	0,14 V	CONFORME
374 V	150,000 V	50,00 Hz	150,01 V	0,01 V	0,18 V	2,0	1030	0,37 V	CONFORME
	250,000 V	50,00 Hz	250,0 V	0,00 V	0,21 V	2,0	1292	0,4 V	CONFORME
	300,000 V	50,00 Hz	300,0 V	0,00 V	0,23 V	2,0	1208	0,4 V	CONFORME
1000 V	380,000 V	50,00 Hz	380,0 V	0,00 V	0,38 V	2,0	476	1,0 V	CONFORME
	500,000 V	50,00 Hz	500,0 V	0,00 V	0,44 V	2,0	669	1,0 V	CONFORME
	1000,00 V	50,00 Hz	1000,0 V	0,00 V	0,70 V	2,0	1037	1,0 V	CONFORME
Fase L2-N									
136 V	5,00000 V	50,00 Hz	5,01 V	0,0100 V	0,0095 V	2,2	16	0,14 V	CONFORME
	10,0000 V	50,00 Hz	10,00 V	0,0000 V	0,0079 V	2,0	2030	0,14 V	CONFORME
	30,0000 V	50,00 Hz	30,00 V	0,000 V	0,017 V	2,0	187	0,14 V	CONFORME
	100,000 V	50,00 Hz	99,99 V	-0,010 V	0,066 V	2,0	1052	0,14 V	CONFORME
374 V	150,000 V	50,00 Hz	149,99 V	-0,01 V	0,18 V	2,0	1030	0,37 V	CONFORME
	250,000 V	50,00 Hz	250,0 V	0,00 V	0,21 V	2,0	1292	0,4 V	CONFORME
	300,000 V	50,00 Hz	300,0 V	0,00 V	0,23 V	2,0	1208	0,4 V	CONFORME
1000 V	380,000 V	50,00 Hz	380,0 V	0,00 V	0,38 V	2,0	476	1,0 V	CONFORME
	500,000 V	50,00 Hz	500,1 V	0,10 V	0,44 V	2,0	648	1,0 V	CONFORME
	1000,00 V	50,00 Hz	1000,0 V	0,00 V	0,70 V	2,0	1037	1,0 V	CONFORME
Fase L3-N									
136 V	5,00000 V	50,00 Hz	5,02 V	0,0200 V	0,0066 V	2,0	1550	0,14 V	CONFORME
	10,0000 V	50,00 Hz	10,02 V	0,020 V	0,010 V	2,1	25	0,14 V	CONFORME
	30,0000 V	50,00 Hz	30,01 V	0,010 V	0,016 V	2,0	1317	0,14 V	CONFORME
	100,000 V	50,00 Hz	100,01 V	0,010 V	0,067 V	2,0	1047	0,14 V	CONFORME
374 V	150,000 V	50,00 Hz	150,00 V	0,00 V	0,18 V	2,0	1028	0,37 V	CONFORME
	250,000 V	50,00 Hz	250,0 V	0,00 V	0,21 V	2,0	1292	0,4 V	CONFORME
	300,000 V	50,00 Hz	300,0 V	0,00 V	0,23 V	2,0	1208	0,4 V	CONFORME
1000 V	380,000 V	50,00 Hz	380,0 V	0,00 V	0,38 V	2,0	476	1,0 V	CONFORME
	500,000 V	50,00 Hz	500,0 V	0,00 V	0,44 V	2,0	669	1,0 V	CONFORME
	1000,00 V	50,00 Hz	1000,0 V	0,00 V	0,70 V	2,0	1037	1,0 V	CONFORME

RESULTADOS

Função/Gama	Leitura no Padrão	Leitura no Equipamento	Erro	Incerteza Expandida	k'	v'ef	EMA	Avaliação de Conformidade
Corrente Alternada								
0,5 A a 1000 A								
I1 - Sonda amperimétrica METREL A 1227 | Nº série: 15391351								
(30/ 300/ 3000) A x 50								
220,000 mA	**11 A**	11,07 A	0,07 A	0,11 A	2,0	1006	0,19 A	CONFORME
65,00 Hz								
0,7200 A	**36 A**	36,26 A	0,26 A	0,54 A	2,0	1000	0,63 A	CONFORME (#)
65,00 Hz								
2,4000 A	**120 A**	120,7 A	0,7 A	1,1 A	2,0	1006	2,1 A	CONFORME
50,00 Hz								
7,2000 A	**360 A**	362,2 A	2,2 A	3,5 A	2,0	1001	6,3 A	CONFORME
50,00 Hz								
11,0000 A	**550 A**	553,4 A	3,4 A	4,8 A	2,0	1000	9,7 A	CONFORME
50,00 Hz								
I2 - Sonda amperimétrica METREL A 1227 | Nº série: 15330293								
(30/ 300/ 3000) A x 50								
220,000 mA	**11 A**	11,03 A	0,03 A	0,11 A	2,0	1006	0,19 A	CONFORME
65,00 Hz								
0,7200 A	**36 A**	36,08 A	0,08 A	0,54 A	2,0	1000	0,63 A	CONFORME
65,00 Hz								
2,4000 A	**120 A**	120,4 A	0,4 A	1,1 A	2,0	1006	2,1 A	CONFORME
50,00 Hz								
7,2000 A	**360 A**	361,2 A	1,2 A	3,5 A	2,0	1001	6,3 A	CONFORME
50,00 Hz								
11,0000 A	**550 A**	551,8 A	1,8 A	4,8 A	2,0	1000	9,6 A	CONFORME
50,00 Hz								
I3 - Sonda amperimétrica METREL A 1227 | Nº série: 15330319								
(30/ 300/ 3000) A x 50								
220,000 mA	**11 A**	10,99 A	-0,01 A	0,11 A	2,0	1006	0,19 A	CONFORME
65,00 Hz								
0,7200 A	**36 A**	35,99 A	-0,01 A	0,54 A	2,0	1000	0,63 A	CONFORME
65,00 Hz								
2,4000 A	**120 A**	120,1 A	0,0 A	1,1 A	2,0	1009	2,1 A	CONFORME
50,00 Hz								
7,2000 A	**360 A**	360,1 A	0,1 A	3,5 A	2,0	1001	6,3 A	CONFORME
50,00 Hz								
11,0000 A	**550 A**	550,2 A	0,2 A	4,8 A	2,0	1000	9,6 A	CONFORME
50,00 Hz								

RESULTADOS:

Função/Gama	Leitura no Padrão	Leitura no Equipamento	Erro	Incerteza Expandida	k'	v'ef	EMA	Avaliação de Conformidade
Corrente Alternada (continuação)								
0,5 A a 1000 A								
IN - Sonda amperimétrica METREL A 1227 | Nº série: 18030408								
(30/ 300/ 3000) A x 50								
	220,000 mA **11 A**	10,97 A	-0,03 A	0,11 A	2,0	1006	0,19 A	**CONFORME**
	65,00 Hz							
	0,7200 A **36 A**	35,92 A	-0,08 A	0,54 A	2,0	1000	0,63 A	**CONFORME**
	65,00 Hz							
	2,4000 A **120 A**	119,8 A	-0,2 A	1,1 A	2,0	1006	2,1 A	**CONFORME**
	50,00 Hz							
	7,2000 A **360 A**	359,6 A	-0,4 A	3,5 A	2,0	1001	6,3 A	**CONFORME**
	50,00 Hz							
	11,0000 A **550 A**	549,3 A	-0,7 A	4,8 A	2,0	1000	9,6 A	**CONFORME**
	50,00 Hz							